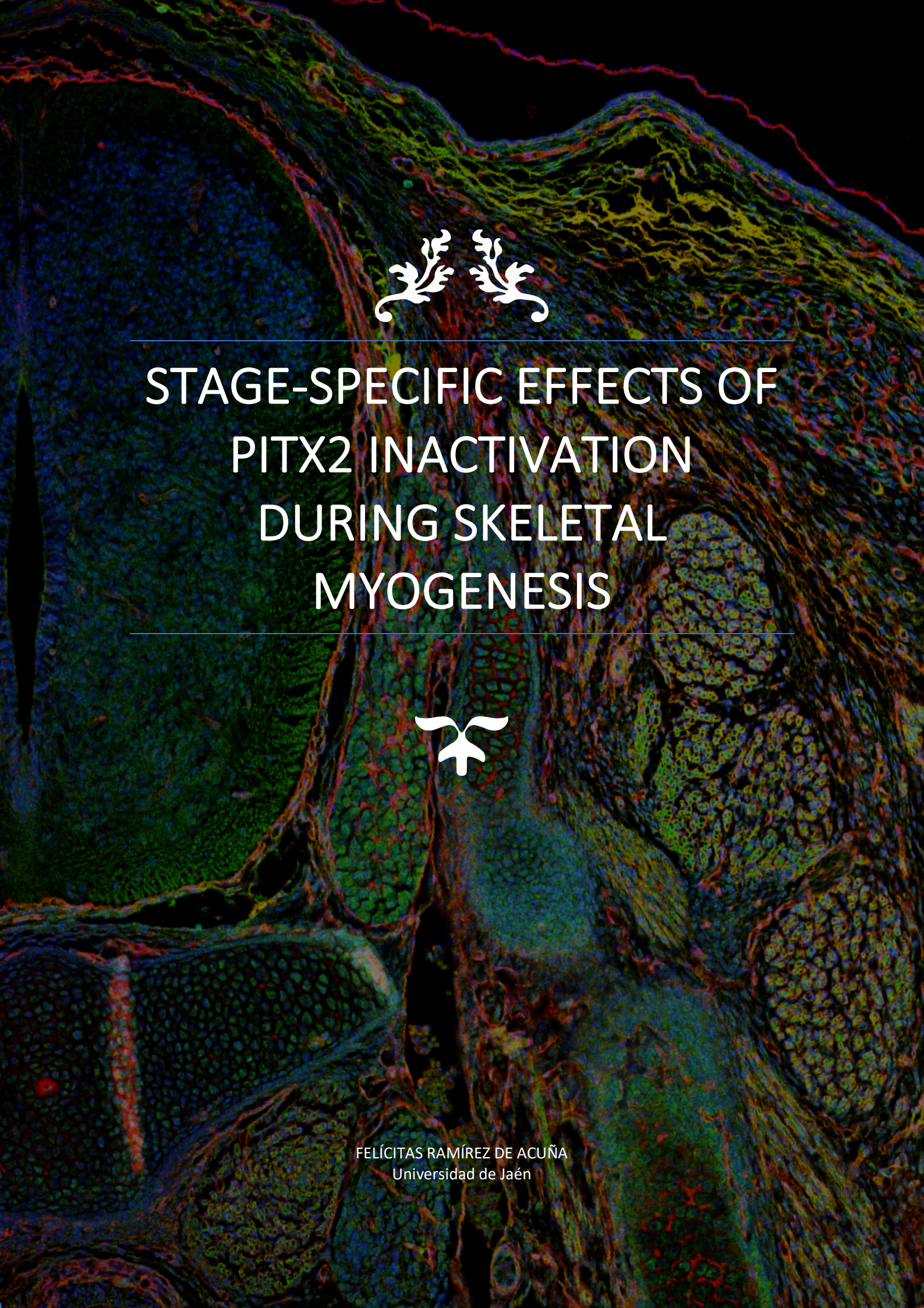

STAGE-SPECIFIC EFFECTS OF PITX2 INACTIVATION DURING SKELETAL MYOGENESIS

FELÍCITAS RAMÍREZ DE ACUÑA
Universidad de Jaén

Index

Chapter I:

General Introduction

Chapter I: General Introduction:

1. The skeletal muscle

Striated muscle is the most abundant tissue in the body of vertebrates and it forms, together with the skeleton, the locomotory system required both for movement and the creation of the specific body shape of a species. The skeletal muscle is a highly organized tissue containing several bundles of muscle fiber (myofibers). Each myofiber (containing several myofibrils), represents a muscle cell with its basic cellular unit called the sarcomere. Bundles of myofibers form the fascicles, and bundles of fascicles form the muscle tissue, with each layer successively encapsulated by the extracellular matrix (Lieber, 2011) and supported by the cytoskeletal networks. The skeletal muscle is highly vascularized and innervated, and embedded with components of the metabolic machinery, supporting efficient energy production and cellular homeostasis (**Figure 1**). Precisely coordinated activity between all of these components is crucial for shaping the state of muscular health and associated motor activity.

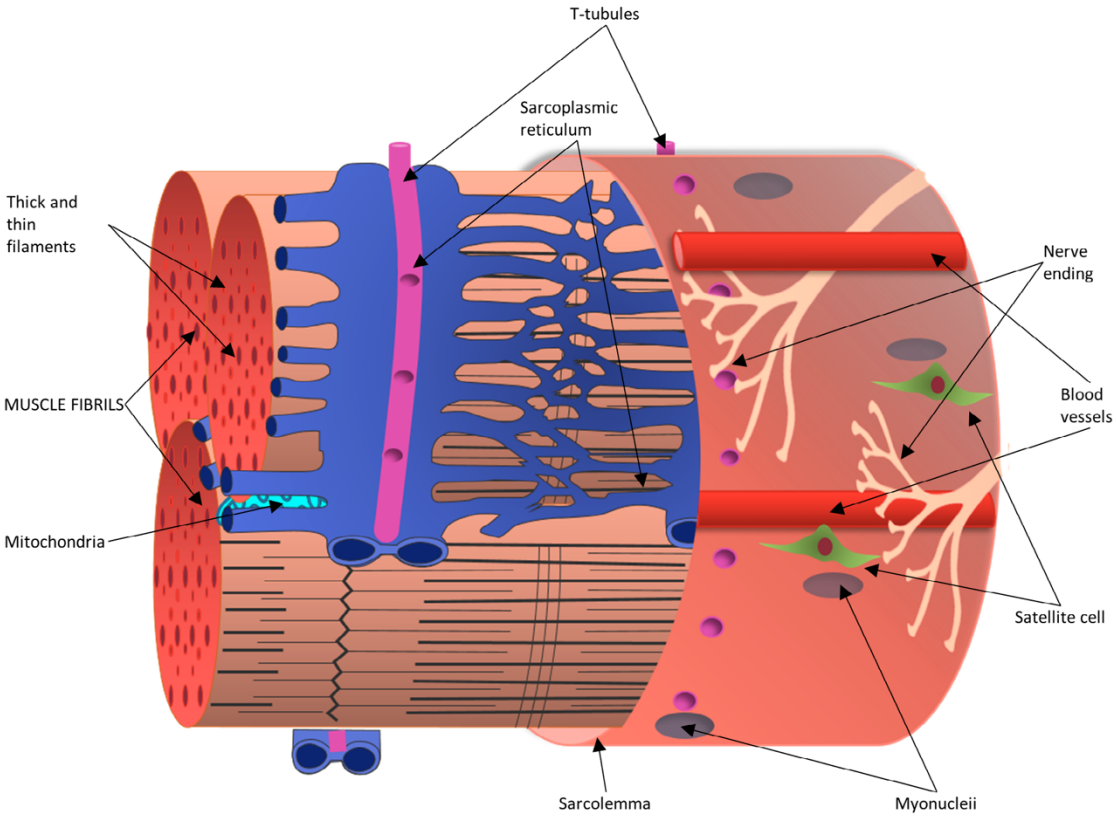

Figure 1: Schematic mature skeletal muscle fiber where can be shown a myofibrils bundle covered by the sarcolemma. Capillaries and nerve fibers prolong along the muscle fiber while the satellite cells are place under the basal lamina and in a closeness position of the myonuclei fibers (Lieber, 2011).

2. Making muscle: Embryonic and adult myogenesis

The myogenic process is the result of different extrinsic (morphogens, muscle damage) and intrinsic elements like gene regulatory elements, that giving rise to the mature muscle.

- Embryonic development of the skeletal muscle

A large variety of signalling molecules coordinates myogenesis during embryonic development and in postnatal life. The presence of cells surface

receptor and its activation by these signals stimulates intracellular pathways join on a series of specific transcription and chromatin-remodeling factors. These factors translate the extracellular signals in to the gene and microRNA expression program, which gives its own myogenic identity every muscle progenitors (Bentzinger, Wang, & Rudnicki, 2014).

The limb and trunk muscles procced from the somites, structures formed by a process termed somitogenesis. The somitogenesis starts with local oscillations in gene expression and morphogen gradients inducing, in the paraxial mesoderm, pairwise condensation structures on either side of the neural tube (Bentzinger et al., 2014) (Buckingham & Vincent, 2009). These structures called somites are developed progressively from head to tail, and approximately one pair of somites is formed every 2 h to ultimately a total of 60 pairs of somites in the developing mouse embryo (Buckingham et al., 2003).

The somitogenesis involves directly or indirectly participanting genes in *Notch* and *Wnt* pathways together with morphogen gradients of *Wnt*, *FGF* and retinoic acid (Bentzinger et al., 2014). Through the influence of signalling molecules –such as Sonic Hedgehog (*Shh*), *Wnt*, and *BMP* emanating from the notochord, neural tube, surface ectoderm, and lateral plate mesoderm –. The somites undergo a transition, partitioning into an underlying mesenchymal sclerotome, sited on the ventral part of the somite and which contains precursors to connective tissue for cartilage, bone and tendons, and an overlying dermomyotome localized in the most dorsal part which remain epithelial and give rise to all skeletal muscles of the body, brown fat, endothelial cells and dorsal dermis (Deries & Thorsteinsdóttir, 2016). Around embryonic day E8.00

expression of MRFs is first detected in these structures (Ott, Bober, Lyons, Arnold, & Buckingham, 1991).

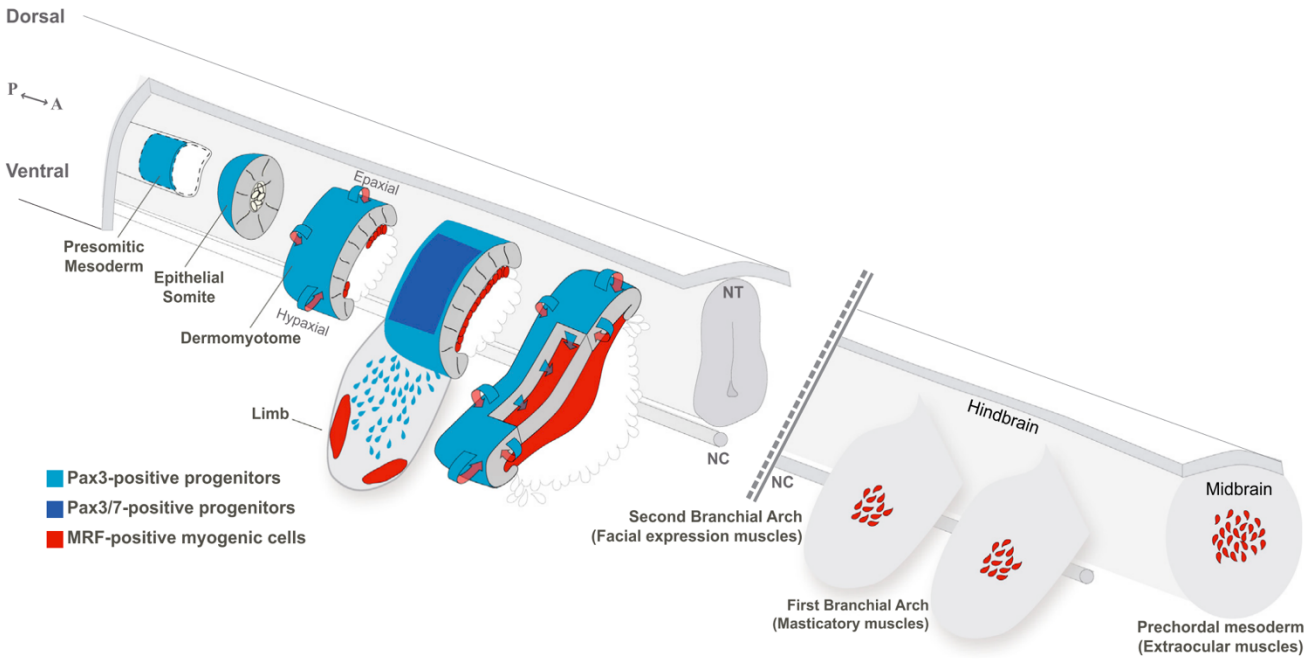

Figure 2: Schematic representation of somites, First and Second Branchial Arches, and Prechordal Mesoderm that are the sources of skeletal muscles shown for the mouse embryo somites mature following an anterior (A) to posterior (P) developmental gradient. NT, neural tube; NC, notochord (Buckingham & Rigby, 2014).

The gene regulatory network that controls muscle progenitor cell behaviour and activation of the myogenic determination genes is controlled by Paired box factor 3 (*Pax3*), which is first expressed in pre-somitic mesoderm immediately anterior to the first somite and then throughout the early epithelial somite (Buckingham, 2017) (**Figure 2**). *Pax3* is required for cell survival in the somite and also contributes to control the balance between self-renewal vs. differentiation program by FGF signalling (Buckingham, 2017).

The cells from the dermomyotome are marked by the expression of the paired box transcription factor *Pax3* and *Pax7*, and low expression of the basic

helix-loop-helix transcription factor *Myf5* (Bentzinger et al., 2014). These cells are distributed in two lips and carry out an epithelial- mesenchymal transition (EMT) which integrate the myotome, a structure composed by myocytes (Buckingham & Relaix, 2015) which containing committed muscle cells expressing high levels of *MyoD* and *Myf5*. Both genes are considerate myogenic terminal specification markers.

The myotome is considered the first myogenic structure of the embryonic development and eventually forms the skeletal muscles of the body and limbs, as a result of *Shh* and *Wnt* signalling from the notochord and floor plate, which induces *Myf5* expression by the mab-related transcription factor 2 (*Dmrt2*) (Sato, Rocancourt, Marques, Thorsteinsdóttir, & Buckingham, 2010). *Dmrt2* is also implicated in the maintaining somite integrity and is a direct *Pax3* target (Buckingham, 2017). *MyoD* acts downstream from *Pax3* and *Pax7* in the genetic hierarchy of myogenic regulators, whereas *Myf5* can acts in parallel with Pax factor depending of the context. After that, the central part of the dermomyotome disintegrates and the muscle progenitors intercalate into the primary myotome (Bentzinger et al., 2014). The epaxial part of the dermomyotome give rise to the dorsal and back muscle whereas the trunk muscles, the limbs and body walls come from the hypaxial myotome (Buckingham & Relaix, 2015) where *MyoD* expression is induced at E10.5 by *Wnt* signalling from the dorsal endoderm and by *BMP4* from the lateral mesoderm (Cazenave, Souriau, & Kien, 1989). Cell migration from cervical somites is also important for the formation of the diaphragm muscle (Buckingham, 2017).

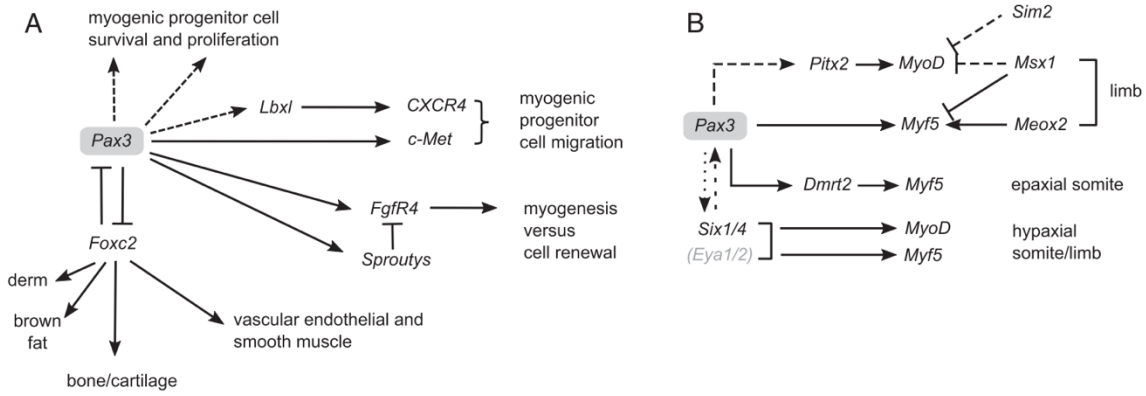

Figure 3: Gene regulatory networks at the onset of myogenesis in the trunk and limbs, where *Pax3* plays a central role in controlling many aspects of myogenic progenitor cell behavior (A) including choice of the myogenic cell fate, survival, proliferation, migration, and entry into the differentiation program, which depends on activation of the myogenic determination genes at different sites where skeletal muscle formation is initiated in the mouse embryo (B). derm refers to the dorsal dermis (Buckingham, 2017).

MyoD activation also depends on the paired-like-homeodomain factor 2 (*Pitx2*), which lies genetically upstream of *Pax3* (L'Honore, Ouimette, Lavertu-Jolin, & Drouin, 2010). Sine oculis homeobox transcription factors 1/4 (*Six1/4*), with their coactivators *Eya1/2*, are also important players in *MyoD* expression. Together with *Pax3*, they respond to enhancer elements responsible for hypaxial somite and limb expression of *Myf5* and *MyoD* (Buckingham, 2017) (**Figure 3**). At last, the limbs progenitor cells, hypaxial myoblasts adjacent to the nascent limbs buds which show an extensive migratory capacity, delaminate and undergo an EMT with the aim to originate dorsal and ventral muscle masses in mature fore and hind limbs (Deries & Thorsteinsdóttir, 2016).

Delamination and migration depend on the presence of *c-met*, a tyrosine kinase receptor which interacts with its ligand HGF, produced by non-somitic mesodermal cells which thus delineate the migratory route and which depends of *Pax3*. The chemokine receptor type 4 (*CXCR4*) is also required for migration of

a subset of myogenic progenitors into the limb (**Figure 3**). Activation of this gene depends on a transcription factor encoded by Ladybird homeobox 1 (*Lbx1*), which lies genetically downstream of *Pax3*. This, *Pax3* orchestrates key steps (cell fate choice, survival, self-renewal, and migration) in the progression of progenitor cells toward myogenesis (Buckingham, 2017).

Pax3^{+} cells migrate to their target sites where they later differentiate to form the muscles. Muscle progenitor cells migrating to the limbs enter to the limb mesenchyme and after they scope their target sites in the proximal limb buds, they proliferate before some differentiate into myoblasts/myocites (Murphy & Kardon, 2011). The pool of muscle cells divides into dorsal and ventral muscle masses, differentiated cells fuse to form multinucleated muscle fibers which either aggregate with, or split from, neighbouring fibers, originating all the different limbs muscles (Deries & Thorsteinsdóttir, 2016). Muscle cell differentiation and myotube formation starts proximally and proceeds in a proximal to distal direction in analogy to the rostral to caudal maturation gradient observed in the trunk (Deries & Thorsteinsdóttir, 2016). Limb muscle morphogenesis then takes place together with the formation of bones and tendons to forms the definitive limb musculoskeletal system.

In this line, during the primary (embryonic) myogenesis, the primary muscle fibers are generated between embryonic day (E) 9.5E and 14.5E in the mouse embryo. The final fate of the progenitor cells in the embryonic myogenesis is orchestrated by transcription factors during the specification, determination, and differentiation progression. *MyoD*, *Myf5*, *Myogenin* and *Myogenic Regulatory Factor 4* (*MRF4*) act at multiple points in the muscle lineage to determine the

skeletal muscle phenotype through regulation or proliferation, irreversible cell cycle arrest of precursor cells, followed by regulated activation of sarcomeric and muscle specific genes to facilitate differentiation and sarcomere assembly (Buckingham & Rigby, 2014).

Transcripts for myogenin and MRF4 are first detected at E8.5 and E9.00, and their expression is evenly distributed throughout the myotome (Cazenave et al., 1989). Consistent with a dual role in both determination and differentiation of the muscle linage, MRF4 transcripts show biphasic expression, whereby they are downregulated by E11.5, but reappear at E16.0 in differentiated muscle fibers. Differences between the epaxial and hypaxial pool of myoblasts are evidenced at the molecular level by differing dependencies upon *Myf5* and *MyoD*.

MyoD, Myf5, Myogenin and *MRF5* contain a basic helix-loop-helix (bHLH) domain that confers them with the ability to identify the E-box sequence (CANNTG) in the regulatory sequence of target genes upon heterodimerization with a member of the ubiquitously expressed E-protein family of bHLH proteins (Lassar et al., 1991). Localization, timing and expression levels of the MRFs during development are finely modulated to guarantee the correct progression of the developmental process.

The onset of the trunk myogenesis starts with the expression of *Pax3*, a transcription factor placed at dermomyotome which is the first specification marker to the myogenic lineage, and continues with the activation of *Pax7* on the *Pax3*$^{+}$ myogenic precursor, giving rise the myogenic progenitor (Buckingham & Relaix, 2007) of the embryonic and fetal muscles in trunk and limbs. These

progenitor cells delaminating and migrating from the somite to the limbs (Buckingham & Relaix, 2015). Myogenic cells that have activated the myogenic determination genes *Myf5/Myf6* and *MyoD* downregulate *Pax3* and delaminate from the edges of the dermomyotome (Buckingham & Relaix, 2015). The early epaxial myotome depends of the early epaxial activation of *Myf5* which is driven by *Wnt* and *Shh* without any requirement of *Pax3* or *Pax7* (Buckingham & Relaix, 2015). These cells differentiate deprived of *MyoD* and *MyoG*. On the other hand, *Myf5* is activated under PAX3 control in the hypaxial somites and limbs (Buckingham & Relaix, 2015). In the rest of the dermomyotome and limbs MyoD is expressed after the activation of *Myf5* (Hu, Geles, Paik, DePinho, & Tjian, 2008). Finally, the terminal differentiation needs the transcription factor MYOG and *Myf6* for fusion of myocytes and the formation of myotubes (Bentzinger, Wang, & Rudnicki, 2012).

In parallel to myofiber formation, can be detected adjacent to the myofibers a subpopulation of myogenic precursor cells that do not express the MRFs and maintain *Pax3/Pax7* expression late during mouse fetal development, around E16.5-18.5 (Kassar-duchossoy et al., 2005). It is hypothesized that these cells give rise to the satellite cell population found in adult muscle.

Instead, the head skeletal muscle derives from the unsegmented head mesoderm which is remodelled at early stage during embryonic development. The unsegmented head mesoderm gives rise to all craniofacial skeletal muscles, which can be classified like four different population: extra-ocular (EOMs), branchial, laryngoglosal and axial neck muscles. Cells from cranial paraxial

mesoderm migrate through the first branchial arch as well as the prochordal mesoderm form the EOMs (Hernandez-Torres, Rodríguez-Outeiriño, Franco, & Aranega, 2017). For branchial arch muscles, the cells migrate from the cranial paraxial mesoderm and the lateral splanchnic mesoderm, while the laryngoglossal muscles develop from myoblasts arising from occipital somites. Finally, the axial neck muscles are formed from medio-dorsal and latero-ventral region of occipital a cervical somites (Hernandez-Torres et al., 2017). The genetic hierarchy leading myogenesis in the head is different of the trunk muscle formation. For example, branchial-arch-derived muscles depend on *Myf5/Myo6/MyoD*, whereas extraocular muscle formation is initiated by *Myf5/Myf6* and in their absence, cannot be restored by *MyoD*.

On the other hand, during the secondary (fetal) myogenesis the fusion of the different myoblasts give rise to the secondary muscle fibers formed initially at the site of innervation of the primary fibers and are under the same basal lamina ("The origin of secondary myotubes in mammalian skeletal muscles: Ultrastructural studies," 1989) around E14.00. These fibers continue enclosed for a short period to primary fibers and which can be differentiate from primary fibers by their relative small size (Costamagna, Mommaerts, Sampaolesi, & Tylzanowski, 2016). In parallel to myofiber formation, a subpopulation of myogenic precursor cells that do not express the MRFs and maintain *Pax3/Pax7* expression is observed adjacent to the myofibers late during mouse fetal development, at around E16.5-18.5 (Dumont, Wang, & Rudnicki, 2015). It is hypothesised that these cells give rise to the satellite cell population found in adult

muscle. Although adult satellite cells do not express *MyoD* in resting conditions, the progenitors of essentially all adult satellite cells transcribed *MyoD* prenatally.

Finally, a third wave of progenitors residing adjacent to existing fibers, called satellite cells, appear at the end of postnatal development and will allow for the hypertrophic growth of skeletal muscle after birth. At the end of postnatal development, some satellite cells enter quiescence but remain primed for activation. In this way, have been show that during the first three postnatal weeks increase the myofiber length, cross-sectional area and number of myonuclei (White, Biérinx, Gnocchi, & Zammit, 2010).

- Post-natal myogenesis

At the postnatal satellite cell stage, *Pax3* and *Pax7* mark the presence of these muscle progenitors placed underneath the basal lamina of adult myofibers. While *Pax7* is present in all satellite cells in the postnatal fibers, not all satellite cells express *Pax3*. Whereas *Pax3* binds a subset of *Pax7* targets genes implicated in the regulation of embryonic functions and maintenance of an undifferentiated phenotype, *Pax7* specifically activates genes involved in the maintenance of adult satellite cell phenotype from regulation of proliferation to inhibition of differentiation (Soleimani et al., 2012). Although in adult satellite cells *MyoD* is not express in resting conditions, the use of a *MyoD*-iCre mouse strain with a lineage-tracing reporter allele, suggests that regardless of their anatomical localization and embryological origin, all the progenitors derived from satellite cells transcribe *MyoD* prenatally (Kanisicak, Mendez, Yamamoto, Yamamoto, & Goldhamer, 2009). Distinct population of $Myf5^{+}$ and $Myf5^{-}$ satellite cells are

present in adult muscles, as have been show in *Myf5-nlacZ* reporter mice and by the direct detection of *Myf5* protein levels (Kuang, Kuroda, Le Grand, & Rudnicki, 2007).

- Adult myogenesis

The muscular tissue is made up of specialized cells called fibers (myofibers) which are characterized by the presence of specific filaments of myosin and actin that give to this kind of cells the contractile capacity. Each myofiber is a syncytium developing from the fusion of mononucleated muscle cells (myoblasts) (Kim, Jin, Duan, & Chen, 2015). Every skeletal muscle is surrounded and protected by connective tissue at three different levels; *episysium*, *perimysium* and *endomysium*.

A large number of similarities can be described between embryonic and adult myogenesis, such as common transcription factors and signalling molecules (Bentzinger et al., 2014). During the adulthood, the regulatory pathways that control the embryonic myogenesis are reactivated during the muscle homeostasis and the regeneration process. Tissue regeneration requires the recruitment of an undifferentiated progenitors to the site on injury. In adult skeletal muscle, the satellite cells (SC) are the skeletal-muscle stem cells indispensable in this process. While SCs of the body and limbs arise from somites (Schienda et al., 2006) the SCs located in head muscles also originate from the cranial mesoderm. Under a physical stimulation situation, the SCs enter in an

activation stage, proliferate, differentiate and fuse to create multinucleated myofibers (Miersch et al., 2017).

Satellite cells depend of the same genetic hierarchy that governs embryonic myogenesis (Rudnicki, Le Grand, McKinnell, & Kuang, 2008) and represent 2-10% of the total myonuclei ($2 \cdot 10^5$ to $1 \cdot 10^6$ cells/g muscle) (White et al., 2010). These cells employ asymmetric division for self-maintenance where give rise one cell which is identically to the original stem cell and a second committed cell. In this way, with this kind of division allow the satellite cell pool be renewed at the same time that give rise to more committed myogenic progeny. This pool remains constant even after multiple traumas (Shi & Garry, 2006). The satellite cells population is very disparate, and the precise nature of the least committed adult muscle progenitor is extensively debated in the field (Bentzinger et al., 2014)(Dumont et al., 2015). The capacity of the satellite cells to balance quiescence, self-renewal and commitment is crucial to guarantee the life-long maintenance of skeletal muscle. Several studies support the idea that the heterogeneous population of satellite cells involve a subpopulation of committed satellite cells more disposed to progress into the myogenic lineage and a subpopulation of satellite cells that are more predisposed to undergo self-renewal (Rocheteau, Gayraud-Morel, Siegl-Cachedenier, Blasco, & Tajbakhsh, 2012).

Somatic stem cells depend on a particular situation called the “stem niche”, which is a localization in an organ that maintenances self-renewal of cells while blocking them form differentiation (Bentzinger et al., 2014). The satellite cells are placed closely to the myofiber under its basal membrane (**Figure 4**). Until their

activation by a muscle injury or other stimuli, their niche permit adult satellite cells to continue in a quiescent, non-proliferative state. In the same line to developmental processes have been described how during postnatal myogenesis, *Wnt* proteins have arisen as a key regulator of satellite cell commitment and self-renewal (Bentzinger et al., 2014).

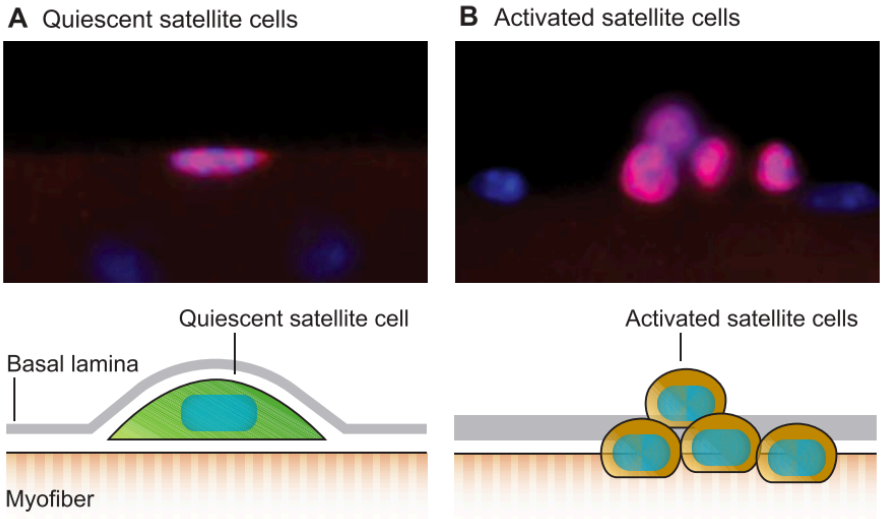

Figure 4: Satellite cells marked by Pax7 (red) in a quiescent stage (**A**) and in an activated stage (**B**) placed in their niche under its basal lamina. (Dumont et al., 2015)

Satellite cells are characterized by the expression of the *Pax7* transcription factor (**Figure 4**). After an injury situation or growth stimulus, the activated SCs (myoblasts) express the myogenic regulation factors *Myf5* and or/ *MyoD* and proliferate massively to generate enough myogenic progenitor for the muscle regeneration. Successively, *Pax7* expression is decreased in the myoblast and start to be activate myogenic regulator factors such myogenin (*MyoG*) and Myogenic Regulatory Factor 4 (*MRF4*) to exit the cell cycle, differentiate and fuse to form myofibers (**Figure 5**).

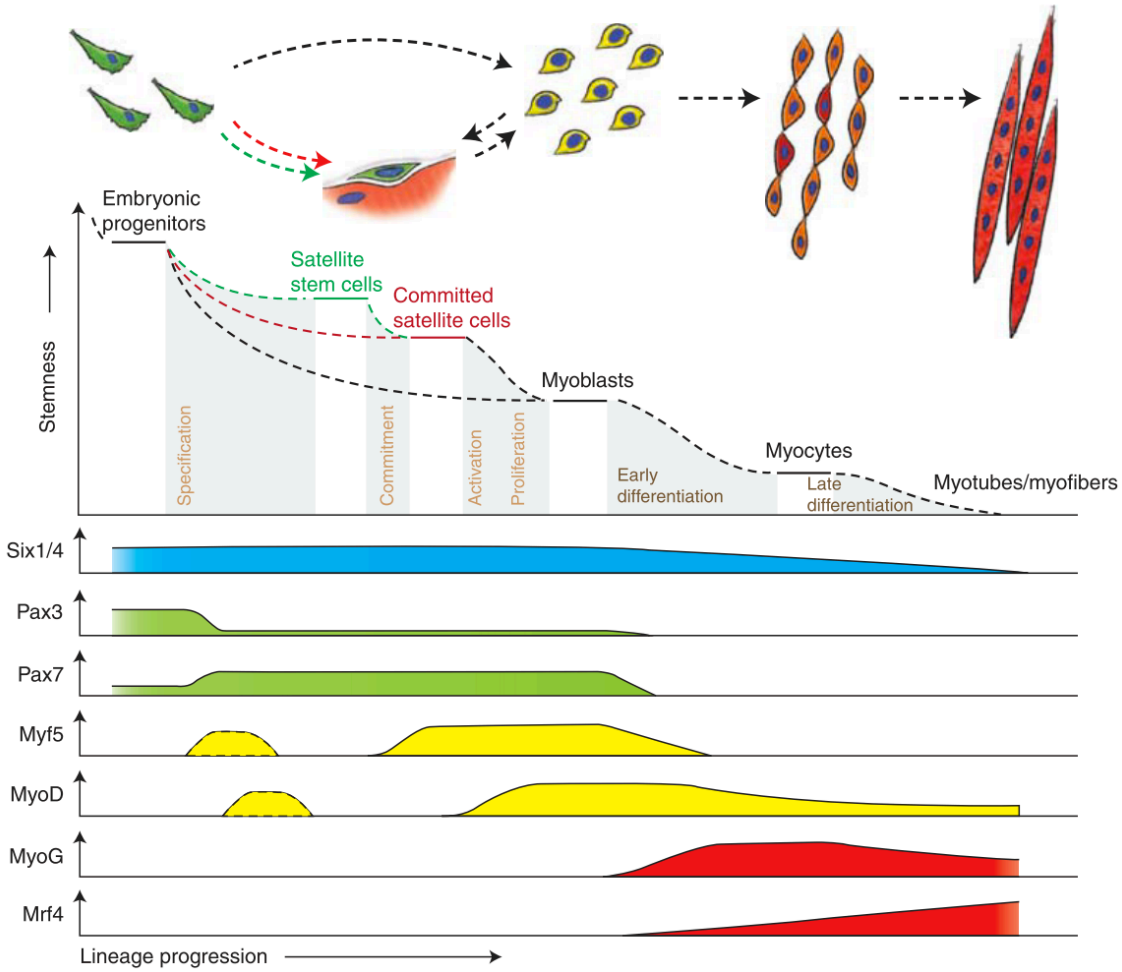

Figure 5: Schema of the transcription factor hierarchy that drives the myogenic lineage. During the embryonic myogenesis, muscle progenitor cells carry out muscle differentiation until myoblast missing the satellite cell stage. For the myocytes fusion and the myotube formation is required the expression of the terminal differentiation genes such *MyoG* and *MRF4* (Bentzinger et al., 2012).

Although adult satellite cells do not express *MyoD* in resting conditions, the progenitors of basically all adult satellite cells transcribe *MyoD* prenatally. Contrary to *MyoD* expression, distinct population of *Myf5*$^{+}$ and *Myf5*$^{-}$ satellite cells are present in the adult muscles (Dumont et al., 2015). Have been show that a subpopulation of around 10% of total satellite cells never expresses *Myf5* during development.

This heterogeneity in the developmental origins of satellite cells raises the possibility that subsets of satellite cells have self-renewal capacity and act as muscle stem cells. *Myf5*$^{-}$ cells posse higher self-renewal ability than *Myf5*$^{+}$ cells which are more prone to commit into myogenic progenitors. Satellite cells are a heterogeneous population that can be divided into subpopulations of committed satellite cells (predisposed to progress through the myogenic lineage once activated) as well as subpopulation of satellite stem cells (that are able to self-renew and maintain the satellite cell pool (Dumont et al., 2015)).

Muscle regeneration is characterized by different myogenic stages; activation, proliferation, differentiation and self-renewal/ return to quiescence **(Figure 6)**.

In resting adult muscles, satellite cells exist in an inactive state known as quiescence or the reversible G_0 stage. The ability of satellite cells to continue quiescence in the resting state is essential for the long-term conservation of the satellite cell pool. This quiescence state is different from the cell cycle exit observed prior to differentiation, the most notable variance being its reversibility, which permits cells to return to a proliferative state in reaction to injury (Dumont et al., 2015) **(Figure 6)**. Impairments in the ability of satellite cells to maintain quiescence reduce self-renewal capacity and muscle regeneration.

Notch pathway has emerged as a master regulator of satellite cell quiescence. Notch signalling activity is higher in quiescent satellite cells than in activated myogenic cells. This increased activity could be mediated by the interaction between the Notch ligand Delta1 which is expressed by myofibers,

and the Notch receptor which is present on satellite cells (Pisconti, Cornelison, Olguín, Antwine, & Olwin, 2010). *Notch1* and *Notch3* receptors is activated by the forkhead transcription factor *Foxo3* (Gopinath, Webb, Brunet, & Rando, 2014), which is also enriched in quiescent satellite cells. Upon binding of Notch ligand to its receptor, the Notch intracellular domain (NICD) is released and translocated into the nucleus where it interacts with recombining binding protein suppressor of hairless (*Rbpj*) and triggers the transcription of various genes, including those in the Hes and Hey families. During regeneration, downregulation of Notch is mandatory to allow myogenic cell lineage progression. Satellite cell quiescence is also maintained by microRNAs (miRNAs). The overall requirement of miRNAs in satellite cells quiescence is exemplified by their precocious activation after deletion of *Dicer*, the enzyme involved in pre-miRNA hairpin cleavage (Cheung et al., 2012). Muscle-specific miRNAs, such miR-1/206 and miR-133, are thought to maintain the myogenic program and facilitate the transition into differentiation (G. Ma et al., 2015). The lack of skeletal muscle phenotypes in the knockout of any single miR-1/206/133 cluster suggests that they share overlapping functions or that alternative mechanisms could circumvent their function in these specific knockout models. miR-489 is highly enriched in quiescent satellite cells where it post-transcriptionally represses the oncogene *Dek* and prevents cell cycle entry. The ability of satellite cells to maintain quiescence but to be poised for activation was shown to be at least partially due to the sequestration of miRNAs together with mRNAs (Dumont et al., 2015).

During the activation, mitogenic factors liberated following injury drive quiescent satellite cells to re-enter the cell cycle. The intermediate stage between

the G_0 quiescent and activated cell stated is called G_{Alert} (**Figure 6**). These "alert" satellite cells express a number of cell cycle genes similar to those expressed in activated satellite cells. This intermediate G_{Alert} state allows satellite cells to perform their first division faster than satellite cells in the G_0 state. This pre-activation state is particularly important because the first cell cycle takes much longer to complete than subsequent cell cycles, which indicates that exit from quiescence is a relatively slow process (Dumont et al., 2015). Satellite cells in the G_{Alert} state have greater regenerative potential. Release of hepatocyte growth factor (*Hgf*) at the site of injury could have a systemic effect and activate mTOR signalling in distant quiescent satellite cells, thereby driving their entry into the G_{Alert} state.

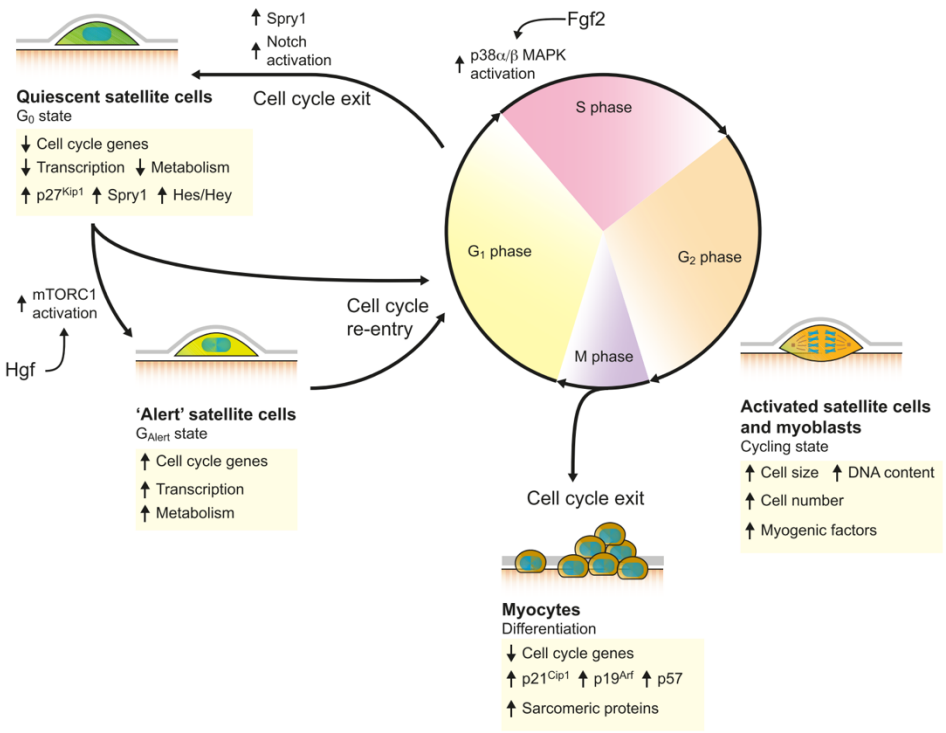

Figure 6: Regulation of the cell cycle in satellite cells. In resting conditions, intrinsic regulators of the cell cycle maintain satellite cells in a reversible and quiescent G_0 state. Activated satellite cells then re-enter the cell cycle, either directly or via an intermediate state referred to as G_{Alert}. After activation, satellite cells can exit the cell cycle and return to quiescence by upregulating *Spry1* or by increasing *Notch* signalling. Proliferating

myoblasts also exit the cell cycle to differentiate into myocytes and progress into the myogenic lineage (Dumont et al., 2015).

Once activated, satellite cells are then instructed to undergo differentiation (into myocytes) or to return to quiescence, two processes that involve cell cycle exit requires the upregulation of specific cyclin-dependent kinase inhibitors. The tyrosine kinase signalling inhibitor *Spry1* is expressed at low levels in activated satellite cells, but is upregulated in satellite cells returning to quiescence because *Spry1* promotes cell cycle exit by inhibiting the ERK signalling pathway (Shea et al., 2010). Activation of Notch signalling is also crucial for satellite cells to return to quiescence. During the asymmetric division of activated satellite stem cells, the daughter cell that is committed to differentiate expresses high levels of *Delta1*, whereas the daughter satellite cell expresses the *Notch3* receptor, which results in the activation of Notch signalling in this cell and promotes its return to quiescence. Notch activation also inhibits the expression of *MyoD* and promotes the expression of *Pax7*, this encouraging maintenance of the primitive satellite cell state (Dumont et al., 2015). In order for satellite cells to return to quiescence in vivo, cell-cell adhesion and ECM deposition are necessary checkpoints that are ultimately intrinsically regulated through autocrine mechanisms.

Activated satellite cells must also determine the cell fate of their daughter cells, in particular whether they self-renew or generate myogenic progenitors. Stem cell subpopulation are able to undergo both symmetric and asymmetric modes of self-renewal to maintain satellite cell numbers through repetitive rounds of regeneration.

Symmetric division is promoted by activation of the planar cell polarity pathway, which leads to the symmetric distribution of polarity effectors such as *Vangl2* in daughter cells (Le Grand, Jones, Seale, Scimè, & Rudnicki, 2009). Asymmetric division is characterized by the segregation of different cell fate determinants into the daughter cells. During the asymmetric division of *My5*$^{-}$ satellite stem cells, the *Nocth3* receptor is enriched in the daughter satellite stem cell, whereas the committed daughter cell inherits the Notch ligand Delta1, consistent with the role of Notch in promoting satellite cell return to quiescence and self-renewal. After asymmetric division, the ability of the two daughter cells to activate the myogenic program is also controlled by *Pax7* transcriptional activity. *Pax7* must be methylated by the arginine methyltransferase *Carm1* because during the asymmetric division, interaction between *Carm1* and *Pax7* in the nucleus of the committed daughter cell activates the transcriptional expression of *Myf5* (Dumont et al., 2015). Have been shown that *MyoD* is able to asymmetrically distribute in the two daughter cells, giving rise to one *Pax7*$^{+}$*MyoD*$^{-}$ reserve cell and one *Pax7*$^{-}$*MyoD*$^{+}$ committed myogenic cell.

The capacity of satellite cells to choose whether to perform symmetric or asymmetric division allows then to coordinate their activity with the needs of the regenerating muscle. An increased proportion of symmetric divisions would promote expansion of the satellite stem cell pool, whereas increased asymmetric division would favour the generation of myogenic progenitors and maintenance of the stem cell pool. In regenerating muscle, satellite cell symmetric division occur mostly in a planar orientation, whereas asymmetric divisions occur in a

apicobasal orientation, suggesting that cell division orientation is a decisive factor in cell fate determination (Dumont et al., 2015).

3. Pitx2 and myogenesis

Homeodomain proteins are one of the most important group of proteins/transcription factors regulating plan of body structure and organogenesis in eukaryotes. Homeodomain protein are characterized by specific 60 amino acid long helix-turn-helix DNA binding homeodomain motif. The homeodomain is a very highly conserved structure consists of three helical regions folded into a tight globular structure that binds a 5'-TAAT-3' core motif. The DNA sequence that encodes the homeodomain is called the "homeobox".

The Pitx proteins belong to the bicoid-related subclass of homeodomain proteins with the lysine residue at position nine of the third helix, being the major determinant of DNA and RNA binding specificity and are highly conserved at the amino acid level at the C-terminal while significantly diverging at the N-terminal (Gage, Suh, & Camper, 1999).

The homeotic transcription factor PITX2 (Pituitary homeobox 2 or Paired-like homeodomain transcription factor 2) have arisen in the last two decades like a key element during the cardiac and skeletal myogenesis. The Pitx2 expression have been described in different tissues and organ such in the lateral plate mesoderm, mesenchyme of the eye, the first and second branchial arches,

pituitary gland, the fore and hind limbs as well as at somite stages E8.5 and E10.5 in mouse at dermomyotome level (Hernandez-Torres et al., 2017). Furthermore, is proposed in left-right asymmetry as the molecular transducer of embryonic left-right signalling during early developmental stages at the level of organs such as heart. The absence of Pitx2 in mice is characterized by body-wall closure and ocular defects, right pulmonary isomerism and defects in cardiac, tooth, and pituitary development (Hernandez-Torres et al., 2017).

Pitx2 gene is placed on chromosome 3 (3G3; 3 57.84 cM) in the mouse (Gage et al., 1999) and consists of six exonic sequences separated by five introns (Knopp, Figeac, Fortier, Moyle, & Zammit, 2013) (**Figure 7**). Three isoforms can be transcribed from this gene; *Pitx2a* and *Pitx2b*, which use the same promotor and *Pitx2c* which use an alternative promotor placed upstream the exon 4 (Schweickert, Campione, Steinbeisser, & Blum, 2000) a left side-specific enhancer (ASE) upstream of exon 6. These three isoforms share exons 5 and 6, but differ in other; exon 3 is Pitx2b specific, while exon 4 is Pitx2c specific. In human, Pitx2 is placed in the 4q25 locus and generate a new isoform (Pitx2d) using an alternative promoter of Pitx2c and differential splicing.

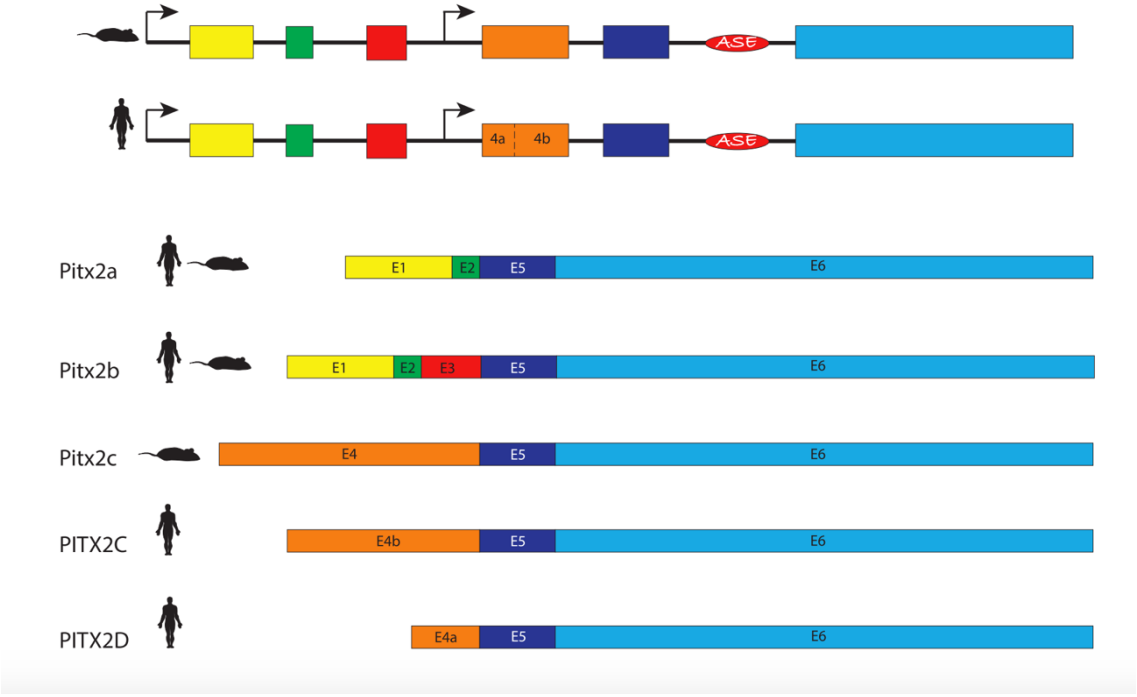

Figure 7: The Pitx2 gene: Genomic structure and splice variants in the mouse. (A) Genomic structure. (B) Pitx2a isoform. (C) Pitx2b isoform. (D) Pitx2c isoform. The arrows in (A) indicate the promoters used by the Pitx2a and Pitx2b isoforms (P2, blue arrow) and Pitx2c (P1, red arrow). ASE: Asymmetric enhancer. Exons: E followed by the corresponding number. The coding region (ORF) and the region of the Homeodomain (HD) as well as the start (AUG) and end (UGA) codons of the translation are indicated.

- Pitx2 and skeletal development

Pitx2 is detected on an early skeletal muscle structure, the dermomyotomes, where co-localize with the muscle specification marker *Pax3*. *Pax3* is a key role player during the delamination and migration of the somitic muscle progenitor cells from the dermomyotomes to the emerging limb buds (Tajbakhsh, Rocancourt, Cossu, & Buckingham, 2016). Indeed, the PITX2 protein is detected here at E10.25 in *Pax3*$^{+}$ *Myod1*$^{+}$ myoblasts of the ventrolateral dermomyotome at forelimb levels, showing an expression pattern similar to PAX3

and MYOD (Marcil, 2003). Start in other somites developments in both the rostral and caudal direction from this place, and is closely associated with adjacent apposition of a non-somitic Pitx2^{+} cell population that shows to originate from an early body wall *Pitx2* expression domain (C. N. Chang, Singh, Gross, & Kioussi, 2019). Six hours later, *Pitx2*$^{+}$*Pax3*$^{+}$*Myod1*$^{+}$ cells are also observed intermixed with the central myotome, where *Myod1*$^{+}$ cells are known to secondarily colonize the primary myotome (C. N. Chang et al., 2019). Early *Lbx1*$^{+}$*Pax3*$^{+}$*Myod1*$^{-}$ limb muscle precursors delaminate from forelimb level somites at E9.25 and migrate into the limb. The dorsal and ventral muscle masses of E10.25 forelimbs contain mostly of *Pax3*$^{+}$*Lbx1*$^{+}$*; Myod1*$^{+}$ *and MyoG*$^{+}$ cells (C. N. Chang et al., 2019). At this time, *Pitx2*$^{+}$ cells start to appear in the forelimb bud along the interior surface of the muscle masses at E10.25. They co-express *Pax3* and *Myod1*, but not *Pax7*, and by E10.75 they are intermingled with muscle masses. At E10.5, a few *Pax7*$^{+}$ cells are observed in the forelimb, but by E11.5 the limb muscle masses contain *Pitx2*$^{+}$ mixtures of *Pax3*$^{+}$*Pax7*$^{-}$, *Pax3*$^{+}$*Pax7*$^{+}$ and *Pax3*$^{-}$*Pax7*$^{+}$ cells. The absence of *Pitx2* from early Pax3^{+}Pax7^{-} limb muscle precursors and its presence later is consistent with the idea *Pitx2* is expressed in the fetal muscle progenitor lineage, but not in the preceding embryonic muscle progenitor lineage. This fetal muscle lineage derives from *Pax3*$^{+}$*Pax7*$^{-}$ progenitors that activate *Pax7* expression in the limb bud (C. N. Chang et al., 2019).

In this way, only subsets of *Pitx2*$^{+}$ cells are marked by *Pax3* and the muscle-regulatory factors (MRFs) in these regions, and essentially all *Pitx2*$^{+}$ cells placed in this region express as a minimum one of these myogenic markers (Shih, Gross, & Kioussi, 2007). However, have been describe how the PAX3^{+} cells that

have concluded migration until the proximal limb bud express PITX2 at the same time, while not all PITX2^{+} cells expressed PAX3, suggesting the role of *Pitx2* like a key player within the molecular pathways which orchestrate muscle-progenitor fate (L'Honoré et al., 2007). In the same line, have been showed how *MyoD* is regulates by PITX2 through binding to its core enhancer, describing in what way the *Pitx2*$^{-/-}$ mice display a delay in the myogenic differentiation and a *MyoD* down regulation in the limb buds (L'Honoré, Ouimette, Lavertu-Jolin, & Drouin, 2010).

Myf5 and *Myf6* control *MyoD* expression during the early limb-bud myogenesis collaborating with *Pitx2*. Nevertheless, *MyoD* expression in the myotome is not delayed in Pitx2$^{-/-}$ mice. It is necessary the inactivation of *Myf5* and/or *Myf6* in the *Pixt2*$^{-/-}$ to obtain a similar loss of *MyoD* expression at myotome level than at the limbs level (L'Honore et al., 2010). These evidences suggest that during myotome development, PITX2 is helped by MYF5 and/or MYF6 to control *Myod* expression (**Figure 8**). Furthermore, have been suggested that *Pitx2* is downstream of *Pax3* during myotome development because *Splotch* mice, which are *Pax3* mutants, show *Pitx2* deficit expression at myotome but not in the adjacent mesenschyme (L'Honoré et al., 2010). In gain-of-function screens for PAX3 targets, they found an up-regulation of *Pitx2* in somites but not in limb buds. These results indicate that, at least in the myotome, *Pitx2* could be acting in parallel with *Myf5* downstream of *Pax3*. However, not all PITX2^{+} were positive for PAX3, and limb expression of *Pitx2* precedes *Myf5* (L'Honoré et al., 2010).

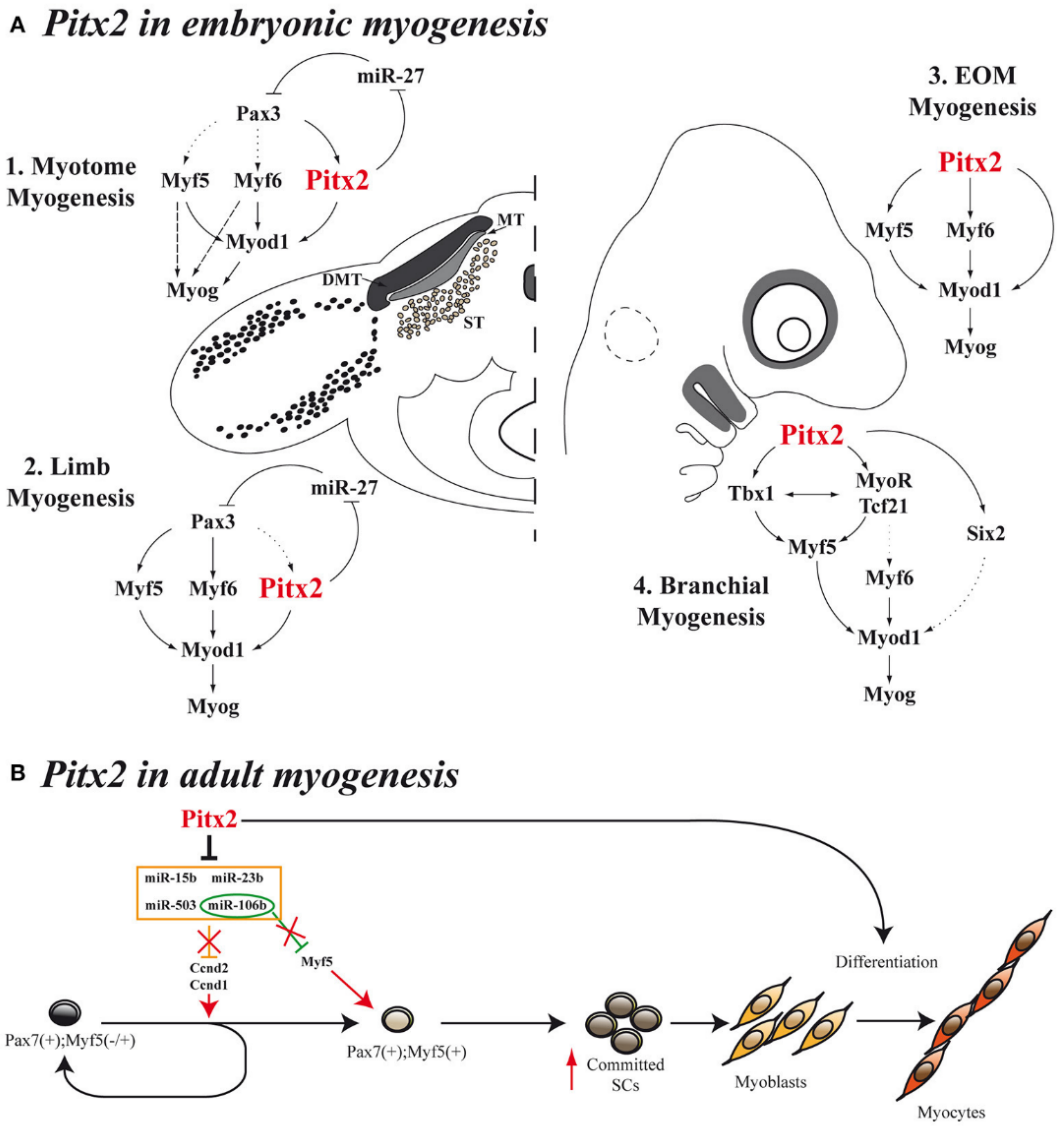

Figure 8: Models for Pitx2 functions in myogenesis. (A) During embryonic stages, Pitx2 contribution is different depending on the initial muscle-cell clusters [myotome myogenesis (A1), limb myogenesis (A2), EOM myogenesis (A3), or branchial myogenesis (A4)]. First myocytes of the myotome differentiate through Myf5 and/or Myf6 directly to Myog without turning on MyoD. This is represented by dashed arrows. Dotted arrows represent direct molecular relationships that still remain elusive (B) Proposed model for Pitx2 in adult myogenesis promoting activation and commitment of SCs (Hernandez-Torres et al., 2017).

The fetal muscle progenitor lineage only appears to be responsive to ß-catenin as myofiber assembly proceeds in the limb muscle of the fetal period. ß-catenin signalling increases expression of the Pitx2-expressing organs (including

muscle), acts together with Pitx2 protein to remove deacetylases from Pitx2-bound, suppressed promoters, and activates a serial recruitment of coactivators to Pitx2-bound promoters of growth control genes acting at early to mid G1. Wnt signalling, acting through Pitx2 to increase proliferation. The ß-catenin responsiveness in “fetal” but not “embryonic” muscle cells is also coherent with the model that Pitx2 plays a role in former rather than the latter (C. N. Chang et al., 2019).

Pitx2 is target of the *Wnt/Dvl2/beta-catenin* pathway controlling proliferation by regulating expression of *Ccnd1, Ccnd2* and *c-Myc* (Kioussi et al., 2011). Previous results from our laboratory have demonstrated that the overexpression of Pitx2c in Sol8 cells increase the proliferative capacity of the myoblasts and completely blocked terminal differentiation, essentially because this led to maintained high levels of *Pax3* expression (Martínez-Fernandez et al., 2006). In the same way, in vivo experiments in chicken embryos showed a reduction of differentiated myocytes/myofibers number in somites in *Pitx2* loss of function, while *Pitx2* overexpression led to a raise of myocytes/myofibers numbers, and more concretely at epaxial level of the myotome (Abu-Elmagd et al., 2010). According to that, have been described using *Pitx2*$^{-/-}$ embryos how *Pitx2c* plays a crucial function in the controlling the equilibrium between proliferation and differentiation during limb and trunk myogenesis. This control is carry out by balancing *Pax3*$^{+}$/*Pax7*$^{+}$ myogenic population *in vivo* together with regulating key myogenic transcription factors such as *Pax3* through the repression of *miR-27* (Lozano-Velasco et al., 2011).

The adult skeletal muscle homeostasis depends of a special stem cells localized under the basal laminate of every fiber called satellite cells. All Pitx2 isoform can be detected in myoblast derivative of satellite cells (Ono, Boldrin, Knopp, Morgan, & Zammit, 2010). While in the proliferative stage, the SCs express very low levels of *Pitx2a*, *Pitx2b*, and *Pitx2c* isoforms, these levels increase during the early stages of myogenic differentiation. In this way, the expression of any *Pitx2* isoform inhibited SC proliferation, leading the cells to myogenic differentiation (Knopp et al., 2013). Have been describe in our laboratory that *Pitx2c* expression is higher in early-activated SCs than in long-term activated ones, and our in vitro *Pitx2c* gain-of- function experiments have revealed that *Pitx2c* stimulates *Ccnd1* and *Ccnd2* expression, accelerating cell proliferation during early satellite-cell activation (Lozano-Velasco et al., 2015). Also, we have demonstrated the existence of the Pitx2-miRNA pathway on SCs proliferation where Pitx2c mediate downregulation of the miRNAs miR-15b, miR-106b, miR-23b, and miR-503 (Figure 7B). This Pitx2-miRNA pathway orchestrate the expression of crucial regulatory cell-cycle genes in early-activated SCs shown a function of Pitx2 in satellite- cell activation (Lozano-Velasco et al., 2015). Besides, Myf5 can increase expression by Pitx2c by mean of down-regulating miR-106b (**Figure 8B**), thereby the $Myf5^{+}$ satellite-cell population is expanded and revealing a role for Pitx2c in stimulating satellite-cell populations more primed for myogenic commitment (Lozano-Velasco et al., 2015).

- Pitx2 and cardiac development

The heart is an asymmetric organ which is partitioned in two halves, driving double blood circulation. The atrial and ventricular chambers, as well as the great vessels, in the left and right halves of the heart have distinct anatomical features, which are adapted to the systemic and pulmonary circulation. The position and alignment of the cardiac segments are crucial for heart function. This is prefigured in the embryo, during the process of heart looping. The rightward looping of the heart primordium is the first sign of asymmetric organogenesis. It corresponds to the transformation of a straight cardiac tube into a loop. By determining the relative position of cardiac chambers, heart looping in amniotes is essential for the asymmetric partition of the heart (Desgrange, Garrec, & Meilhac, 2018).

The cardiac development is an elaborate morphogenetic process that involve different cells lineages. It begins when the precardiogenic mesoderm is specified (Anderson, Webb, Brown, Lamers, & Moorman, 2003). The bilateral cardiogenic subpopulations merge at the embryonic midline shaping a linear cardiac tube (García-Martinez, V., 1993). (**Figure 9**) At this stage of development, the heart is symmetrical, but shortly subsequently, bilateral asymmetry is established as the cardiac tube bulges on its ventral side and then twists rightward. Future embryonic atrial and ventricular chambers become soon established with a common inlet, atrioventricular canal and outlet segments (Moorman & Christoffels, 2003) (**Figure 9**). These cardiac regions are derivative from distinct cardiogenic cell subpopulations, the first heart field (FHF) and the second heart field (SHF). The formation of a series of cardiac septa separate into systemic and venous components all cardiac chambers and segments.

Ventricular chambers are divided by the establishment of interventricular muscular and membranous septa, and distinct aortic and pulmonary trunks are divided with the formation of the outflow track septum (Moorman & Christoffels, 2003).

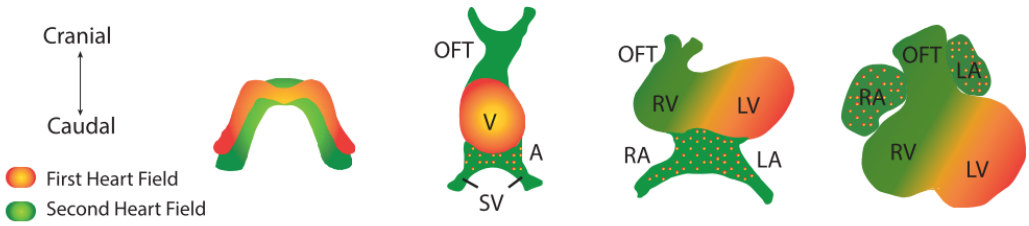

Figure 9: Schematic representation of the developing heart delineating distinct developmental stages (Franco, Sedmera, & Lozano-Velasco, 2017).

The exactly mechanism that orchestrate cardiovascular development is not completely understood. A large number of transcription factors has been identified during cardiogenesis. *Hand1* and *Hand2* transcription factors display ventricular chamber-specific expression in the systemic and venous components (Srivastava, 2006). Tbx1 is delimited to the arterial pole without significant influence to the developing myocardial component, but essential for aortic arch formation and remodelling (Baldini, Fulcoli, & Illingworth, 2017). *Tbx2* is restricted to small areas of the developing heart, sus as the outflow tract and atrioventricular canal with a similar pattern to Tbx3. Tbx5 is confined to the systemic ventricle, as well as both atrial chambers whereas Tbx18 is limited to a minor subset of ventricular cardiomyocites, as well as to the venous pole of the heart (Greulich, Rudat, & Kispert, 2011).

Pitx2 expression is already present in the developing embryo soon after gastrulation. The first signs of bilateral asymmetry are detected while the developing heart bulges ventrally and bends to the right. Large of these asymmetric regulators present left/right differential expression in the lateral plate mesoderm (LPM), while others already display asymmetric expression in the embryonic midline left/right organizer (LRO), with the developing node (Franco et al., 2017). The node plays an essential role in establishing left/right symmetry break and particularly node cilia and node cilia-related flow. The left/right symmetric break is conserved morphogenetic process in most vertebrate phyla having a core signalling cascade represented by *Nodal* > *Pitx2* with different variable players in distinct species. In this way, early during embryogenesis, *Pitx2* is directly regulated by the Nodal-mediated left-right asymmetry (LRA) pathway, which confers lift-sided morphogenesis onto all organs in the body such heart, lug and gut, among others (Franco et al., 2017). *Nodal* is a Tgfβ family signalling molecule that participates in the early break in symmetry in mammalian embryos and *Nodal*-mediated regulation of *Pitx2* takes place via an asymmetric cis-regulatory element located within the *Pitx2* gene body. As a downstream effector of LRA signalling, Pitx2 plays an essential function at the late stages of LRA (Hill et al., 2019).

The left LPM provides different signals controlling embryonic left-right asymmetry. *Pitx2* expression is confined to left LPM in chick, frog and mouse, as well as the cardiogenic precursors of the left SHF (Nowotschin et al., 2006). During development, *Pitx2* continues to be expressed asymmetrically in several organs. Over-expression studies in Xenopus and chicken demonstrate that *Pitx2*

is important in the determination of vertebrate heart and gut looping (Franco et al., 2017).

Pitx2 isoforms distinctly contribute to the regulation of left-right asymmetry. *Pitx2a*, *Pitx2b* and *Pitx2c* are symmetrically expressed in the head at the beginning of development, but *Pitx2c* in only expressed asymmetrically in the LPM from two to four somite stages in the mouse. During development and adulthood, *Pitx2c* expression still remains in the developing heart (Chinchilla et al., 2011). Experimental models of gain and loss of function demonstrated that *Pitx2* is dispensable in driving looping directionality in mice (Franco et al., 2017).

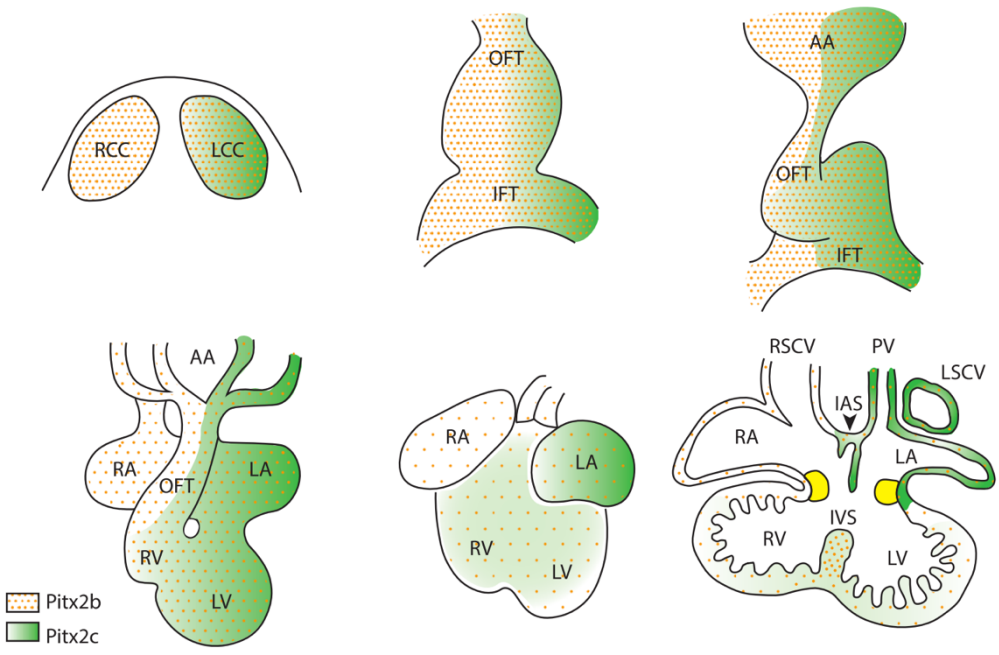

Figure 10: Schematic representation of the Pitx2 isoform (Pitx2b and Pitx2c) expression patterns during cardiac development (Franco et al., 2017).

During heart development, *Pitx2* has two main functions: morphogenesis of the outflow tract (OFT) and lift-right specification of the atria. *Pitx2* is required for complete OFT septation (Liu, Liu, Lu, Brown, & Martin, 2001). Conditional

mutagenesis revealed that *Pitx2* function in the second heart field (SHF) to regulate proliferation of OFT myocardium, and that *Pitx2* was dispensable in the cardiac neural crest. In the left atrium, Pitx2 confers left atrial morphology (Liu et al., 2001). *Pitx2* null mutant left atria have right-sided morphologic characteristics including venous valves and trabeculated myocardium.

In addition to OFT morphogenesis, *Pitx2* has also been implicated in atrioventricular valve development. Morphogenesis of both the AV cushion and the dorsal mesenchymal protrusion are defective in *Pitx2* null embryos, suggesting an essential function for *Pitx2* during ventricular septation (Hill et al., 2019).

On E10.5 *Pitx2* is highly expressed and atrial septation, valvulogenesis, atrioventricular junction formation and OFT remodeling begin to occur.

Chapter II:

Hypotheses and Objectives

Chapter II: Hypotheses and Objectives

Hypothesis: Although several previous evidences have revealed that the transcription factor *Pitx2* might be a player within the molecular pathways controlling somite-derived muscle progenitors' fate; the specific role of *Pitx2* in the development of trunk muscles remains unsolved. In this Doctoral Thesis we plan to investigate the hypothesis that *Pitx2* might play a sequential role at different stages of somite-derived myogenesis.

General Objective: To explore the role of *Pitx2* in multipotent $Pax3^{+}$ muscle progenitors and in myogenic committed $Myf5^{+}$ progenitors.

Specific Objectives:

Objective 1: To investigate the role of *Pitx2* in multipotent $Pax3^{+}$ muscle progenitors by generating the conditional *Pitx2* mutant mice $Pax3Cre^{+/-}/Pitx2^{loxp/loxp}$.

Objective 2: To investigate the role of *Pitx2* in myogenic committed $Myf5^{+}$ progenitors by generating the conditional *Pitx2* mutant mice $Myf5Cre^{+/-}/Pitx2^{loxp/loxp}$.

Chapter III: Materials and Methods

Chapter III: Materials and Methods

1. Generation of conditional tissue-specific null mutant mice:

Animals procedures were approved by the University of Jaen Ethics Committee, and it was conducted according the national and European community guidelines regulations for animal care and handling. All mice were maintained inside a barrier facility where food and water were administered *ad libitum.*

B6;129-Pax3tm1(cre)Joe/J (ref. 005549) transgenic mice were supplied by The Jackson Laboratory. Myf5Cre+ were kindly supplied by Victor Luis Ruiz Pérez, (Instituto de Investigaciones Biomédicas de Madrid). Both transgenic mice were crossed into homozygous Pitx2 floxed mice kindly supplied by Marina Campione (Pathophysiology of Striated Muscle Group, Universitá degli Studi di Padova). $Pax3Cre^{+/-}$ $Pitx2^{fl+/-}$ heterozygotes were backcrossed. In the same way, $Myf5Cre^{+/-}$ $Pitx2^{fl+/-}$ and $Myf5Cre^{+/-}$ $Pitx2^{fl+/+}$ were backcrossed too. The littermates were PCR screened with Pitx2- and Cre-specific primers (Table 1). $Pitx2^{fl+/+}$ homozygotes mice were selected as wild-type controls. All mice were maintained inside a barrier facility, and experiments were performed in accordance with University of Jaen regulations for animal care and handling.

2. PCR genotyping:

The DNA was isolated from different tissues depending of the animal age. For adult animals, ear DNA was used for genotyping by PCR while for new-borns the DNA was isolated from the tail and from the yolk sac for embryo stages. One microliter of neutralized DNA samples was used for PCR reaction using DreamTaq DNA Polymerase (ThermoFisher) with buffers supplied by the manufacturer with 0.4 mM dNTPs and 4 mM $MgCl_2$. The PCR products were resolved in agarose gel (2% for Pitx2 PCR product and 1,5% for $Pax3Cre^{+}$ and $Myf5Cre^{+}$ PCR product), stained with 0.5 µg ml^{-1} ethidium bromide (Gibco), and digitally imaged for record keeping.

Primer	Sequence	
Pitx2ln4_f01	GGTGGGGGTGTCTGTAAAAC	$Pitx2^{fl+/-}$
Pitx2ln5_r01	CAAGCCTTGCGTGTTTCTG	$Pitx2^{fl+/-}$
oIMR6977	CTGCACTCAAGGGACTCCTC	$Pax3Cre^{+/-}$
oIMR6978	GTGAAGGCGAGACGAAAAAG	$Pax3Cre^{+/-}$
oIMR9074	AGGCAAATTTTGGTGTACGG	$Pax3Cre^{+/-}$
AF-Cre1	CGGTCGATGCAACGAGTGATGAGG	$Myf5Cre^{+/-}$
AF-Cre2	CCAGAGACGGAAATCCATCGCTCG	$Myf5Cre^{+/-}$

Table 1: Genotyping primers

3. Cardiotoxin (CTX) and muscle injury:

Cardiotoxin (Sigma) was prepared by dissolving a freshly opened tube in PBS at 10 µM. The solution was divided into Eppendorf tubes as 50 µl aliquot stocks, flash frozen, and stored at -80 °C. Each tube was thawed fresh before injection and not re-used. Animals were anaesthetized by intraperitoneal injection of ketamine/xylazine. The tibialis anterior muscles of 4 months old mice were injected with 50 µl of cardiotoxin using an insulin needle. Cardiotoxin animals were kept on a warming blanket until recovery before being returned to a normal cage rack. For immunohistochemistry and histological analysis, the animals were killed and TA muscles were collected at 3, 7, 15 and 30 days after cardiotoxin injection.

4. Exercise tolerance test:

An exhaustion treadmill was performed to evaluate the endurance of the mice by using the motorized treadmill LE8708 single mouse, Treadmill, PanLab, Harvard Apparatus supplied with shocker plate as described elsewhere (Benchaouir et al., 2007). The treadmill was run at an inclination of 0° at 5 m/min for 5 min, after which the speed was increased 1 m/min every minute. The test was then stopped when the mouse remained on the shocker plate for 20 seconds without any attempt to reengage the treadmill. Distance (meters) and the time to exhaustion (expressed in minutes) was determined. For immunohistochemistry and histological analysis, the animals were killed and TA muscles were collected, frozen in liquid nitrogen cooled isopentane for sectioning and preserved at -80ºC.

5. Tibialis anterior muscle collection:

Mice were sacrificed by cervical dislocation. TA were collected and frozen in liquid nitrogen-cooled isopentane for sectioning or in liquid nitrogen for total RNA isolation and store at -80ºC.

For histological analysis tissue specimens were sliced using a cryostat microtome to 10 µm thick and mounted onto Thermo Scientific™ SuperFrost Ultra Plus™ Adhesion Slides.

6. Whole-mount in situ hybridization:

Mouse embryos from E10.5 and E12.5 were fixed and store in 4% PFA at 4ºC. Complementary RNA digoxigenin-labelled probes of Pax3, Pax7, Myf5, MyoD and MyoG were generated using standard protocols. Embryos head were holed carefully to avoid the trapping. The embryos were washed in PBT (PBS x10, 0,1% Tween® 20) and MetOH to be dehydrated before be bleached (6% H_2O_2/MetOH) in darkness. After be rehydrated with PBT, the embryos were treated with Proteinase K and postfix (0,2% glutaraldehyde 4% PFA). Prehybridization washes (50% Formamide, 25% SSC x20 pH4.5, 2% SDS, 2% BBR, 0,025% yeast tRNA, 1% Heparin) and hybridization were carried out at 70ºC with following washes (50% Formamide, 20% SSC x20 pH4.5, 2% SDS) at the same temperature. The staining (0,15% NBT, 0,2% BCIP on NTMT) was realized at RT.

7. Inmunohistochemistry

Series of 10 µm transverse cryosections cut over the mouse tibialis anterior muscles (TA) length were examined by immunohistochemical staining. The tissue sections were fixed in 4% PFA for 10 min at RT. For PAX7, immunostaining, epitopes were unmasked in citrate buffer (10 mM Sodium Citrate, 0.05% Tween-20, pH 6.0) in a pre-heat water bath 30 min at 95ºC. Afterwards, all samples were washed twice in PBS and incubated in TBSA-BSAT (10 mM Tris, 0.9% NaCl, 0.02% sodium azide, 2% BSA and 0.1% Triton X-100) at RT for 30 min. The antibodies were diluted to 5 µg/µl into TBSA-BSAT and incubated overnight at 4°C in a humidified chamber. The antibody solutions were removed and the samples were washed with TBSA-BSAT twice at RT. Alexa-conjugated secondary antibodies (Thermo Fisher Scientific, 1/200) were applied to the samples and incubated for 2 hours at RT. The antibody solutions were then removed and washed two times in PBS. Finally, sections were incubated with DAPI in PBS 1/2000 for 15 min at RT. The samples were mounted with Hydromount (National Diagnosis. HS-106) after two PBS and two H_2O milliQ washes.

For tissue samples from paraffin, the slides were heated at 60ºC during 10 minutes and dewax in xylene washes and rehydrated in diminishing alcohol washes before be blocked with TBSA solution.

Antibody	Source	Identifier
Rabbit Anti-Laminin	Sigma-Aldrich	L9393; RRID: AB_477163
Mouse Anti-MF20	Developmental Studies Hybridoma Bank (DSHB)	RRID: AB_2147781
Mouse Anti-Pax7	Developmental Studies Hybridoma Bank (DSHB)	RRID: AB_528428
Goat Anti-Pax3 (C-20)	Santa Cruz Biotechnology	Sc-34916
Mouse Anti-Desmin	Sigma-Aldrich	D1033
AlexaFluor® Goat Anti-rabbit 546	Thermo Fisher Scientific	A-11035; RRID: AB_2534093
AlexaFluor® Goat Anti-mouse 488	Thermo Fisher Scientific	A-11001; RRID: AB_2534069
DAPI	Thermo Fisher Scientific	D1306; RRID: AB_2629482

Table 2: Antibodies

8. Cross-section area:

To analyse the size of skeletal muscle fibers, we measured the fibre cross-sectional area as described (Moresi et al., 2009) using ImageJ software on adult and neonatal TA sliced.

9. Total RNA extraction and reverse transcription

Muscle total RNA was extracted from treated tibialis anterior muscles by using Direct-zol™ RNA MiniPrep-Zymo Research kit (Zymo Research, R2050) following manufacturer's instructions. One microgram of total RNA was reverse transcribed using Maxima First Strand cDNA Synthesis Kit (Thermo Fisher, K1642) following manufacturer's instructions. As a reverse transcription negative

control, each sample was subjected to the same process without reverse transcriptase.

10. qRT-PCR analyses:

Real-time PCR was performed by using an MxPro Mx3005p PCR thermal cycler (Stratagene, Spain) using SsoFast™ EvaGreen® Supermix (Bio-Rad, 1725201) and primers listed in supplementary information Table 3. The relative level of expression of each gene was calculated as the ratio of the extrapolated levels of expression of each gene and Gapdh and Gusb genes as mRNA normalizers. Each PCR reaction was performed in triplicate and repeated at least in three different biological samples to have a representative average. Relative measurements were calculated as described Pfaffl MW

qPCR program consisted in 95ºC for 30 seconds (initial denaturalization), followed by 40 cycles of 95ºC for 5 seconds (denaturalization); 60ºC for 10 seconds (annealing) and 75ºC for 7 seconds (extension). Finally melt curves were determined by an initial step of 95ºC for 5 seconds followed by 0,5ºC increments for 7 seconds from 65 to 95ºC. The relative level of expression of each gene was calculated as the ratio of the extrapolated levels of expression of each gene and *Gapdh* and *Gusb* genes as normalizers.

Gene	Primer sequence
Gapdh (NM_008084.2)	**MmGapdhF:** GGCATTGCTCTCAATGACAA
	MmGapdhR: TGTGAGGGAGATGCTCAGTG
Gusb (NM_010368.1)	**MmGusbF:** ACGCATCAGAAGCCGATTAT
	MmGusbR: ACTCTCAGCGGTGACTGGTT
Myf5 (NM_008656.5)	**MmMyf5F:** TGAGGGAACAGGTGGAGAAC
	MmMyf5R: AGCTGGACACGGAGCTTTTA
Myod1 (NM_010866.2)	**MmMef2cF:** TGGTTTCCGTAGCAACTCCT
	MmMef2cR: AGTTACAGAGCCGAGGTGGA
Pitx2c (NM_001042502.1)	**MmPitx2cF:** CCTCACCCTTCTGTCACCAT
	MmPitx2cR: GCCCACATCCTCATTCTTTC
Pax3 (IsoaNM_008781.4, Isob NM_001159520.1)	**MmPax7F:** TCTTACTGCCCACCCACCTA
	MmPax7R: GTGGACAGGCTCACGTTTTT
Pax7 (NM_011039.2)	**MmPax7F:** TCTTACTGCCCACCCACCTA
	MmPax7R: GTGGACAGGCTCACGTTTTT

Table 3: Primers for qPCR analysis

11. Quantification and statistical analysis

For comparison between two groups, two- tailed paired, unpaired Student's t tests were performed to calculate p-values and to determine statistically significant differences. The number of independent experimental replications (n value ≥ 3: mice, experiments, wells or counted cells/muscles). Mean ± SD and statistical test (p-value) are reported in each corresponding figure legend. All statistical analyses were performed with GraphPad Prism. Image were processed for quantification with ImageJ software.

12. Electroporation:

Eggs are incubated with the blunt end up in a humidified incubator at 37ºC. To obtain HH10 embryos we incubated fertile eggs for approximately 38h.

Remove shell pieces until embryo is easily accessible and in a shallow angle inject ink-mix (1:500 PBS/ Pen Strep (PS) on with Indian ink beneath the embryo for contrast and apply 2 drops PBS/PS-solution on top to increase elasticity of extra-embryonic tissues (EET).

Use syringe needle to cut open the vitelline membrane. Perform injection in area of interest using a needle for microinjection (borosilicate glass capillaries 1.00 mm O.D. × 0.78 mm I.D.). Load needle with ~1.5 µl Morpholino at 1 µM using Microloader™ (Eppendorf) and mount onto microinjector (20 Volts, 4 pulses, 950 milliseconds space, 50 milliseconds/pulse). Remove needle and visually confirm injection.

Slide the needle of the large syringe down along the inside of the egg shell and remove albumen until the embryo is sufficiently lowered and will not touch the sealing tape.

Apply a few drops PBS/PS-solution. Seal the egg using clear adhesive tape and Return the egg to an incubator immediately. Collect the embryos after 24h or 48h.

Chapter IV:

Results

Chapter IV: Results

1. Loss of Pitx2 in Pax3^{+} multipotent myogenic progenitors decrease migration of Pax3^{+} cells and led to perinatal lethality

To better understand the role *Pitx2* in Pax3^{+} multipotent myogenic progenitors we have generated *Pax3Cre*$^{+/-}$/Pitx2$^{loxp/loxp}$ conditional mutant mice. Deletion of Pitx2 in Pax3^{+} cells lead to perinatal lethality since the number of Pax3Cre-Pitx2-loxp homozygous mutants dramatically decrease around day one after birth and no homozygous mice survive after day 1/day 2 afterbirth indicating perinatal lethality **(Figure 11).**

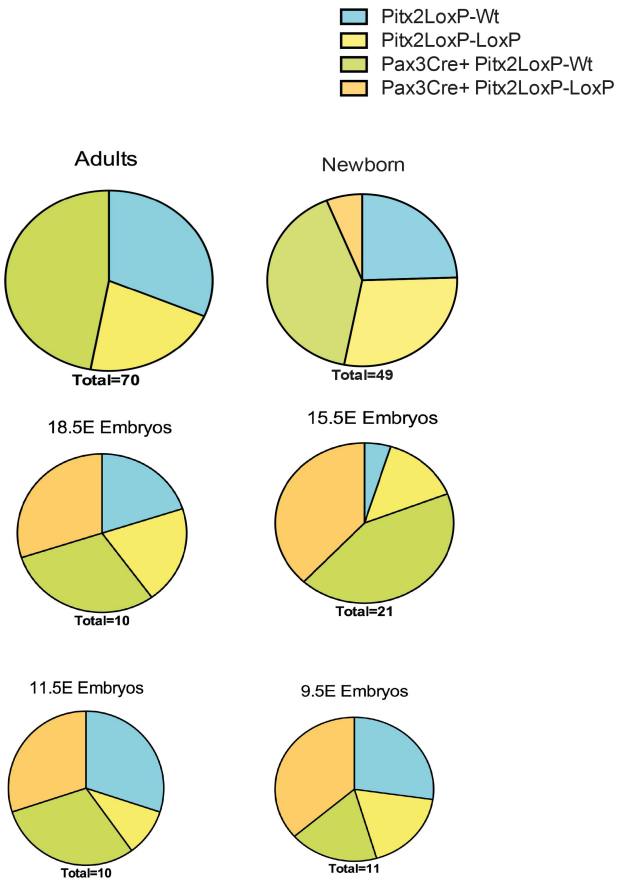

Figure 11: Mendelian ratios and survival rates for Pitx2$^{loxp/loxp}$, *Pax3Cre*$^{+/-}$/Pitx2$^{loxp/wt}$ and *Pax3Cre*$^{+/-}$/Pitx2$^{loxp/loxp}$ mice.

We first check for myogenic precursors population in these mutants by evaluating *Pax3* expression, at E10.5 no evident changes in *Pax3* expression pattern in somites were detected in *Pax3Cre*$^{+/-}$/Pitx2$^{loxp/loxp}$ conditional mutant mice **(Figure 12A).** However, we observed that the number of Pax3^{+} cells in the limb buds is reduced in homozygous conditional mutant embryos respect to heterozygous and wild type mice **(Figure 12B),** suggesting that the number of Pax3 cells that migrate into limb bud is decreased in these mutant mice.

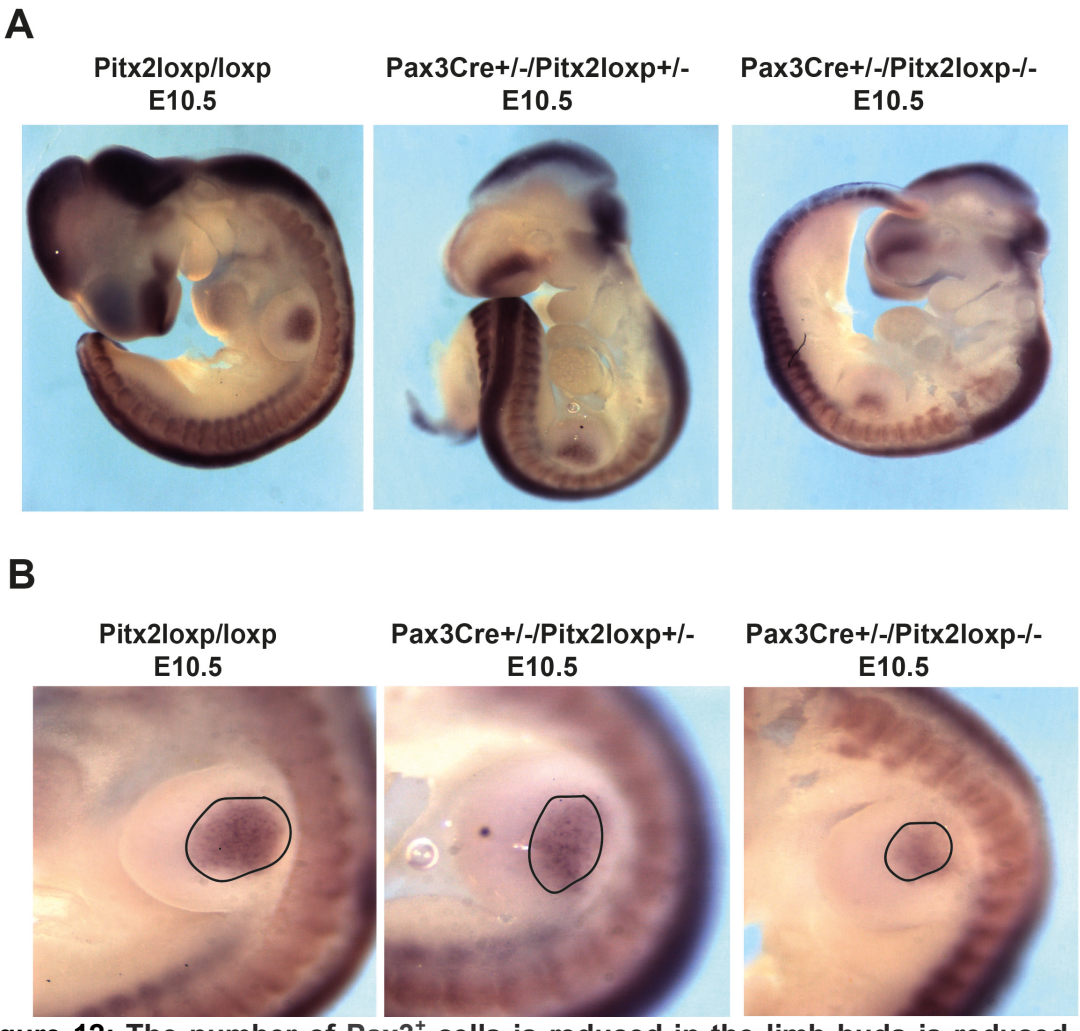

Figure 12: The number of Pax3^{+} cells is reduced in the limb buds is reduced in homozygous conditional mutant embryos of Pax3Cre$^{+/-}$/Pitx2$^{loxp/loxp}$: A: Representative images of in situ hybridization for Pax3 in Pitx2$^{loxp/loxp}$, *Pax3Cre*$^{+/-}$/Pitx2$^{loxp/wt}$ and *Pax3Cre*$^{+/-}$/Pitx2$^{loxp/loxp}$ embryo at E10.5 stage. **B:** Magnified view of representative images of in situ hybridization for Pax3 in Pitx2$^{loxp/loxp}$, *Pax3Cre*$^{+/-}$/Pitx2$^{loxp/wt}$ and *Pax3Cre*$^{+/-}$/Pitx2$^{loxp/loxp}$ embryo at E10.5 stage. *Pax3* positive cells are dotted.

Because migration of Pax3^{+} cardiac neural crest (CNC) cells is required for proper septation of the outflow tract (OFT) during in the developing heart (Chan, Cheung, Yung, & Copp, 2004; Olaopa et al., 2011) and the role of *Pitx2* in the formation of OFT septum remains controversial (Ai et al., 2006; Bajolle et al., 2006; H. Y. Ma, Xu, Eng, Gross, & Kioussi, 2013), we first evaluate in mouse and chick embryos *Pitx2* expression pattern in Pax3^{+} CNC migrating cell population by immunohistochemistry, and we found a clear co-location on *Pitx2* in Pax3^{+} CNC cells **(Figure 13A).**

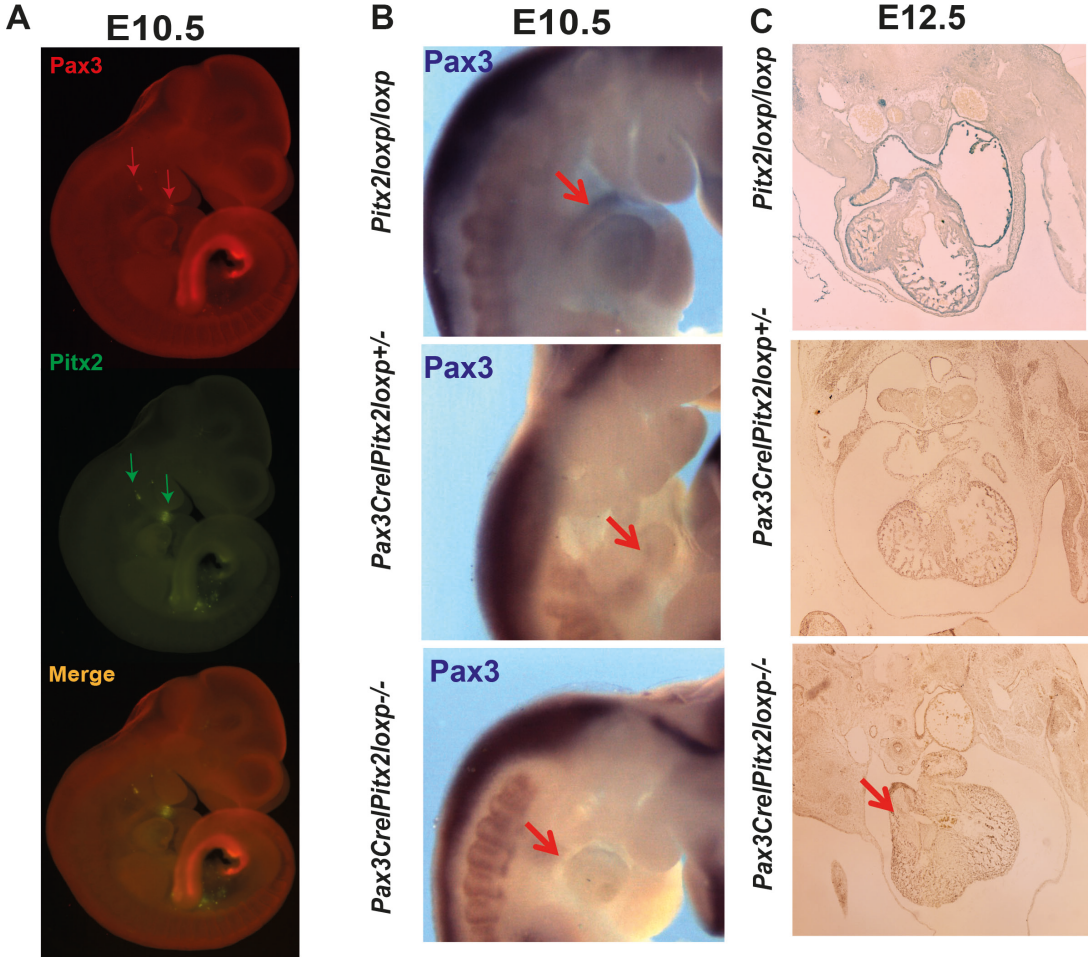

Figure 13: *Pitx2* is required for migration of CNC cells. A: Representative images of *Pax3* and *Pitx2* immunostaining in the mouse embryo at E10.5 stage. **B:** Representative images of in situ hybridization for *Pax3* in Pitx2$^{loxp/loxp}$, *Pax3Cre*$^{+/-}$/Pitx2$^{loxp/wt}$ and *Pax3Cre*$^{+/-}$/Pitx2$^{loxp/loxp}$ embryo at E10.5 stage. The arrows shown *Pax3*-expressing cells. **C:** Representative images showing the presence of DORV (arrow) *Pax3Cre*$^{+/-}$/Pitx2$^{loxp/loxp}$ embryo at E12.5.

Notably, and as observed in **Figure 13A** the migration of Pax3^{+} CNC cells contributing to cardiac chamber septation is also compromised in *Pax3Cre*$^{+/-}$ /Pitx2$^{loxp/loxp}$ homozygous mutant mice **(Figure 13B)**. As a consequence, around 40% of the homozygous mutants display cardiac defects such as Double outlet right ventricle (DORV) **(Figure 13C).**

This cardiac anomaly could explain, at least in part, the perinatal lethality and reveal a *Pitx2* requirement for the migration of Pax3^{+} cardiac neural crest. To further address the role of *Pitx2* in CNC cell migration we have performed *Pitx2* loss-of function experiments by Morpholinos in pre-migrating cardiac neural crest of the chick embryo (HH 10) and interestingly we observed that *Pitx2* blockage by morpholino electroporation in the presumptive CNC at HH10 lead to a clear decrease in the migration of electroporated cells through the brachial arches **(Figure 14)** reinforcing the notion of that *Pitx2* is required for migration of Pax3^{+} CNC cells.

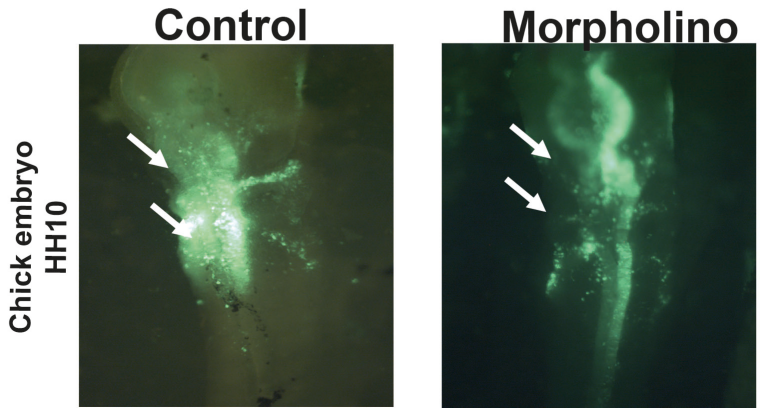

Figure 14: *Pitx2* loss-of function experiments by Morpholinos in pre-migrating cardiac neural crest of the chick embryo (HH10). The arrows indicate electroporated migrating CNC cells.

2. Pax3Cre$^{+/-}$/Pitx2$^{-/-}$ conditional mutant mice display retarded myogenesis and muscle hypotrophy

Next, we look for the impact of *Pitx2* deletion on myogenic lineage progression by analysing *MyoD* and *myogenin* expression pattern. A delay of myogenic differentiation only in the limb buds of systemic *Pitx2* null mutant have been previously reported (L'Honore et al., 2010). However, in *Pax3Cre*$^{+/-}$*/Pitx2*$^{loxp/loxp}$ conditional mutant mice we observed a clear deficit of *MyoD* and *myogenin* expression in myotomes at E10.5 but *MyoD* expression is rescued later at E12.5 **(Figure 15).**

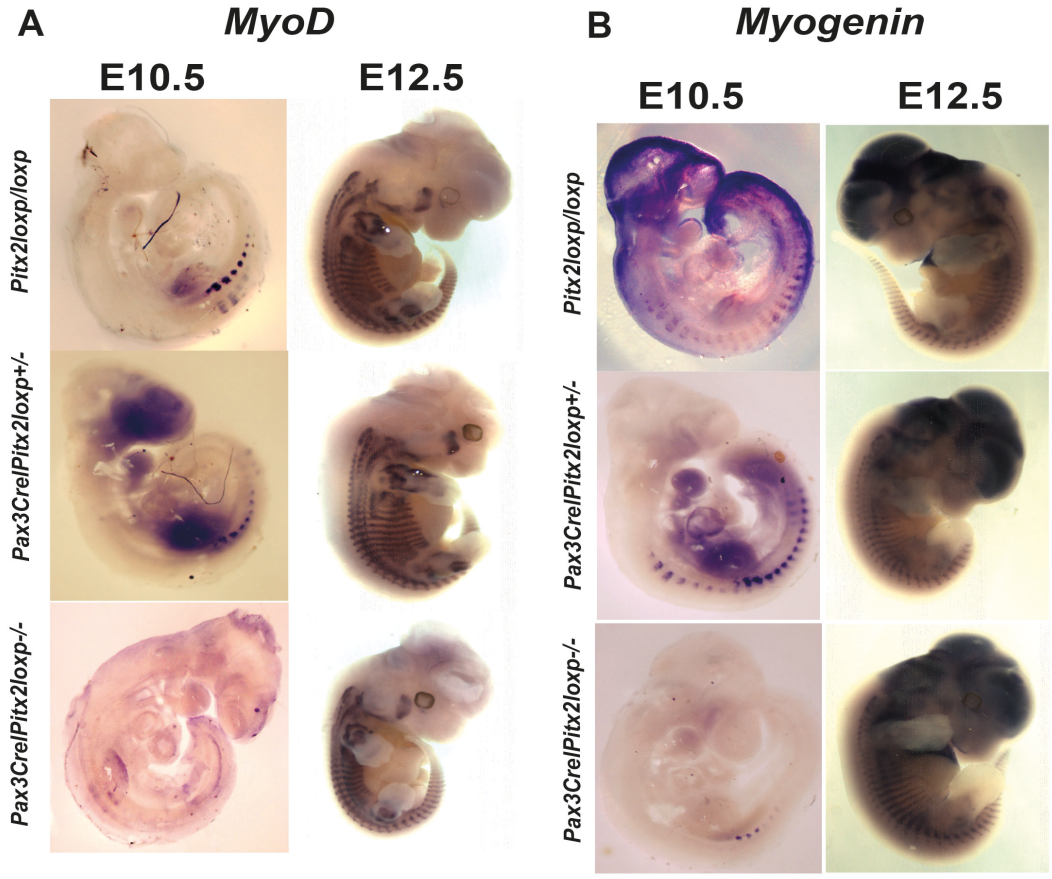

Figure 15: The onset of *MyoD* and *miogenin* expression is delayed in the myotome at E10.5 and reduced in the limb buds at E12.5 in *Pax3Cre*$^{+/-}$*/Pitx2*$^{loxp/loxp}$ embryos. **A:** Representative images of in situ hybridization for *MyoD* in *Pitx2*$^{loxp/loxp}$, *Pax3Cre*$^{+/-}$/Pitx2$^{loxp/wt}$ and *Pax3Cre*$^{+/-}$*/Pitx2*$^{loxp/loxp}$ embryo at E10.5 and E12.5 stages. **B:** Representative images of in situ hybridization for *Myogenin* in *Pitx2*$^{loxp/loxp}$, *Pax3Cre*$^{+/-}$*/Pitx2*$^{loxp/wt}$ and *Pax3Cre*$^{+/-}$*/Pitx2*$^{loxp/loxp}$ embryo at E10.5 and E12.5 stages.

Consistent with our previously reported analysis in *Pitx2* systemic mutants indicating a role of *Pitx2* in cell proliferation in myogenic precursors; we observed a clear decrease in the number of proliferative cells in the myotome of *Pax3Cre*$^{+/-}$*/Pitx2*$^{loxp/loxp}$ mutant mice at E10.5 **(Figure 16)** indicating that delayed *MyoD* expression is concomitant with retarded cell proliferation of myogenic progenitors joining the myotome.

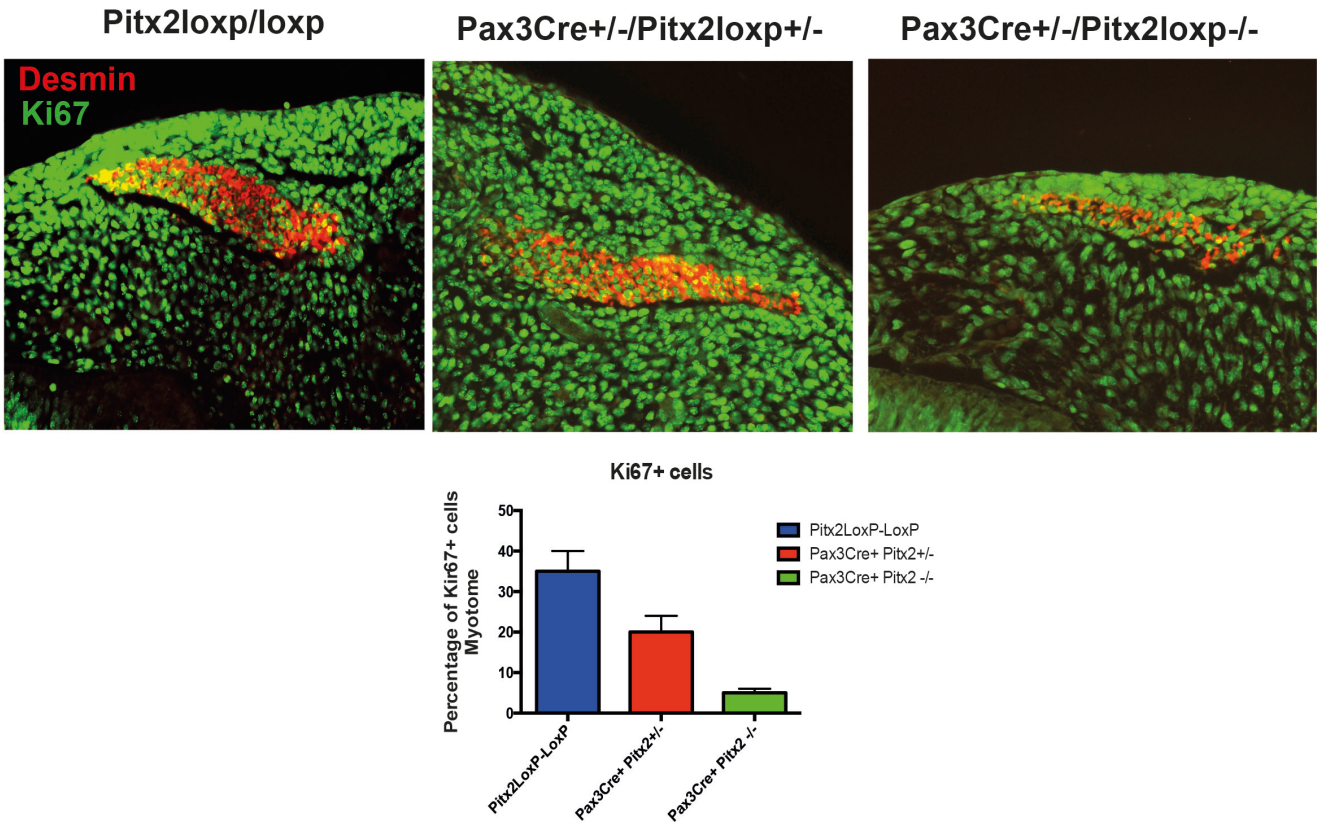

Figure 16: Representative images of Desmin and Ki67 immunostaining in the myotome of *Pitx2*$^{loxp/loxp}$, *Pax3Cre*$^{+/-}$*/Pitx2*$^{loxp/wt}$ and *Pax3Cre*$^{+/-}$*/Pitx2*$^{loxp/loxp}$ mice at E10.5 stage.

In addition, and in agreement with the idea to a decreased migration of Pax3^{+} myogenic precursors, we detected a decrease in *MyoD* and *myogenin* expression in the limb buds at E12.5 **(Figure 17)**.

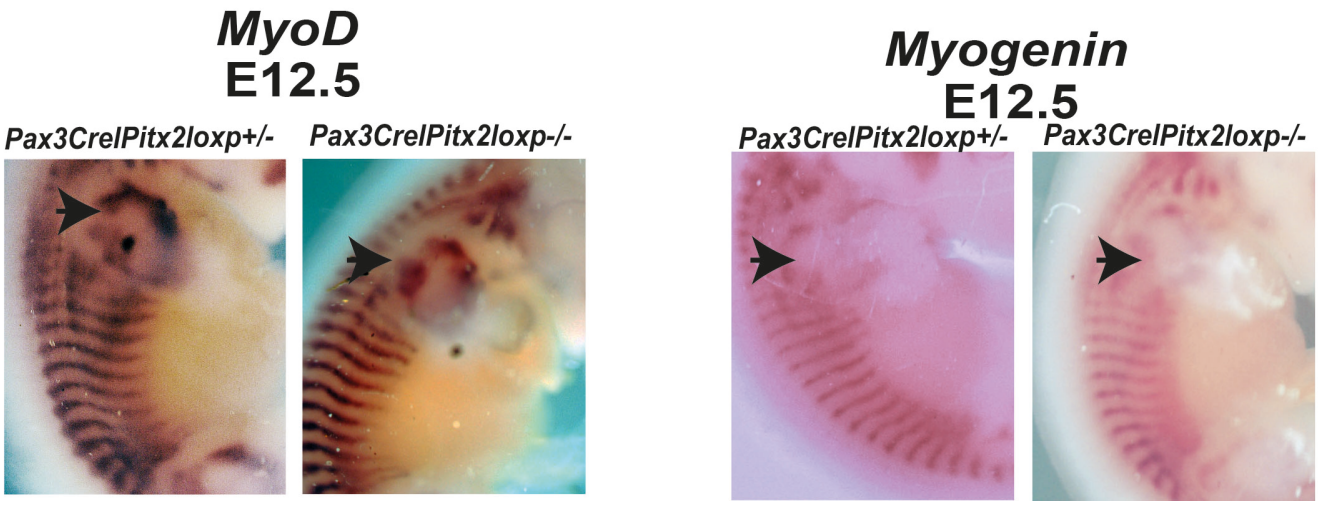

Figure 17: Magnified view of representative images of in situ hybridization for *MyoD* and *Myogenin* of *Pax3Cre*$^{+/-}$*/Pitx2*$^{loxp/wt}$ and *Pax3Cre*$^{+/-}$*/Pitx2*$^{loxp/loxp}$ embryo at E12.5 stage. The arrows indicate *MyoD* and *Myogenin* expression in the limb buds.

To evaluate the consequences of *Pitx2* deletion during subsequent fetal myogenesis, we analysed the epaxial and hypaxial muscle mass at E14.5 by MF20 staining. As observed in **Figure 18** *Pax3Cre*$^{+/-}$*/Pitx2*$^{loxp/loxp}$ conditional mutant mice display muscle hypotrophy in epaxial and hypaxial fetal muscles as well in the diaphragm. This observation indicate that *neonatal lethality may be also due a to* severe *diaphragm* hypotrophy. Beginning at E14.5, secondary myotubes form in tight association with primary myotubes, and they account for much of the muscle growth during fetal development (Buckingham M, Bajard L, Chang T, Daubas P, Hadchouel J, Meilhac S,Montarras D, Rocancourt D, Relaix F (2003) J Anat 202:59–68.). Thus, in order to evaluate secondary myogenesis, the number of MHC^{+} secondary myotubes formed in mutant embryos.

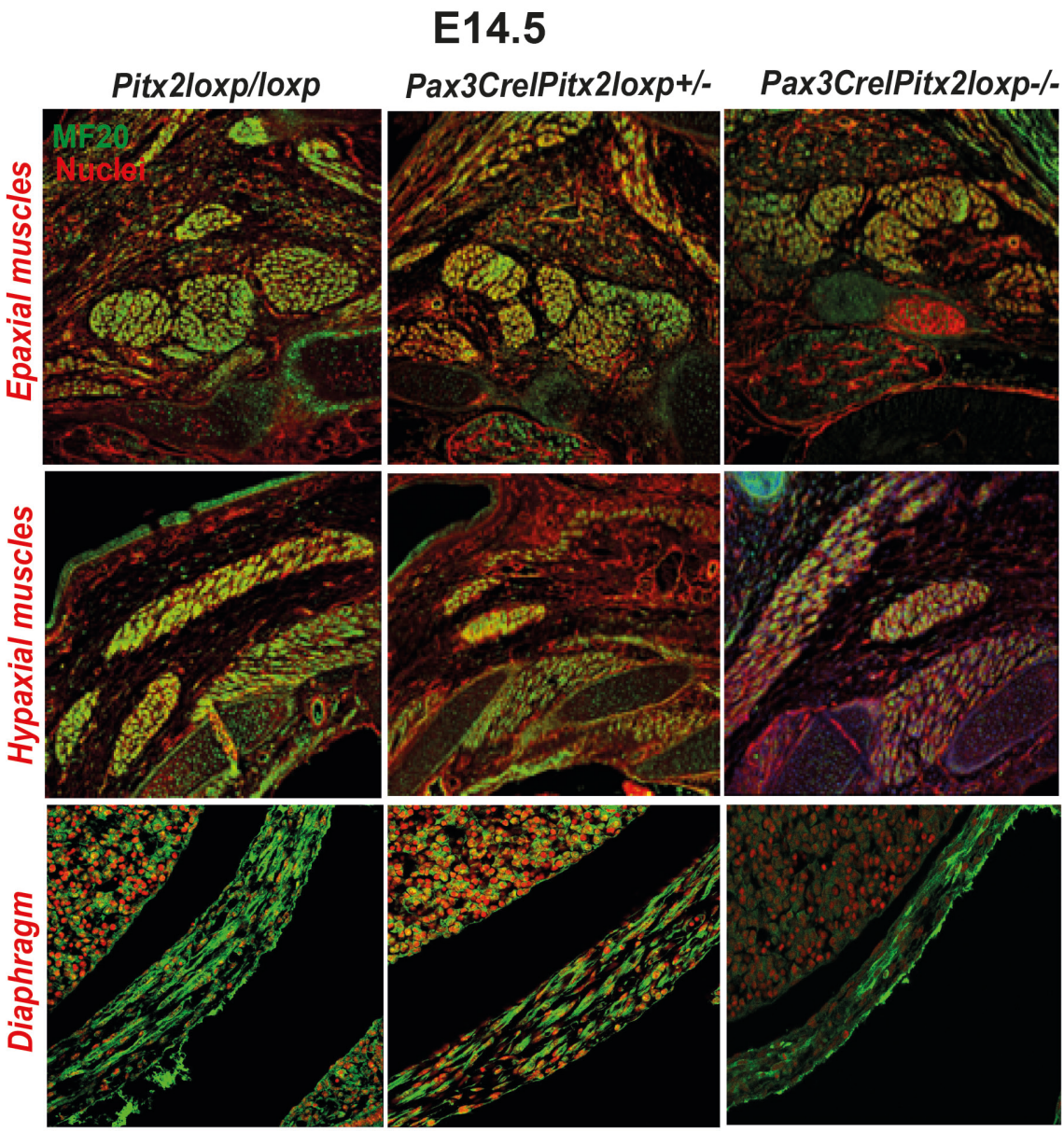

Figure 18: *Pax3Cre*$^{+/-}$*/Pitx2*$^{loxp/loxp}$ mice display muscle hypotrophy and retarded secondary myogenesis at fetal stages. A: Representative images of MF20 immunostaining in Epaxial muscles, Hypaxial muscles and diaphragm in *Pitx2*$^{loxp/loxp}$, *Pax3Cre*$^{+/-}$*/Pitx2*$^{loxp/wt}$ and *Pax3Cre*$^{+/-}$*/Pitx2*$^{loxp/loxp}$ embryo at E14.5 stage.

Our results showed that the number of secondary myotubes were severely reduced in mutant muscles, but they were frequently observed in wild-type **(Figure 19)** indicating that secondary myogenesis is also impaired in these mutant mice.

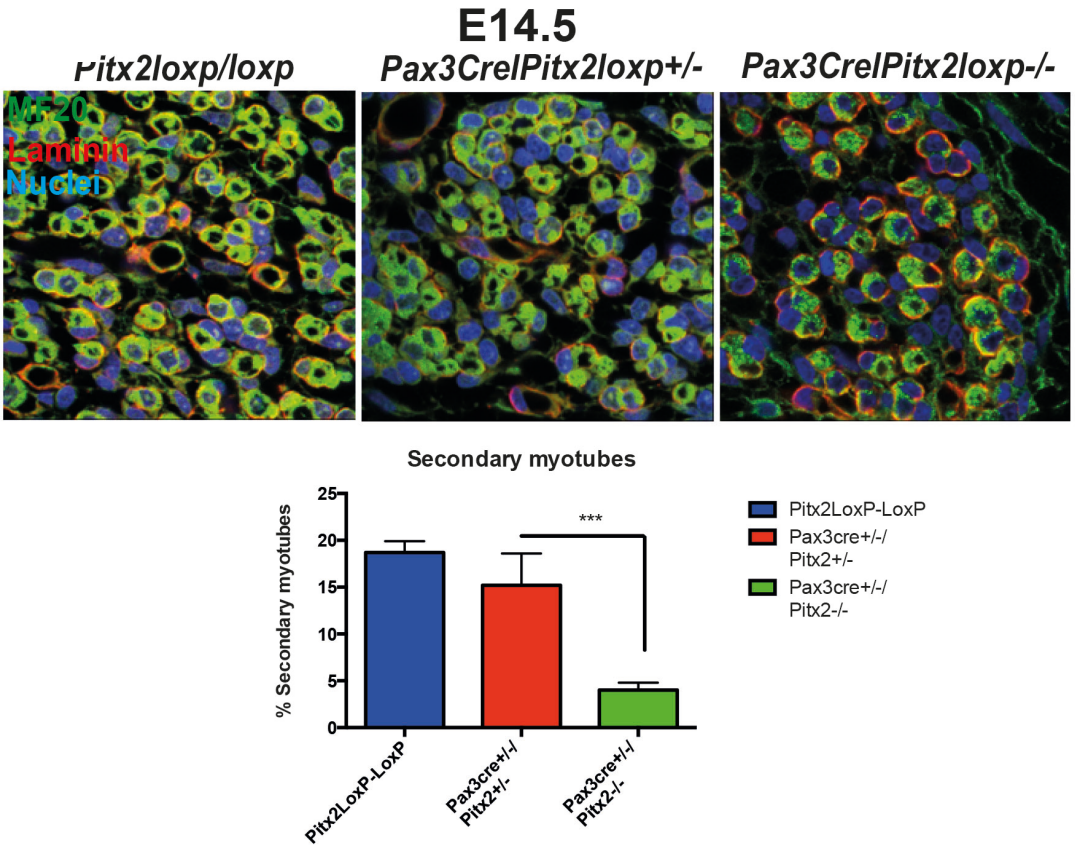

Figure 19: Representative images of MF20 and Laminin immunostaining in *Pitx2*$^{loxp/loxp}$, *Pax3Cre*$^{+/-}$*/Pitx2*$^{loxp/wt}$ and *Pax3Cre*$^{+/-}$*/Pitx2*$^{loxp/loxp}$ embryo at E14.5 stage. Percentage of secondary myotubes is shown.

Muscle hypotrophy persist in this mutant at neonatal stages as observed by a decreased in the number of muscle fibers together a shift in the distribution of the fiber size to the lowest area classes **(Figure 20).** Since Pax3^{+}/Pax7^{+} embryonic progenitor cells are the major source of adult satellite cells in trunk and limb muscles, we also looked for satellite cells in Pax3Cre-Pitx2 mutant and, as illustrated in **Figure 20**, the number of satellite cells was also decreased indicating that *Pitx2* inactivation on myogenic precursors also impact the pool of satellite cell population that remain in the adult muscle.

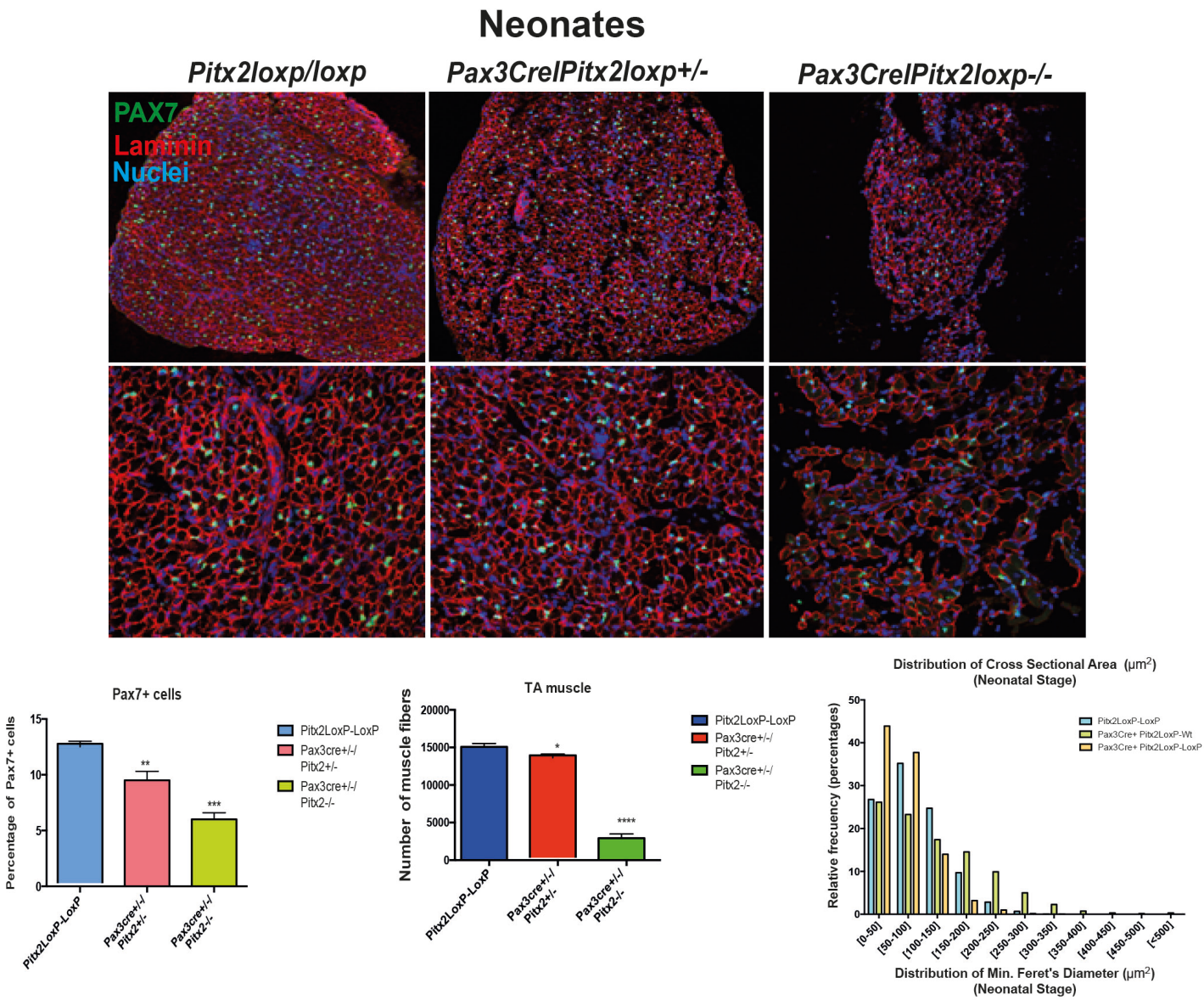

Figure 20: Representative images of PAX7 and Laminin co-immunostaining in the TA muscles of *Pitx2*$^{loxp/loxp}$, *Pax3Cre*$^{+/-}$*/Pitx2*$^{loxp/wt}$ and *Pax3Cre*$^{+/-}$*/Pitx2*$^{loxp/loxp}$ mice at neonatal stage. The percentage of PAX7 positive cells, number of muscles fibers and distribution of cross-sectional area are shown.

The adult phenotypic analysis of these conditional mutant mice was completed by using adult heterozygous mutant mice. As observed in **Figure 21**, the muscles of adult *Pax3Cre*$^{+/-}$*/Pitx2*$^{loxp/wt}$ heterozygous mice also displayed a shift in the distribution of the fiber size to the lowest area classes as well as a reduced number of satellite cells **(Figure 21).**

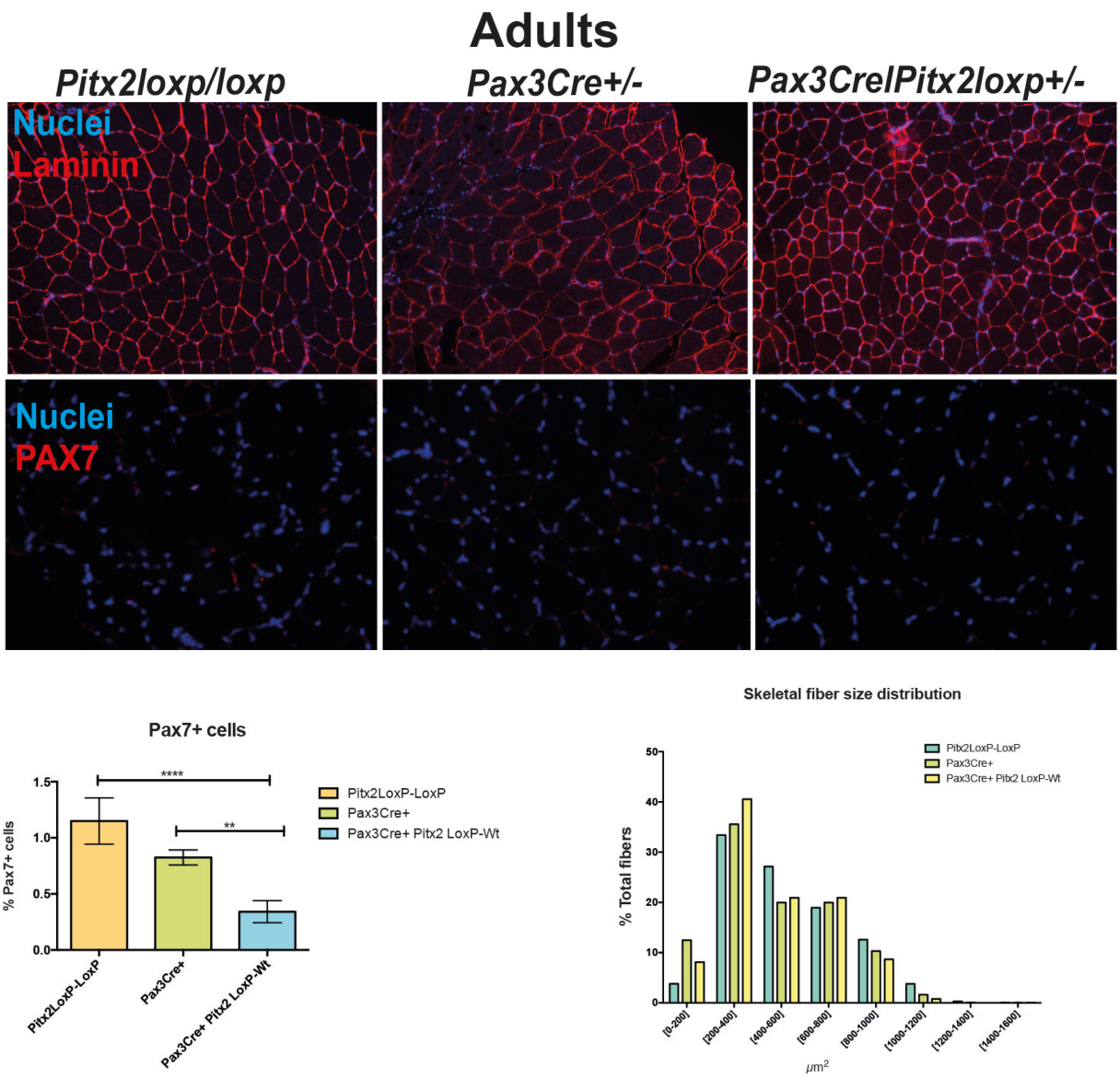

Figure 21: Representative images of PAX7 and Laminin in the TA muscles of *Pitx2*$^{loxp/loxp}$, *Pax3Cre*$^{+/-}$ and *Pax3Cre*$^{+/-}$*/Pitx2*$^{loxp/loxp}$ mice at adult stage. The percentage of PAX7 positive cells, number of muscles fibers and skeletal fiber size distribution area are shown.

3. Regeneration-related activity is diminished in Pax3Cre$^{+/-}$ /Pitx2$^{+/-}$ heterozygous mice

Since we have observed a reduction of satellite cell number in *Pax3Cre*$^{+/-}$ */Pitx2*$^{loxp/wt}$ heterozygous mice, we decided to evaluate satellite cell function in these mice. Because *Pax3Cre*$^{+/-}$*/Pitx2*$^{-/-}$ homozygous mutant neonates were born

alive but died soon after birth, we have used 4-month-old *Pax3Cre*$^{+/-}$*/Pitx2*$^{+/-}$ heterozygous mice. Heterozygosis for a deletion in the *Pitx2* gene in Pax3^{+} cells lowered the number of differentiated myotubes during *in vitro* differentiation **(Figure 22A)** also decreasing the number of *Myogenin*$^{+}$ nuclei **(Figure 22B)**. These findings agree with our *Pitx2c*-siRNA experiments, reinforcing the notion that the loss of *Pitx2* expression alters the behaviour of activated satellite cells, diminishing their performance to form myofibres.

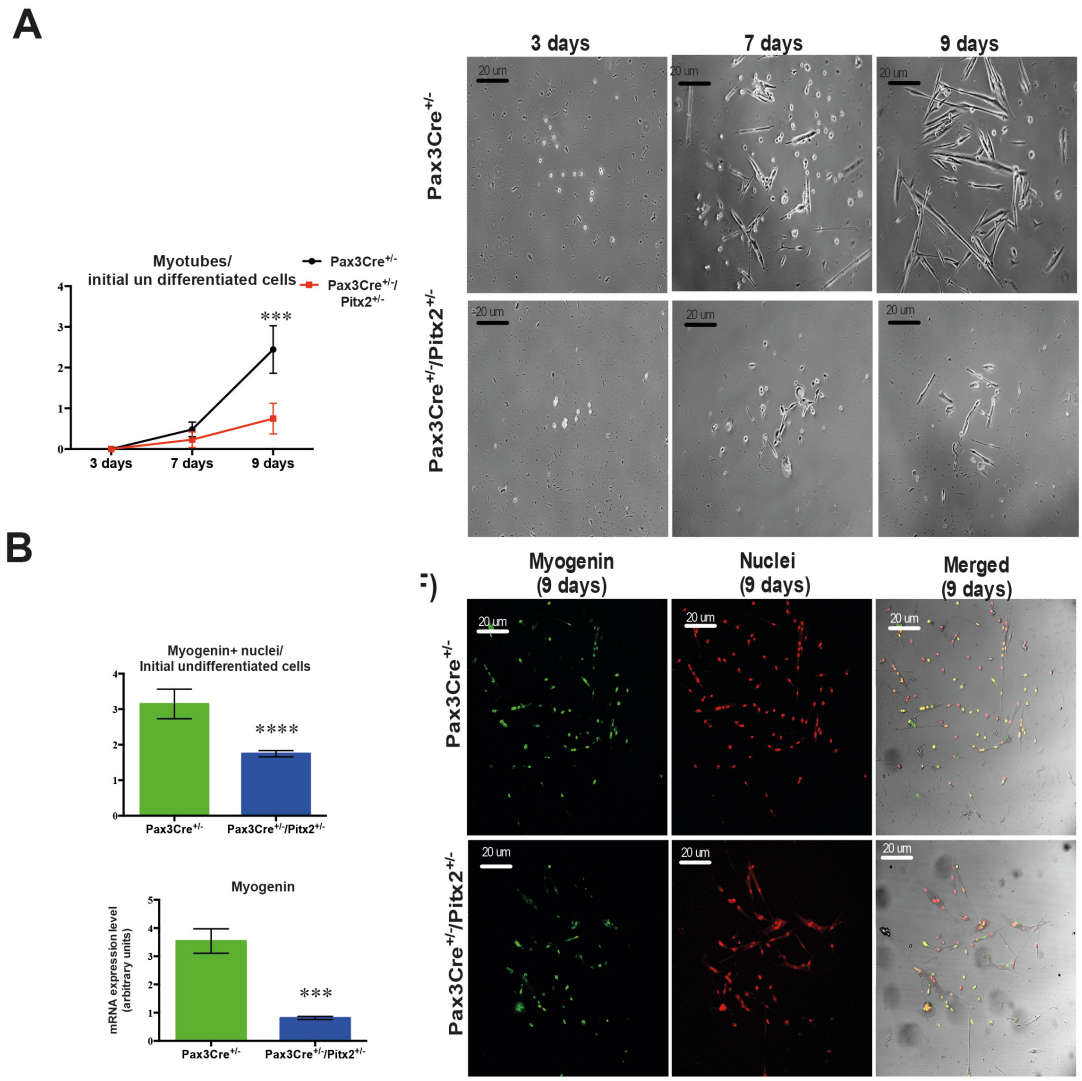

Figure 22: A Satellite cell isolated from *Pax3Cre*$^{+/-}$*/Pitx2*$^{loxp/wt}$ heterozygote mice, in which *Pitx2* expression is reduced by around 50%, exhibited a lower number of differentiated myotubes during in vitro differentiation **B**: a decreased *myogenin* expression as well as a diminished number of *Myogenin*+ nuclei. *p<0.1, ***p<0.001, ****p<0.0001.

To further investigate the role of *Pitx2* during muscle regeneration *in vivo*, we induced skeletal-muscle damage by cardiotoxin injection (CTX) in the tibialis anterioris (TA) of 4-month-old *Pax3Cre*$^{+/-}$*/Pitx2*$^{+/-}$ heterozygote mice and *Pax3Cre*$^{+/-}$ control mice. After skeletal-muscle injury, we evaluated the impact of genetic loss of *Pitx2* on the myogenic response during the initial waves of muscle regeneration by analysing the number of *Pax7*$^{+}$*/MyoD*$^{+}$ satellite cells at 3 days after damage **(Figure 23 A)**

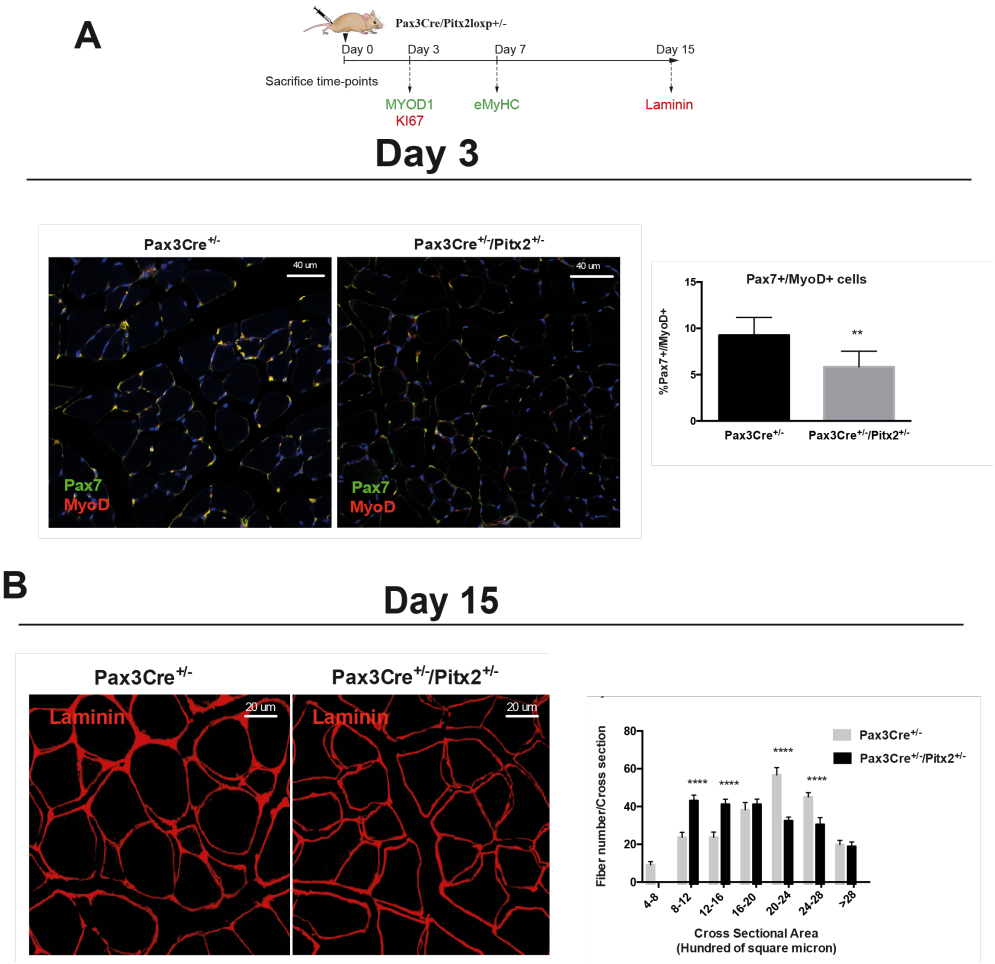

Figure 23: Muscle regeneration is impaired in *Pax3Cre*$^{+/-}$*/Pitx2*$^{+/-}$ heterozygote mice. **A** Representative image of Pax7^{+}/MyoD^{+} cells at day 3 after cardiotoxin injection in tibialis anterioris muscle (TA) of *Pax3Cre*$^{+/-}$*/Pitx2*$^{+/-}$ heterozygote mice *vs.* controls *Pax3Cre*$^{+/-}$ mice. Percentage of *Pax7*$^{+}$*/MyoD*$^{+}$ cells at day 3 after cardiotoxin injection in *Pax3Cre*$^{+/-}$*/Pitx2*$^{+/-}$ heterozygote mice *vs.* controls *Pax3Cre*$^{+/-}$ mice. **B:** Cross-sectional area in tibialis anterioris (TA) muscles of *Pax3Cre*$^{+/-}$*/Pitx2*$^{+/-}$ heterozygote mice *vs.* controls *Pax3Cre*$^{+/-}$ mice at day 15 after cardiotoxin injection and representative images.

Moreover, regeneration was impaired, as indicated by smaller myofibre size 15 days after injury compared to *Pax3Cre*$^{+/-}$ mice **(Figure 23 B)**, emphasizing the requirement of *Pitx2* for *in vivo* myogenic differentiation.

To evaluate muscle function, *Pax3Cre*$^{+/-}$*/Pitx2*$^{+/-}$ heterozygote mice were submitted to treadmill tests until exhaustion 30 days after injury. Strikingly, the running time and distance in the transgenic mice diminished by 23% and 34%, respectively **(Figure 24)**. These results further support the notion that the reduced number of Pax7^{+} satellite cells in *Pax3Cre*$^{+/-}$*/Pitx2*$^{+/-}$ heterozygote mice trigger muscle regeneration.

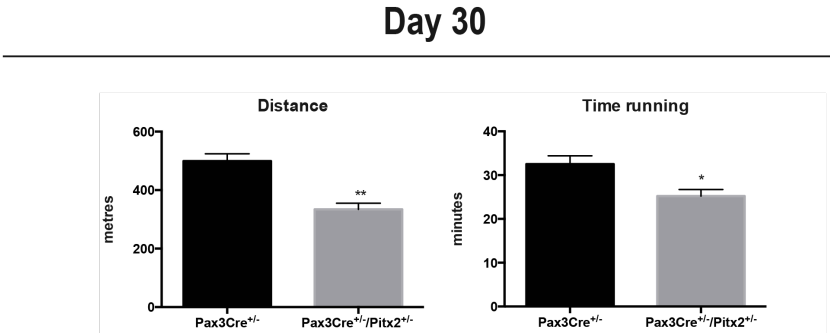

Figure 24: Treadmill Test: Running time and distance of *Pax3Cre*$^{+/-}$*/Pitx2*$^{+/-}$ heterozygote mice *vs.* controls *Pax3Cre*$^{+/-}$ mice at day 30 after muscle injury. *p<0.1,**p<0.01, ***p<0.001,****p<0.0001.

4. The lack of *Pitx2* function in Myf5^{+} committed myogenic precursors give rise to normal muscles with satellite cells expressing high levels of Pax7

The first sign of myogenic compromise during development is the activation of the myogenic factor *Myf5* in the progenitor's cells into somites. Thus, to full address how *Pitx2* acts in myogenic progression during skeletal myogenesis, we genetically ablated *Pitx2* in myogenic committed progenitor cells by intercrossing a *Pitx2* floxed mouse line with a *Cre* deletor mouse line (B195AP-Cre), which rendered muscle-lineage-specific *Myf5Cre* recombination (Naldaiz-Gastesi, Stem Cell Reports, 2016). Mice lacking *Pitx2* in Myf5^{+} myogenic precursors developed into normal adults and their muscles to have normal fiber size **(Figure 25A-B).** Because it has been previously established that adult satellite cells derive from progenitors that express the myogenic determination gene *Myf5* during fetal stages of myogenesis (Biresi et al, 2013); we wondered if the lack of *Pitx2* function in *Myf5* progenitors' cell may affect to the satellite cell population in the adult muscle. To check this; we performed *Pax7* and laminin co-immunostaining in 4 months old Myf5Cre/Pitx2 conditional mutants. Quantification of the number of Pax7^{+} sublaminar cells showed a not significative tendency to a high number of satellite cells in the muscle *Myf5Cre*$^{+/-}$*/Pitx2*$^{loxp/loxp}$ homozygous mutant mice respect to heterozygous and wild-type mice **(Figure 25B)**.

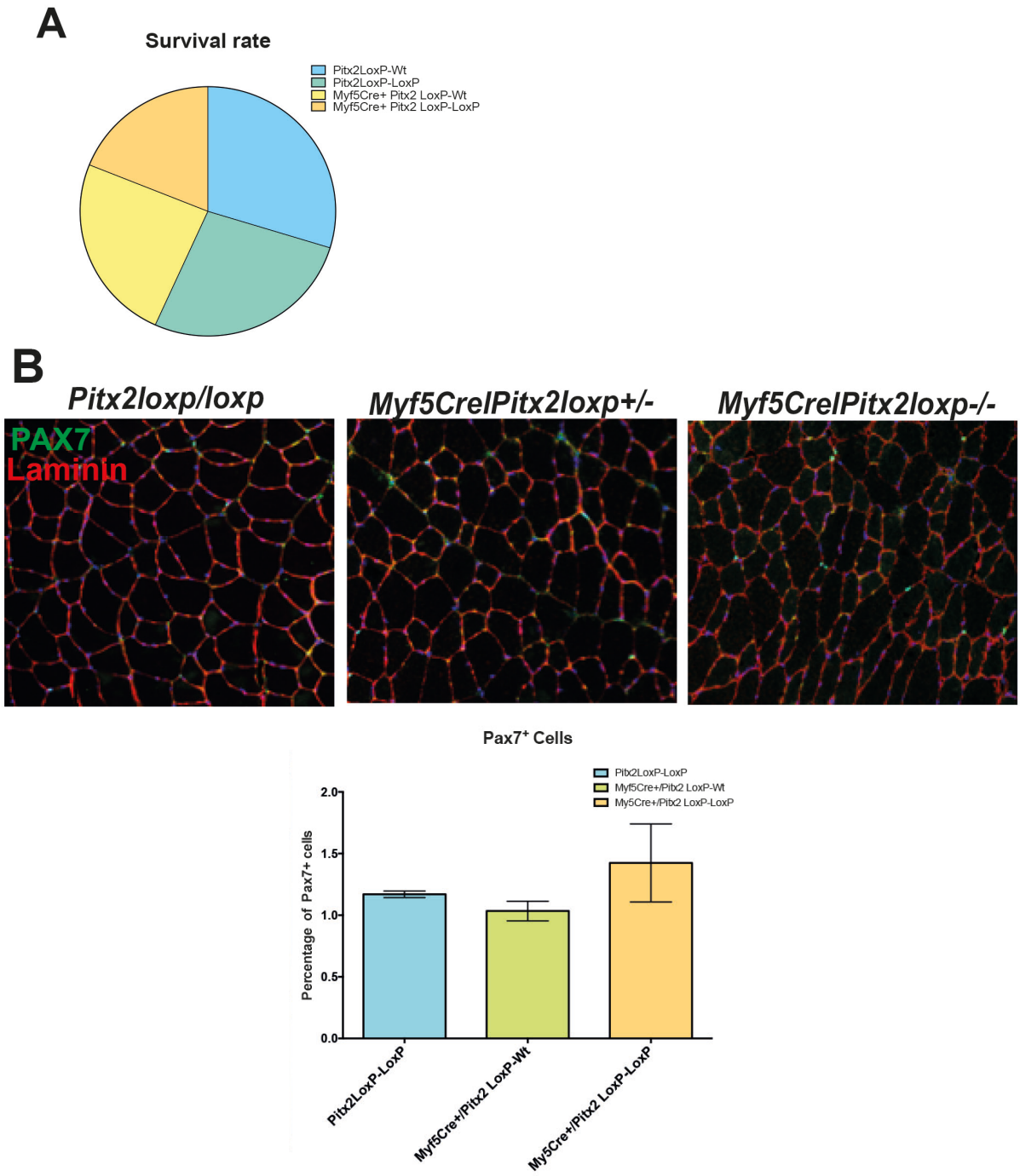

Figure 25: *Myf5Cre*$^{+/-}$*/Pitx2*$^{loxp/loxp}$ **mice have normal survival rates but posses satellite cells with high Pax7 expression. A:** Survival rates for Pitx2$^{loxp/loxp}$, *Myf5Cre*$^{+/-}$*/Pitx2*$^{loxp/wt}$ and *Myf5Cre*$^{+/-}$*/Pitx2*$^{loxp/loxp}$ mice. **B:** Representative images of PAX7 and Laminin co-immunostaining in the TA muscles of Pitx2$^{loxp/loxp}$, *Myf5Cre*$^{+/-}$*/Pitx2*$^{loxp/wt}$ and *Myf5Cre*$^{+/-}$*/Pitx2*$^{loxp/loxp}$ mice. The percentage of PAX7 positive cells is shown.

However, RT-PCR analyses for Pax7 expression levels revealed that the level of Pax7 expression was two-fold increase in *Myf5Cre*$^{+/-}$*/Pitx2*$^{loxp/loxp}$ homozygous mutant mice **(Figure 26)** indicating that satellite cells in these mutants exhibit high levels of *Pax7* expression. We further evaluate this satellite cell phenotype in neonates; no changes in the muscle fiber size and in the number of Pax7^{+} sublaminar satellite cells that achieve muscle growth after birth were detected in the neonatal muscles of *Myf5Cre*$^{+/-}$*/Pitx2*$^{loxp/loxp}$ homozygous mutant respect to control. These results show that *Pitx2*-loss of activity in Myf5 progenitors did not impact on satellite cell activity of the neonatal muscle.

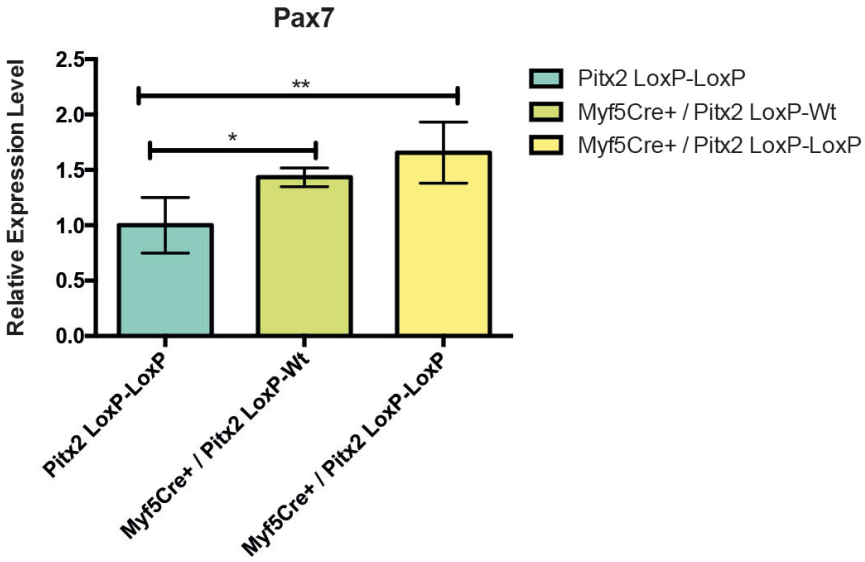

Figure 26: RT-PCR analyses for Pax7 in the TA muscles of Pitx2$^{loxp/loxp}$, *Myf5Cre*$^{+/-}$*/Pitx2*$^{loxp/wt}$ and *Myf5Cre*$^{+/-}$*/Pitx2*$^{loxp/loxp}$ mice.

5. Myf5Cre$^{+/-}$/Pitx2$^{-/-}$ mutant mice display severe defects on muscle regeneration

On account of the maintenance of high levels of *Pax7* on satellite cells might alter proper myogenic terminal differentiation finally affecting its

regenerative capacity (Olguin & Olwin; Dev Biol, 2004; Olguin et al; 2007, Von Maltzahn et al, 2013); we next set up to explore if high *Pax7* expression in satellite cells in *Myf5Cre*$^{+/-}$*/Pitx2*$^{loxp/loxp}$ mutant mice might modify muscle regeneration potential. To check that, skeletal-muscle damage was induced in 4-month-old *Myf5Cre*$^{+/-}$*/Pitx2*$^{loxp/loxp}$ homozygous, *Myf5Cre*$^{+/-}$*/Pitx2*$^{loxp/wt}$ heterozygotes and *Myf5Cre*$^{+/-}$ control mice. We found that satellite cells of *Myf5Cre*$^{+/-}$*/Pitx2*$^{loxp/loxp}$ mice display a lower propensity to proliferate at day 3 of muscle injury, as observed by the lowest number of Ki67^{+} cells **(Figure 27).** In addition, the differentiation kinetics was decreased, as measured by the number of MYOD1^{+} cells 3 days after cardiotoxin injection, which suggests that the inactivation of *Pitx2* in Myf5^{+} cells **(Figure 27)** decrease the functional ability of SCs to activate and participate in tissue repair.

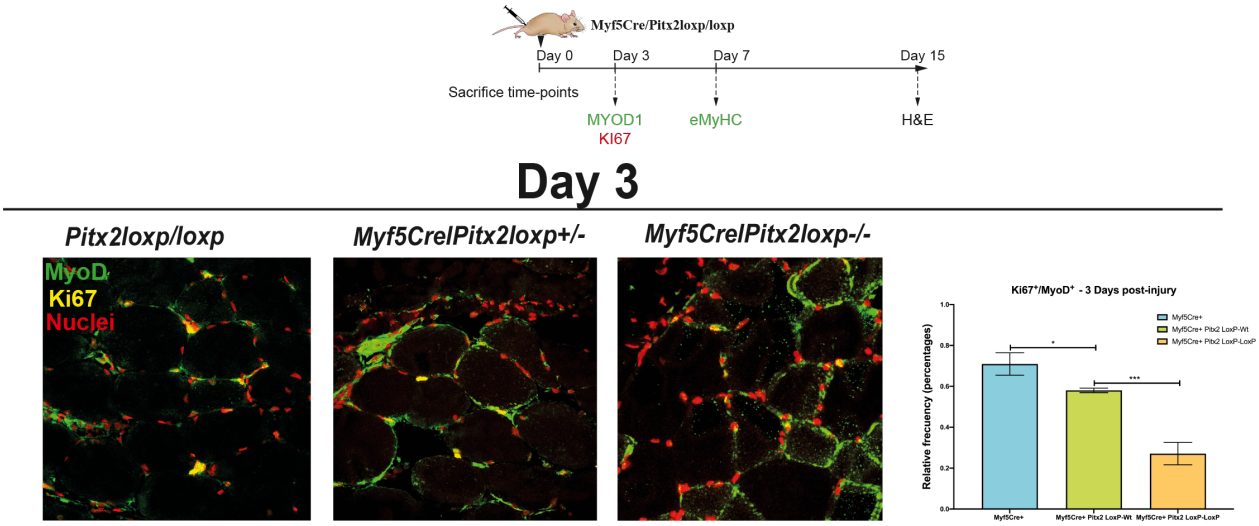

Figure 27: Muscle regeneration is dramatically affected in *Myf5Cre*$^{+/-}$*/Pitx2*$^{loxp/loxp}$ mice: Scheme of CTX injection in the TA of C57BL/6 mice *Pitx2*$^{loxp/loxp}$, *Myf5Cre*$^{+/-}$*/Pitx2*$^{loxp/wt}$ and *Myf5Cre*$^{+/-}$*/Pitx2*$^{loxp/loxp}$ mice and representative images of Ki67 and MyoD co-immunostaining in the TA muscles at 3 days of cardiotoxin-muscle damage. The percentages of Ki67^{+}/MyoD^{+} positive satellite cell are shown.

We also tested tissue regeneration by analysing the newly formed myofibers by using an eMyHC antibody on day 15 of cardiotoxin injection. As observed in **Figure 28**, the number of eMyH^{+} myofibers was dramatically decreased in the injured muscles of *Myf5Cre$^{+/-}$/Pitx2$^{loxp/loxp}$* homozygous respect to *Myf5Cre$^{+/-}$/Pitx2$^{loxp/wt}$* heterozygotes and *Myf5Cre$^{+/-}$* control mice.

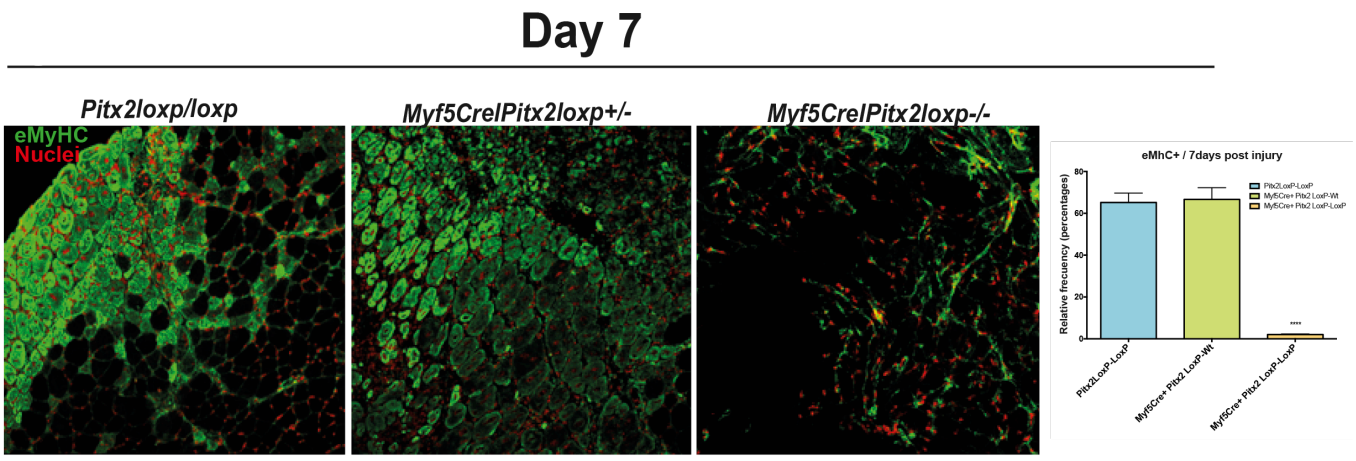

Figure 28: Representative images of eMyHC immunostaining in the TA muscles at 7 days of cardiotoxin-muscle damage. The percentages of eMyHC positive myofibers are shown.

The histological analysis of the TA fat 15 days after muscle damage clearly showed a lower percentage of fibers with centralised nuclei **(Figure 29)** as well as a shift in the distribution of the regenerating fiber size to the lowest area classes **(Figure 29).** Together, these findings indicate that the regenerative potential of satellite cells in *Myf5Cre$^{+/-}$/Pitx2$^{loxp/loxp}$* homozygous mice was clearly decreased.

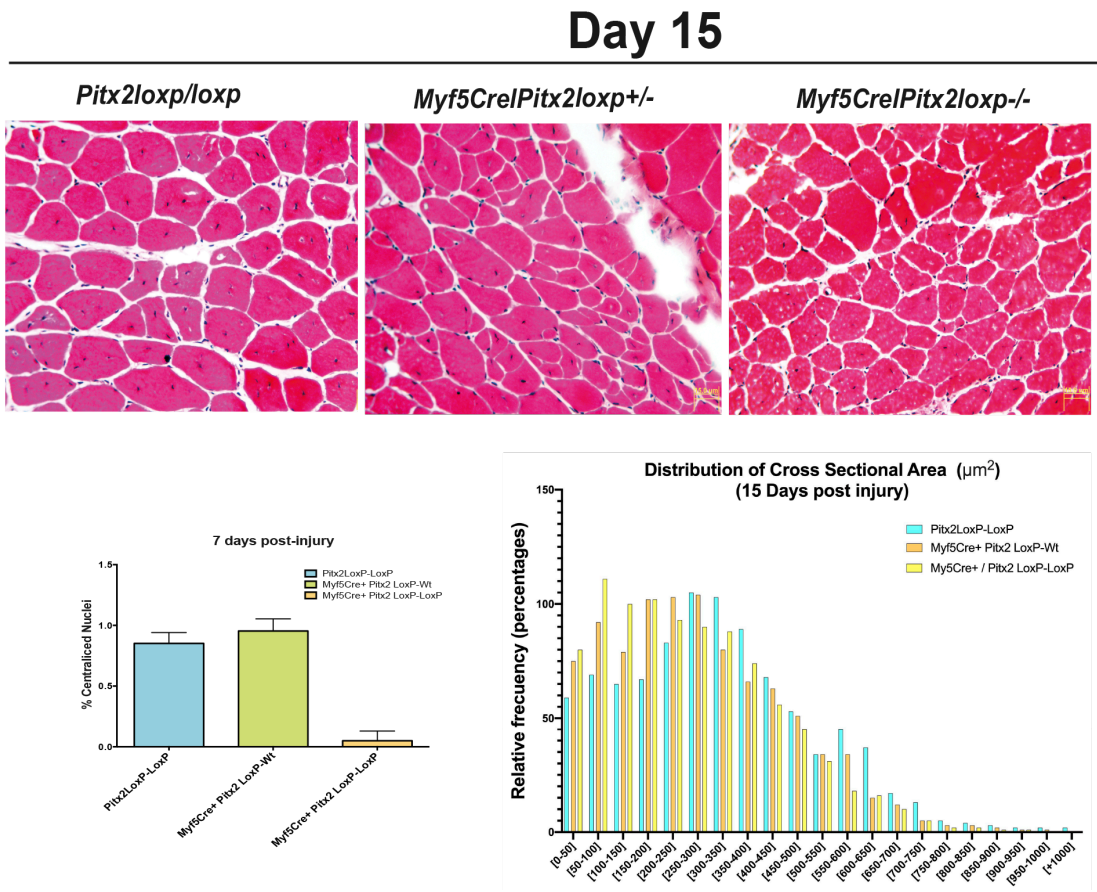

Figure 29: Representative images of the TA muscles at 15 days of cardiotoxin-muscle damage (H/E). The skeletal fiber size distribution area and the centralized nuclei percentage are shown.

Chapter V:

Discussion

Chapter V: Discussion

Several previous evidences have revealed that the transcription factor Pitx2 might be a player within the molecular pathways controlling somite-derived muscle progenitors cell fate (Kioussi et al., 2011; L'Honore et al., 2010; Lozano-Velasco et al., 2011; Martínez-Fernandez et al., 2006). However, the hierarchical position occupied by *Pitx2* within the genetic cascade that control somite-derived myogenesis as well as its role on later foetal muscle mass remain unsolved. To get insight into this issue, we have differentially generated two conditional *Pitx2* mutant mice to specifically inactivate *Pitx2* in multipotent $Pax3^{+}$ muscle progenitors ($Pax3Cre^{+/-}/Pitx2^{loxp/loxp}$ mice) and in myogenic committed progenitors ($Myf5Cre^{+/-}/Pitx2^{loxp/loxp}$ mice). Our analyses revealed that *Pitx2* inactivation in $Pax3^{+}$ precursors lead to impaired myogenesis with severe muscle hypotrophy while the loss of *Pitx2* in $Myf5^{+}$ myogenic cells have an impact satellite cell activity with severe consequences in muscle regeneration.

Although, several seminal works suggest that *Pitx2* could be acting downstream of *Pax3* and in parallel with *Myf5*, at least in the myotome,(L'Honoré et al., 2007; L'Honore et al., 2010; Lagha et al., 2010); the specific role of *Pitx2* in multipotent muscle progenitors and/or myogenic committed progenitors during skeletal muscle development in not well understood. It has been previously showed that systemic $Pitx2^{-/-}$ null mutants display a delay in the onset of *MyoD* and *myogenin* expression in the limb buds (L'Honore et al., 2010). However, our analysis revealed that the lack of *Pitx2* function in $Pax3^{+}$ multipotent myogenic progenitors give rise to a delay of the onset of myogenic differentiation in the

myotome, as observed by a delay in the beginning of *MyoD* and *myogenin* expression at E12.5 in Pax3Cre$^{+/-}$/Pitx2$^{loxp/loxp}$ mutant embryos, indicating that *Pitx2* function is required for initial activation of the *MyoD* gene also in the myotome. In addition, we observed that the number of Pax3^{+} progenitors that migrate into limb buds is decreased in Pax3Cre$^{+/-}$/Pitx2$^{loxp/loxp}$ mutant embryos; leading thus later on to a lower *MyoD* and *myogenin* cell population in the limbs. These results suggest a requirement of *Pitx2* function for proper migration of Pax3 precursors cells.

In agreement with this idea, we also notice that in Pax3Cre$^{+/-}$/Pitx2$^{loxp/loxp}$ mutant embryos display a significant reduction of Pax3^{+} migrating cardiac neural crest cells into the outflow tract (OFT) in the developing heart leading to severe cardiac defects such as double outet right ventricle (DORV). Although previous reports have suggested that mutation of the Pitx2 gene causes defects in OFT based on events in cardiac neural crest (H. Y. Ma et al., 2013) (Kioussi, 2002, 2013); the role of *Pitx2* in cardiac neural crest (CNC) cells is controversial. Therefore, Ai et al Dev Biol 2006, by using the CNC driver *Wnt11*, found that there is no requirement for *Pitx2* in CNCC, but instead it is needed in the cells derived from the second heart field. In this context it has been demonstrated that the onset of Pax3 precedes Wnt1-Cre expression within the neural folds (C. Chang et al., 2009) and Olaopa et al (2011) showed that *Pax3* function in the CNC progenitors is necessary prior to Wnt1-Cre expression. Here, we show that Pax3^{+} CNC express *Pitx2* in the mouse and chick embryo and the lack of *Pitx2* function in CNC cells also lead to a dramatic decrease in CNC cell migration.

Thus, our results point out for the first time the role of Pitx2 in early migration of $Pax3^{+}$ cardiac neural crest cells.

Notably, we observed that $Pax3Cre^{+/-}/Pitx2^{loxp/loxp}$ mutant mice display a clear muscle hypotrophy at fetal stages; this phenotype might probably be due to the defects on cell migration detected at embryonic stages. In parallel secondary myotubes formation is also affected in the foetal muscle stages suggesting that *Pitx2* function is necessary to complete proper secondary myogenesis. This hypotrophic phenotype is maintained in the neonatal muscle of $Pax3Cre^{+/-}/Pitx2^{loxp/loxp}$ mice; together with a reduced number of satellite stem cells. Muscle hypotrophy and a reduced number of satellite cell is also present in the adult muscle of $Pax3Cre^{+/-}/Pitx2^{loxp/wt}$ heterozygous mice. Experiments of induced muscle injury in these heterozygous mice demonstrated that their regenerative capacity were highly compromised. These results are in agreement with our previous reported work highlighting the relevance of *Pitx2* in the context of muscle regeneration.

Contrary to $Pax3Cre^{+/-}/Pitx2^{loxp/loxp}$ conditional mutant mice; $Myf5Cre^{+/-}/Pitx2^{loxp/loxp}$ conditional mutant mice developed into normal adults and their muscles appear to have normal fiber size, indicating that the lack of Pitx2 function in myogenic committed progenitors have not consequences in the developing muscle. However, we detected dramatic defects on satellite cell function $Myf5Cre^{+/-}/Pitx2^{loxp/loxp}$ conditional mutant mice due to high *Pax7* expression suggesting that *Pitx2* is important to satellite cell myogenic differentiation.

Bibliography

Abu-Elmagd, M., Robson, L., Sweetman, D., Hadley, J., Francis-West, P., & Münsterberg, A. (2010). Wnt/Lef1 signaling acts via Pitx2 to regulate somite myogenesis. *Developmental Biology*, *337*(2), 211–219. https://doi.org/10.1016/j.ydbio.2009.10.023

Ai, D., Liu, W., Ma, L., Dong, F., Lu, M. F., Wang, D., … Martin, J. F. (2006). Pitx2 regulates cardiac left-right asymmetry by patterning second cardiac lineage-derived myocardium. *Developmental Biology*, *296*(2), 437–449. https://doi.org/10.1016/j.ydbio.2006.06.009

Anderson, R. H., Webb, S., Brown, N. A., Lamers, W., & Moorman, A. (2003). Development of the heart: (2) Septation of the atriums and ventricles. *Heart*, *89*(8), 949–958.

Bajolle, F., Zaffran, S., Kelly, R. G., Hadchouel, J., Bonnet, D., Brown, N. A., & Buckingham, M. E. (2006). Rotation of the myocardial wall of the outflow tract is implicated in the normal positioning of the great arteries. *Circulation Research*, *98*(3), 421–428. https://doi.org/10.1161/01.RES.0000202800.85341.6e

Baldini, A., Fulcoli, F. G., & Illingworth, E. (2017). Tbx1: Transcriptional and Developmental Functions. In *Current Topics in Developmental Biology* (1st ed., Vol. 122). https://doi.org/10.1016/bs.ctdb.2016.08.002

Benchaouir, R., Meregalli, M., Farini, A., D'Antona, G., Belicchi, M., Goyenvalle, A., … Torrente, Y. (2007). Restoration of Human Dystrophin Following Transplantation of Exon-Skipping-Engineered DMD Patient Stem Cells into Dystrophic Mice. *Cell Stem Cell*, *1*(6), 646–657. https://doi.org/10.1016/j.stem.2007.09.016

Bentzinger, C. F., Wang, Y. X., & Rudnicki, M. A. (2012). Building muscle: molecular regulation of myogenesis. *Cold Spring Harbor Perspectives in Biology*, *4*(2). https://doi.org/10.1101/cshperspect.a008342

Bentzinger, C. F., Wang, Y. X., & Rudnicki, M. A. (2014). *Building Muscle : Molecular Regulation of Myogenesis 2 . MORPHOGEN GRADIENTS AND MYOGENESIS*. 1–19.

Buckingham, M. (2017). Gene regulatory networks and cell lineages that underlie the formation of skeletal muscle. *Proceedings of the National Academy of Sciences of the United States of America*, *114*(23), 5830–5837. https://doi.org/10.1073/pnas.1610605114

Buckingham, M., Bajard, L., Chang, T., Daubas, P., Hadchouel, J., Meilhac, S., … Relaix, F. (2003). The formation of skeletal muscle: From somite to limb. *Journal of Anatomy*, *202*(1), 59–68. https://doi.org/10.1046/j.1469-7580.2003.00139.x

Buckingham, M., & Relaix, F. (2007). The Role of Pax Genes in the Development of Tissues and Organs: Pax3 and Pax7 Regulate Muscle Progenitor Cell Functions . *Annual Review of Cell and Developmental Biology*, *23*(1), 645–673. https://doi.org/10.1146/annurev.cellbio.23.090506.123438

Buckingham, M., & Relaix, F. (2015). PAX3 and PAX7 as upstream regulators of myogenesis. *Seminars in Cell and Developmental Biology*, *44*, 115–125. https://doi.org/10.1016/j.semcdb.2015.09.017

Buckingham, M., & Rigby, P. W. J. (2014). Gene Regulatory Networks and Transcriptional Mechanisms that Control Myogenesis. *Developmental Cell*, *28*(3), 225–238. https://doi.org/10.1016/j.devcel.2013.12.020

Buckingham, M., & Vincent, S. D. (2009). Distinct and dynamic myogenic populations in the vertebrate embryo. *Current Opinion in Genetics and Development*, *19*(5), 444–453. https://doi.org/10.1016/j.gde.2009.08.001

Cazenave, A., Souriau, A., & Kien, D. (1989). © 198 9 Nature Publishing Group. *Nature*, *342*, 189–192. https://doi.org/10.1038/340301a0

Chan, W. Y., Cheung, C. S., Yung, K. M., & Copp, A. J. (2004). Cardiac neural crest of the mouse embryo: Axial level of origin, migratory pathway and cell autonomy of the splotch (Sp2H) mutant effect. *Development*, *131*(14), 3367–3379. https://doi.org/10.1242/dev.01197

Chang, C. N., Singh, A. J., Gross, M. K., & Kioussi, C. (2019). Requirement of Pitx2 for skeletal muscle homeostasis. *Developmental Biology*, *445*(1), 90–102. https://doi.org/10.1016/j.ydbio.2018.11.001

Chang, C., Stankunas, K., Shang, C., Kao, S., Twu, K. Y., & Cleary, M. L. (2009). *NIH Public Access*. *135*(21), 3577–3586. https://doi.org/10.1242/dev.022350.Pbx1

Cheung, T. H., Quach, N. L., Charville, G. W., Liu, L., Park, L., Edalati, A., … Rando, T. A. (2012). Maintenance of muscle stem-cell quiescence by microRNA-489. *Nature*, *482*(7386), 524–528. https://doi.org/10.1038/nature10834

Chinchilla, A., Daimi, H., Lozano-Velasco, E., Dominguez, J. N., Caballero, R., Delpo, E., … Franco, D. (2011). PITX2 insufficiency leads to atrial electrical and structural remodeling linked to arrhythmogenesis. *Circulation: Cardiovascular Genetics*, *4*(3), 269–279. https://doi.org/10.1161/CIRCGENETICS.110.958116

Costamagna, D., Mommaerts, H., Sampaolesi, M., & Tylzanowski, P. (2016). Noggin inactivation affects the number and differentiation potential of muscle progenitor cells in vivo. *Scientific Reports*, *6*. https://doi.org/10.1038/srep31949

Deries, M., & Thorsteinsdóttir, S. (2016). Axial and limb muscle development: dialogue with the neighbourhood. *Cellular and Molecular Life Sciences*, *73*(23), 4415–4431. https://doi.org/10.1007/s00018-016-2298-7

Desgrange, A., Garrec, J. F. Le, & Meilhac, S. M. (2018). Left-right asymmetry in heart development and disease: Forming the right loop. *Development (Cambridge)*, *145*(22). https://doi.org/10.1242/dev.162776

Dumont, N. A., Wang, Y. X., & Rudnicki, M. A. (2015). Intrinsic and extrinsic mechanisms regulating satellite cell function. *Development (Cambridge)*, *142*(9), 1572–1581. https://doi.org/10.1242/dev.114223

Franco, D., Sedmera, D., & Lozano-Velasco, E. (2017). Multiple Roles of Pitx2 in Cardiac Development and Disease. *Journal of Cardiovascular Development and Disease*, *4*(4), 16. https://doi.org/10.3390/jcdd4040016

Gage, P. J., Suh, H., & Camper, S. A. (1999). The <i>bicoid</i> -related Pitx gene family in development. *Mammalian Genome*, *10*(2), 197–200. https://doi.org/10.1007/s003359900970

García-Martinez, V., G. C. S. (1993). *Primitive-Streak Origin of the Cardiovascular System in Avian Embryos*.

Gopinath, S. D., Webb, A. E., Brunet, A., & Rando, T. A. (2014). FOXO3 promotes quiescence in adult muscle stem cells during the process of self-renewal. *Stem Cell Reports*, *2*(4), 414–426.

https://doi.org/10.1016/j.stemcr.2014.02.002

Greulich, F., Rudat, C., & Kispert, A. (2011). Mechanisms of T-box gene function in the developing heart. *Cardiovascular Research*, *91*(2), 212–222. https://doi.org/10.1093/cvr/cvr112

Hernandez-Torres, F., Rodríguez-Outeiriño, L., Franco, D., & Aranega, A. E. (2017). Pitx2 in Embryonic and Adult Myogenesis. *Frontiers in Cell and Developmental Biology*. https://doi.org/10.3389/fcell.2017.00046

Hill, M. C., Kadow, Z. A., Li, L., Tran, T. T., Wythe, J. D., & Martin, J. F. (2019). A cellular atlas of Pitx2-dependent cardiac development. *Development (Cambridge, England)*, *146*(12), 1–12. https://doi.org/10.1242/dev.180398

Hu, P., Geles, K. G., Paik, J. H., DePinho, R. A., & Tjian, R. (2008). Codependent Activators Direct Myoblast-Specific MyoD Transcription. *Developmental Cell*, *15*(4), 534–546. https://doi.org/10.1016/j.devcel.2008.08.018

Kanisicak, O., Mendez, J. J., Yamamoto, S., Yamamoto, M., & Goldhamer, D. J. (2009). Progenitors of skeletal muscle satellite cells express the muscle determination gene, MyoD. *Developmental Biology*, *332*(1), 131–141. https://doi.org/10.1016/j.ydbio.2009.05.554

Kassar-duchossoy, L., Giacone, E., Gayraud-morel, B., Jory, A., Gomès, D., & Tajbakhsh, S. (2005). *Kassar-Duchossoy_etal2005_Pax3Pax7_GenDev 2*. 1–6. https://doi.org/10.1101/gad.345505.1426

Kim, J. H., Jin, P., Duan, R., & Chen, E. H. (2015). Mechanisms of myoblast fusion during muscle development. *Current Opinion in Genetics and Development*, *32*, 162–170. https://doi.org/10.1016/j.gde.2015.03.006

Kioussi, C., Briata, P., Baek, S. H., Rose, D. W., Hamblet, N. S., Herman, T., … Rosenfeld, M. G. (2011). *Identification of a WntDv-Catenin → Pitx2 Pathway.pdf*. *111*, 673–685.

Knopp, P., Figeac, N., Fortier, M., Moyle, L., & Zammit, P. S. (2013). Pitx genes are redeployed in adult myogenesis where they can act to promote myogenic differentiation in muscle satellite cells. *Developmental Biology*, *377*(1), 293–304. https://doi.org/10.1016/j.ydbio.2013.02.011

Kuang, S., Kuroda, K., Le Grand, F., & Rudnicki, M. A. (2007). Asymmetric Self-Renewal and Commitment of Satellite Stem Cells in Muscle. *Cell*, *129*(5), 999–1010. https://doi.org/10.1016/j.cell.2007.03.044

L'Honoré, A., Coulon, V., Marcil, A., Lebel, M., Lafrance-Vanasse, J., Gage, P., … Drouin, J. (2007). Sequential expression and redundancy of Pitx2 and Pitx3 genes during muscle development. *Developmental Biology*, *307*(2), 421–433. https://doi.org/10.1016/j.ydbio.2007.04.034

L'Honore, A., Ouimette, J.-F., Lavertu-Jolin, M., & Drouin, J. (2010). Pitx2 defines alternate pathways acting through MyoD during limb and somitic myogenesis. *Development*, *137*(22), 3847–3856. https://doi.org/10.1242/dev.053421

L'Honoré, A., Ouimette, J. F., Lavertu-Jolin, M., & Drouin, J. (2010). Pitx2 defines alternate pathways acting through MyoD during limb and somitic myogenesis. *Development*, *137*(22), 3847–3856. https://doi.org/10.1242/dev.053421

Lagha, M., Sato, T., Regnault, B., Cumano, A., Zuniga, A., Licht, J., … Buckingham, M. (2010). Transcriptome analyses based on genetic screens for Pax3 myogenic targets in the mouse embryo. *BMC Genomics*, *11*(1), 696. https://doi.org/10.1186/1471-2164-11-696

Lassar, A. B., Davis, R. L., Wright, W. E., Kadesch, T., Murre, C., Voronova, A., … Weintraub, H. (1991). Functional activity of myogenic HLH proteins requires hetero-oligomerization with E12/E47-like proteins in vivo. *Cell*, *66*(2), 305–315. https://doi.org/10.1016/0092-8674(91)90620-E

Le Grand, F., Jones, A. E., Seale, V., Scimè, A., & Rudnicki, M. A. (2009). Wnt7a Activates the Planar Cell Polarity Pathway to Drive the Symmetric Expansion of Satellite Stem Cells. *Cell Stem Cell*, *4*(6), 535–547. https://doi.org/10.1016/j.stem.2009.03.013

Lieber, R. L. (2011). Skeletal muscle structure, function, and plasticity. In *Skeletal Muscle Structure, Function, and Plasticity*. https://doi.org/10.1016/s0031-9406(05)60189-7

Liu, C., Liu, W., Lu, M. F., Brown, N. A., & Martin, J. F. (2001). Regulation of left-right asymmetry by thresholds of Pitx2c activity. *Development*, *128*(11), 2039–2048.

Lozano-Velasco, E., Contreras, A., Crist, C., Hernández-Torres, F., Franco, D., & Aránega, A. E. (2011). Pitx2c modulates Pax3+/Pax7+ cell populations and regulates Pax3 expression by repressing miR27 expression during myogenesis. *Developmental Biology*, *357*(1), 165–178.

https://doi.org/10.1016/j.ydbio.2011.06.039

Lozano-Velasco, E., Vallejo, D., Esteban, F. J., Doherty, C., Hernández-Torres, F., Franco, D., & Aránega, A. E. (2015). A Pitx2 -MicroRNA Pathway Modulates Cell Proliferation in Myoblasts and Skeletal-Muscle Satellite Cells and Promotes Their Commitment to a Myogenic Cell Fate . *Molecular and Cellular Biology*. https://doi.org/10.1128/mcb.00536-15

Ma, G., Wang, Y., Li, Y., Cui, L., Zhao, Y., Zhao, B., & Li, K. (2015). MiR-206, a key modulator of skeletal muscle development and disease. *International Journal of Biological Sciences*, *11*(3), 345–352. https://doi.org/10.7150/ijbs.10921

Ma, H. Y., Xu, J., Eng, D., Gross, M. K., & Kioussi, C. (2013). Pitx2-mediated cardiac outflow tract remodeling. *Developmental Dynamics*, *242*(5), 456–468. https://doi.org/10.1002/dvdy.23934

Marcil, A. (2003). Pitx1 and Pitx2 are required for development of hindlimb buds. *Development*, *130*(1), 45–55. https://doi.org/10.1242/dev.00192

Martínez-Fernandez, S., Hernández-Torres, F., Franco, D., Lyons, G. E., Navarro, F., & Aránega, A. E. (2006). Pitx2c overexpression promotes cell proliferation and arrests differentiation in myoblasts. *Developmental Dynamics*, *235*(11), 2930–2939. https://doi.org/10.1002/dvdy.20924

Miersch, C., Stange, K., Hering, S., Kolisek, M., Viergutz, T., & Röntgen, M. (2017). Molecular and functional heterogeneity of early postnatal porcine satellite cell populations is associated with bioenergetic profile. *Scientific Reports*, *7*(February), 1–14. https://doi.org/10.1038/srep45052

Moorman, A. F. M., & Christoffels, V. M. (2003). Cardiac chamber formation: Development, genes, and evolution. *Physiological Reviews*, *83*(4), 1223–1267. https://doi.org/10.1152/physrev.00006.2003

Moresi, V., Garcia-Alvarez, G., Pristerà, A., Rizzuto, E., Albertini, M. C., Rocchi, M., … Coletti, D. (2009). Modulation of caspase activity regulates skeletal muscle regeneration and function in response to vasopressin and tumor necrosis factor. *PLoS ONE*, *4*(5). https://doi.org/10.1371/journal.pone.0005570

Murphy, M., & Kardon, G. (2011). Origin of vertebrate limb muscle: The role of progenitor and myoblast populations. In *Current Topics in Developmental Biology* (Vol. 96). https://doi.org/10.1016/B978-0-12-385940-2.00001-2

Nowotschin, S., Liao, J., Gage, P. J., Epstein, J. A., Campione, M., & Morrow, B. E. (2006). Tbx1 affects asymmetric cardiac morphogenesis by regulating Pitx2 in the secondary heart field. *Development*, *133*(8), 1565–1573. https://doi.org/10.1242/dev.02309

Olaopa, M., Zhou, H. M., Snider, P., Wang, J., Schwartz, R. J., Moon, A. M., & Conway, S. J. (2011). Pax3 is essential for normal cardiac neural crest morphogenesis but is not required during migration nor outflow tract septation. *Developmental Biology*, *356*(2), 308–322. https://doi.org/10.1016/j.ydbio.2011.05.583

Ono, Y., Boldrin, L., Knopp, P., Morgan, J. E., & Zammit, P. S. (2010). Muscle satellite cells are a functionally heterogeneous population in both somite-derived and branchiomeric muscles. *Developmental Biology*, *337*(1), 29–41. https://doi.org/10.1016/j.ydbio.2009.10.005

Ott, M. O., Bober, E., Lyons, G., Arnold, H., & Buckingham, M. (1991). Early expression of the myogenic regulatory gene, myf-5, in precursor cells of skeletal muscle in the mouse embryo. *Development*, *111*(4), 1097–1107.

Pisconti, A., Cornelison, D. D. W., Olguín, H. C., Antwine, T. L., & Olwin, B. B. (2010). Syndecan-3 and Notch cooperate in regulating adult myogenesis. *Journal of Cell Biology*, *190*(3), 427–441. https://doi.org/10.1083/jcb.201003081

Rocheteau, P., Gayraud-Morel, B., Siegl-Cachedenier, I., Blasco, M. A., & Tajbakhsh, S. (2012). A subpopulation of adult skeletal muscle stem cells retains all template DNA strands after cell division. *Cell*, *148*(1–2), 112–125. https://doi.org/10.1016/j.cell.2011.11.049

Rudnicki, M. A., Le Grand, F., McKinnell, I., & Kuang, S. (2008). The molecular regulation of muscle stem cell function. *Cold Spring Harbor Symposia on Quantitative Biology*, *73*, 323–331. https://doi.org/10.1101/sqb.2008.73.064

Sato, T., Rocancourt, D., Marques, L., Thorsteinsdóttir, S., & Buckingham, M. (2010). A Pax3/Dmrt2/Myf5 regulatory cascade functions at the onset of myogenesis. *PLoS Genetics*, *6*(4). https://doi.org/10.1371/journal.pgen.1000897

Schienda, J., Engleka, K. A., Jun, S., Hansen, M. S., Epstein, J. A., Tabin, C. J., … Kardon, G. (2006). Somitic origin of limb muscle satellite and side population cells. *Proceedings of the National Academy of Sciences*, *103*(4),

945–950. https://doi.org/10.1073/pnas.0510164103

Schweickert, A., Campione, M., Steinbeisser, H., & Blum, M. (2000). Pitx2 isoforms: Involvement of Pitx2c but not Pitx2a or Pitx2b in vertebrate left-right asymmetry. *Mechanisms of Development*, *90*(1), 41–51. https://doi.org/10.1016/S0925-4773(99)00227-0

Shea, K. L., Xiang, W., LaPorta, V. S., Licht, J. D., Keller, C., Basson, M. A., & Brack, A. S. (2010). Sprouty1 Regulates Reversible Quiescence of a Self-Renewing Adult Muscle Stem Cell Pool during Regeneration. *Cell Stem Cell*, *6*(2), 117–129. https://doi.org/10.1016/j.stem.2009.12.015

Shi, X., & Garry, D. J. (2006). Muscle stem cells in development, regeneration, and disease. *Genes and Development*, *20*(13), 1692–1708. https://doi.org/10.1101/gad.1419406

Shih, H. P., Gross, M. K., & Kioussi, C. (2007). Expression pattern of the homeodomain transcription factor Pitx2 during muscle development. *Gene Expression Patterns*, *7*(4), 441–451. https://doi.org/10.1016/j.modgep.2006.11.004

Soleimani, V. D., Punch, V. G., Kawabe, Y. ichi, Jones, A. E., Palidwor, G. A., Porter, C. J., … Rudnicki, M. A. (2012). Transcriptional Dominance of Pax7 in Adult Myogenesis Is Due to High-Affinity Recognition of Homeodomain Motifs. *Developmental Cell*, *22*(6), 1208–1220. https://doi.org/10.1016/j.devcel.2012.03.014

Srivastava, D. (2006). Making or Breaking the Heart: From Lineage Determination to Morphogenesis. *Cell*, *126*(6), 1037–1048. https://doi.org/10.1016/j.cell.2006.09.003

Tajbakhsh, S., Rocancourt, D., Cossu, G., & Buckingham, M. (2016). Redefining the Genetic Hierarchies Controlling Skeletal Myogenesis: Pax-3 and Myf-5 Act Upstream of MyoD. *Cell*, *89*(1), 127–138. https://doi.org/10.1016/S0092-8674(00)80189-0

The origin of secondary myotubes in mammalian skeletal muscles: Ultrastructural studies. (1989). *Development*, *107*(4), 743–750.

White, R. B., Biérinx, A., Gnocchi, V. F., & Zammit, P. S. (2010). *Dynamics of muscle fibre growth during postnatal mouse development*.

Stage-specific effects of Pitx2 inactivation during skeletal myogenesis

Felicitas Ramirez de Acuña; Lara Rodriguez-Outeriño; Francisco Hernández-Torres; Jorge N Dominguez; Diego Franco, Amelia E. Aránega*.

Short title: Pitx2 and myogenesis

[1] Cardiac and Skeletal Myogenesis Group, Department of Experimental Biology, University of Jaen. Spain.

[2] Cardiac and Skeletal Myogenesis Group. MEDINA Foundation. Center for Excellence in Research of Innovative Medicines in Andalusia. Granada. Spain.

***Correspondence:** Amelia Eva Aranega (aaranega@ujaen.es)

ABSTRACT

During embryonic development, the skeletal muscles of the trunk derive from transitory structures called somites. Multipotent muscle progenitor cells (MPCs) that express Pax3 arise from the dermomyotome and acquire their definitive identity via the myogenic regulatory factors (MRFs) Myf5, Mrf4, and MyoD. Moreover, the muscle stem cells (satellite cells) of the body and limbs also arise from somites, in common with the muscle that they are associated with. Several previous evidences have revealed that the transcription factor Pitx2 might be a player within the molecular pathways controlling somite-derived muscle progenitors' fate. However, the hierarchical position occupied by *Pitx2* within the genetic cascade that control somite-derived myogenesis remain unsolved. To get insight into this issue, we have differentially generated two conditional *Pitx2* mutant mice to specifically inactivate Pitx2 in multipotent Pax3+ muscle progenitors (Pax3Cre+/Pitxloxp/loxp mice) and in myogenic committed progenitors (Myf5Cre+/Pitx2loxp/loxp mice). Our analyses revealed that Pitx2 inactivation in Pax3+ precursors lead defective migration of Pax3+ cells and muscle hypotrophy while the loss of Pitx2 in Myf5+ myogenic cells have an impact in satellite stem properties with severe consequences in muscle regeneration. Overall our results suggest a Pitx2 requirement for MPCs migration as well as for the acquisition of a proper satellite cell function.

INTRODUCCION

In vertebrates, the skeletal muscles originate from the paraxial mesoderm during development. The muscles of trunk and limbs derive from transitory mesodermal structures called somites that are generated by a segmentation process of the paraxial mesoderm. As the somite matures, myogenic progenitor cells become confined to the dorso-lateral part of the somite: the dermomyotome [1, 2, 3]. Soon after, the cells in the lateral lips of the dermomyotome undergo an epithelial-to mesenchymal transition and migrate to its ventral surface to form a distinct myotome beneath the dermotome. Myogenic progenitors located in the dorsomedial part of the myotome configurate the epaxial myotome which form the back muscles, while the ventrolateral region or hypaxial myotome gives rise to body wall and limb muscles. Myogenesis then proceeds through diverse waves of differentiation, initially a group of embryonic myoblasts form the primary muscle fibers representing a scaffold for the secondary myofibers formed by the fusion of fetal myoblasts around E14.0 in mice [4]. A third wave of undifferentiated cells, residing adjacent to existing fibers and named satellite cells, appear at the end of postnatal development and will allow for the hypertrophic growth of skeletal muscle during postnatal development and also will achieve the skeletal muscle regeneration during adulthood. However, the muscles of the head and neck are of nonsomitic origin which derive of the unsegmented paraxial and pharyngeal

head mesoderm that form the extra-ocular (EOMs), branchial, laryngoglossal, and axial neck muscles [5,6,7].

The genetic networks that control myogenesis during development is also depending on the location. In the genetic hierarchy that regulates the onset of trunk myogenesis, Pax3 plays a dominant role in somites. Therefore, the paired box gen Pax3 drives cell fate specification of multipotent myogenic precursors, and also orchestrates their survival, self-renewal and migration [8,9,10]. Nonetheless, Pax3 is not expressed in the myogenic precursors of head and some neck muscles where T-box factor 1 (Tbx1) and paired-like homeodomain factor 2 (Pitx2) are key upstream genes. In both cases the entry into the myogenic program depends on the sequential activation of myogenic determination factors Myf5 and MyoD and the transcription factor MYOG is required for the onset of the expression of terminal differentiation genes [1,3].

However, Pitx2 is also expressed in the somite-derived dermomyotome, limb buds and later in the fetal muscle progenitors [11,12]; and several previous works have provided some evidences about the initial role of Pitx2 at the onset of myogenesis. Therefore, the analysis of Pitx2 systemic null mutant performed by L'Honore et al (2010) [13] lead them to conclude that Pitx2 acts at limb level regulating MyoD expression through binding to its core enhancer. Supplementary data by using *Pax3* mutant *Splotch* suggested that Pitx2 could be acting downstream of Pax3. Curiously, contrary to what happens in limb-muscle cells, these authors found that the onset of *Myod* expression was not delayed in *Pitx2*$^{-/-}$ embryos. However, the inactivation of *Myf5* and/or *Myf6* in a

Pitx2$^{-/-}$ background (*Pitx2*$^{-/-}$*;Myf5*$^{nlacZ/nlacZ}$) led to practically a complete loss of *Myod* expression in the myotome, as occurred in limbs [13]; suggesting that MYF5 and/or MYF6 also might cooperate with PITX2 to control *Myod* expression during myotome development. Hence, all these previous data point out that the hierarchical position occupied by *Pitx2* within the genetic cascade that control somite-derived myogenesis remain unsolved.

Additionally, some scientific evidences have related Pitx2 to cell proliferation in myogenic cells and somite derivates. Thus, it has been reported that is a target gene in the Wnt/Dvl2/beta-catenin pathway and operates in myoblasts cell lines to control proliferation by regulating expression of the growth-control genes Ccnd1, Ccnd2 [14,15]. Further, *in vivo* studies have supported the role of Pitx2 in cell proliferation during myogenesis. Pitx2 loss of function in chicken embryos decreased the number of differentiated myocytes/myofibers in the somites, whereas Pitx2 overexpression increased myocyte/myofiber numbers, particularly in the epaxial region of the myotome [16]. Moreover, by using Pitx2-/- mutant embryos, we have previously reported that Pitx2 might be acts balancing the number of Pax3+/Pax7- *versus* Pax3+/Pax7+ myogenic progenitors' populations in the limb bud by controlling cell proliferation [16].

Besides, the continued expression of Pitx2 throughout the myogenic progression makes it difficult to separate early and late Pitx2 functions together with the fact that systemic null mutants show early phenotypes at many non-muscle locations and die between E12.5 and E14.5 [18,19, 20] preclude

evaluation of a complete muscle phenotype and complicate the genetic analysis of Pitx2 function in nascent trunk muscle.

To get insight into this issue, we have differentially generated two conditional *Pitx2* mutant mice to specifically inactivate Pitx2 in multipotent Pax3+ muscle progenitors (Pax3Cre+/Pitxloxp/loxp mice) and in myogenic committed progenitors (Myf5Cre+/Pitx2loxp/loxp mice). Our analyses revealed that Pitx2 inactivation in Pax3+ precursors lead to impaired myogenesis while the loss of Pitx2 in Myf5+ myogenic cells give rise apparent normal musculature containing satellite cells expressing high levels of PAX7 with severe consequences in muscle regeneration.

RESULTS

Loss of Pitx2 in Pax3+ multipotent myogenic progenitors decrease migration of Pax3+ cells and led to perinatal lethality.

To better understand the role *Pitx2* in Pax3+ multipotent myogenic progenitors we have generated Pax3Cre+/Pitxloxp conditional mutant mice. Deletion of Pitx2 in Pax3+ cells lead to perinatal lethality since the number of Pax3Cre-Pitx2-loxp-/- homozygous mutants dramatically decrease around day one after birth and no homozygous mice survived after day 1/day 2 after birth indicating perinatal lethality **(Supplementary Figure 1).** We first check for myogenic precursors population in these mutants by evaluating Pax3 expression; at E10.5 no evident changes in Pax3 expression pattern in somites were detected in Pax3Cre+/Pitx2-loxp-/- conditional mutant mice **(Figure 1A).** However, we observed that the number of Pax3+ cells in the limb buds is reduced in

homozygous conditional mutant embryos respect to heterozygous and wild type mice **(Figure 1B),** suggesting that the number of Pax3 cells that migrate into limb bud is decreased in these mutant mice.

Because migration of Pax3+ cardiac neural crest (CNC) cells is required for proper septation of the outflow tract (OFT) during in the developing heart [21,22, 23, 24]; and the role of Pitx2 in the formation of OFT septum remains controversial [25,26,27]; we first evaluate in mouse and chick embryos Pitx2 expression pattern in Pax3+ CNC migrating cell population by immunohistochemistry, and we found a clear co-location on Pitx2 in Pax3+ CNC cells **(Figure 2A).** Notably, and as observed in **Figure 2B** the migration of Pax3+ CNC cells contributing to cardiac chamber septation is also compromised in Pax3Cre+/ Pitx2loxp-/- homozygous mutant mice. As a consequence, around 40% of the homozygous mutants display cardiac defects such as Double outlet right ventricle (DORV) **(Figure 2C).** This cardiac anomaly could explain, at least in part, the perinatal lethality and reveal a Pitx2 requirement for the migration of Pax3+ cardiac neural crest. To further address the role of Pitx2 in CNC cell migration we have performed Pitx2 loss-of function experiments by Morpholinos in pre-migrating cardiac neural crest of the chick embryo (HH10). Interestingly we observed that Pitx2 blockage by morpholino electroporation in the presumptive CNC at HH10 lead to a clear decrease in the migration of electroporated cells through the brachial arches **(Figure 2D)** reinforcing the notion of that Pitx2 is required for migration of Pax3+ CNC cells.

Pax3Cre+/Pitx2loxp-/- conditional mutant mice display retarded myogenesis and muscle hypotrophy.

Next, we look for the impact of Pitx2 deletion on myogenic lineage progression by analysing MyoD and myogenin expression pattern. A delay of myogenic differentiation only in the limb buds of systemic Pitx2 null mutant have been previously reported [13]. However, in Pax3Cre+/Pitx2-/- conditional mutant mice we observed a clear deficit of MyoD and myogenin expression in myotomes at E10.5 but MyoD expression is rescued later at E12.5 **(Figure 3A and 3B).** Consistent with our previously reported analysis in Pitx2 systemic mutants indicating a role of Pitx2 in cell proliferation in myogenic precursors; we detected a clear decrease in the number of proliferative cells in the myotome of Pax3Cre+/Pitx2-/- mutant mice at E10.5 **(Supplementary Figure 2);** indicating that delayed MyoD expression is concomitant with retarded cell proliferation of myogenic progenitors joining the myotome.

In addition, and in agreement with the idea to a decreased migration of Pax3+ myogenic precursors, MyoD and myogenin expression were decreased in the limb buds of Pax3Cre+/Pitx2-/- mutant mice at E12.5 **(Figure 3C)**.

To evaluate the consequences of Pitx2 deletion during subsequent fetal myogenesis, we analysed the epaxial and hypaxial muscle mass at E14.5 by MF20 staining. As observed in **Figure 4A** Pax3Cre+/Pitx2loxp-/- conditional mutant mice display muscle hypotrophy in epaxial and hypaxial fetal muscles as well in the diaphragm. This observation indicate that neonatal lethality may be

also due a to severe diaphragm hypotrophy. Beginning at E14.5, secondary myotubes form in tight association with primary myotubes, and they account for much of the muscle growth during fetal development [4]. Thus, in order to evaluate secondary myogenesis, the number of MHC+ secondary myotubes formed in mutant embryos. Our results showed that the number of secondary myotubes were severely reduced in mutant muscles, but they were frequently observed in wild-type **(Figure 4B)** indicating that secondary myogenesis is also impaired in these mutant mice.

Muscle hypotrophy persist in this Pax3Cre+/Pitx2loxp-/- conditional mutant at neonatal stages as observed by a decreased in the number of muscle fibers together a shift in the distribution of the fiber size to the lowest area classes **(Figure 5A).** Since $Pax3^{+}/Pax7^{+}$ embryonic progenitor cells are the major source of adult satellite cells in trunk and limb muscles, we also looked for satellite cells in Pax3Cre-Pitx2loxp-/- mutant and, as illustrated in **Figure 5A**, the number of satellite cells was also decreased indicating that Pitx2 inactivation on myogenic precursors also impact the pool of satellite cell population that remain in the adult muscle.

The adult phenotypic analysis of these conditional mutant mice was completed by using adult heterozygous mutant mice. As observed in **Figure 5B**, the muscles of adult Pax3cre/Pitx2loxp+/- heterozygous mice also displayed a shift in the distribution of the fiber size to the lowest area classes as well as a reduced number of satellite cells **(Figure 5B).**

Regeneration-related activity is diminished in Pax3cre/Pitx2+/- heterozygous mice

Since we have observed a reduction of satellite cell number in Pax3cre/Pitx2+/- heterozygous mice, we decided to evaluate satellite cell function in these mice. Heterozygosis for a deletion in the *Pitx2* gene in Pax3+ cells lowered the number of differentiated myotubes during *in vitro* differentiation **(Supplementary Figure 3A)** also decreasing the number of myogenin+ nuclei **(Supplementary Figure 3B)**. These findings reinforce the notion that the loss of *Pitx2* function in Pax3+ myogenic progenitors alters the behaviour of activated satellite cells, diminishing their performance to form myofibres.

To further investigate the role of *Pitx2* during muscle regeneration *in vivo*, we induced skeletal-muscle damage by cardiotoxin injection (CTX) in the tibialis anterioris (TA) of 4-month-old *Pax3Cre*$^{+/-}$*/Pitx2*$^{+/-}$ heterozygote mice and *Pax3Cre+/-* control mice. After skeletal-muscle injury, we evaluated the impact of genetic loss of *Pitx2* on the myogenic response during the initial waves of muscle regeneration by analysing the number of Pax7+/MyoD+ satellite cells at 7 days after damage **(Figures 6A)**. Moreover, regeneration was impaired, as indicated by smaller myofibre size 15 days after injury compared to *Pax3Cre+/-* mice **(Figures 6B)**, emphasizing the requirement of *Pitx2* for *in vivo* myogenic differentiation.

To evaluate muscle function, *Pax3cre*$^{+/-}$*/Pitx2*$^{+/-}$ heterozygote mice were submitted to treadmill tests until exhaustion 30 days after injury. Strikingly, the

running time and distance in the transgenic mice diminished by 23% and 34%, respectively **(Figure 6C)**. These results further support the notion that the reduced number of Pax7+ satellite cells in *Pax3cre*$^{+/-}$*/Pitx2*$^{+/-}$ heterozygote mice trigger muscle regeneration.

The lack of Pitx2 function in Myf5+ committed myogenic precursors give rise to normal muscles with satellite cells expressing high levels of Pax7.

The first sign of myogenic compromise during development is the activation of the myogenic factor Myf5 in the progenitor's cells into somites. Thus, to full address how Pitx2 acts in myogenic progression during skeletal myogenesis, we genetically ablated *Pitx2* in myogenic committed progenitor cells by intercrossing a *Pitx2* floxed mouse line with a *Cre* deletor mouse line (B195AP-Cre)**,** which rendered muscle-lineage-specific *Myf5Cre* recombination [28]. Mice lacking Pitx2 in Myf5+ myogenic precursors developed into normal adults and their muscles to have normal fiber size **(Figure 7A-B).**

Because it has been previously established that adult satellite cells derive from progenitors that express the myogenic determination gene Myf5 during fetal stages of myogenesis [29]; we wondered if the lack of Pitx2 function in Myf5 progenitors' cell may affect to the satellite cell population in the adult muscle. To check this; we performed Pax7 and laminin co-immunostaining in 4 months old Myf5Cre/Pitx2 conditional mutants. Quantification of the number of Pax7+ sublaminar cells showed a not significative tendency to a high number of satellite cells in the muscle Myf5Cre/Pitx2-/- homozygous mutant mice respect

to heterozygous and wild-type mice **(Figure 7B)**. However, RT-PCR analyses for Pax7 expression levels revealed that the level of Pax7 expression was two-fold increase in Myf5Cre/Pitx2-/- homozygous mutant mice **(Figure 7C)** indicating that satellite cells in these mutants exhibit high levels of Pax7 expression.

Myf5Cre/Pitx2-/- mutant mice display severe defects on muscle regeneration

On account of the maintenance of high levels of Pax7 on satellite cells might alter proper myogenic terminal differentiation finally affecting its regenerative capacity [30,31,32]; we next set up to explore if high Pax7 expression in satellite cells in Myf5Cre/Pitx2-/- mutant mice might modify muscle regeneration potential. To check that, skeletal-muscle damage was induced in 4-month-old *Myf5Cre*$^{+/-}$*/Pitx2*$^{-/-}$ homozygous, *Myf5Cre*$^{+/-}$*/Pitx2*$^{+/-}$ heterozygotes and *Myf5Cre+/-* control mice. We found that satellite cells of *Myf5Cre*$^{+/-}$*/Pitx2*$^{-/-}$ mice display a lower propensity to proliferate at day 3 of muscle injury, as observed by the lowest number of MyoD^{pos}/KI67^{pos} cells **(Figure 8A)**, which suggests that the inactivation of Pitx2 in Myf5+ cells **(Figure 8B)** decrease the functional ability of SCs to activate and participate in tissue repair.

We also tested tissue regeneration by analysing the newly formed myofibers by using an eMyHC antibody on day 7 of cardiotoxin injection. As observed in the **Figure 8B**, the number of eMyHC^{pos} myofibers was dramatically decreased in the injured muscles of *Myf5Cre*$^{+/-}$*/Pitx2*$^{-/-}$ homozygous respect to Myf*5Cre*$^{+/-}$

/Pitx2$^{+/-}$ heterozygotes and *Myf5Cre+/-* control mice. The histological analysis of the TA at 15 days after muscle damage clearly showed a lower percentage of fibers with centralised nuclei **(Figure 8C)** as well as a shift in the distribution of the regenerating fiber size to the lowest area classes **(Figure 8C).** Together, these findings indicate that the regenerative potential of satellite cells in *Myf5Cre*$^{+/-}$*/Pitx2*$^{-/-}$ homozygous mice was clearly decreased.

DISCUSSION

Several previous evidences have revealed that the transcription factor Pitx2 might be a player within the molecular pathways controlling somite-derived muscle progenitors cell fate [13,14,15,16, 33]. However, the hierarchical position occupied by *Pitx2* within the genetic cascade that control somite-derived myogenesis as well as its role on later foetal muscle mass remain unsolved. To get insight into this issue, we have differentially generated two conditional *Pitx2* mutant mice to specifically inactivate Pitx2 in multipotent Pax3+ muscle progenitors (Pax3Cre+/Pitxloxp/loxp mice) and in myogenic committed progenitors (Myf5Cre+/Pitx2loxp/loxp mice). Our analyses revealed that Pitx2 inactivation in Pax3+ precursors lead to impaired myogenesis with severe muscle hypotrophy while the loss of Pitx2 in Myf5+ myogenic cells have an impact satellite cell activity with severe consequences in muscle regeneration.

Although, several seminal works suggest that Pitx2 could be acting downstream of Pax3 and in parallel with Myf5, at least in the myotome, [13,34,35]; the specific role of Pitx2 in multipotent muscle progenitors and/or myogenic

committed progenitors during skeletal muscle development in not well understood. It has been previously showed that systemic Pitx2-/- null mutants display a delay in the onset of MyoD and myogenin expression in the limb buds [13]. However, our analysis revealed that the lack of Pitx2 function in Pax3+ multipotent myogenic progenitors give rise to a delay of the onset of myogenic differentiation in the myotome, as observed by a delay in the beginning of MyoD and myogenin expression at E12.5 in Pax3Cre+/Pitx2loxp-/- mutant embryos, indicating that Pitx2 function is required for initial activation of the MyoD gene also in the myotome. In addition, we observed that the number of Pax3+ progenitors that migrate into limb buds is decreased in Pax3Cre+/Pitx2-/- mutant embryos; leading thus later on to a lower MyoD and myogenin cell population in the limbs. These results suggest a requirement of Pitx2 function for proper migration of Pax3 precursors cells.

In agreement with this idea, we also notice that in Pax3Cre+/Pitx2-/- mutant embryos display a significant reduction of Pax3+ migrating cardiac neural crest cells into the outflow tract (OFT) in the developing heart leading to severe cardiac defects such as double outet right ventricle (DORV). Although previous reports have suggested that mutation of the Pitx2 gene causes defects in OFT based on events in cardiac neural crest [14,31]; the role of Pitx2 in cardiac neural crest (CNC) cells is controversial. Therefore, Ai et al Dev Biol 2006 [36]; by using the CNC driver Wnt11, found that there is no requirement for Pitx2 in CNCC, but instead it is needed in the cells derived from the second heart field. In this context it has been demonstrated that the onset of Pax3 precedes Wnt1-Cre expression within the neural folds [37]; and Olaopa et al (2011) [38] showed

that Pax3 function in the CNC progenitors is necessary prior to Wnt1-Cre expression. Here, we show that Pax3 + CNC express Pitx2 in the mouse and chick embryo and the lack of Pitx2 function in CNC cells also lead to a dramatic decrease in CNC cell migration. Thus, our results point out for the first time the role of Pitx2 in early migration of Pax3+ cardiac neural crest cells.

Notably, we observed that Pax3Cre+/Pitx2loxp-/- mutant mice display a clear muscle hypotrophy at fetal stages; this phenotype might probably be due to the defects on cell migration detected at embryonic stages. In parallel secondary myotubes formation is also affected in the foetal muscle stages suggesting that Pitx2 function is necessary to complete proper secondary myogenesis. This hypotrophic phenotype is maintained in the neonatal muscle of Pax3Cre+/Pitx2loxp-/- mice; together with a reduced number of satellite stem cells. Muscle hypotrophy and a reduced number of satellite cell is also present in the adult muscle of Pax3Cre+/Pitx2loxp+/- heterozygous mice. Experiments of induced muscle injury in these heterozygous mice demonstrated that their regenerative capacity were highly compromised. These results agree with our previous reported work highlighting the relevance of Pitx2 in the context of muscle regeneration.

Contrary to Pax3Cre+/Pitx2-loxp/- conditional mutant mice; Myf5Cre+/Pitx2-/- conditional mutant mice developed into normal adults and their muscles appear to have normal fiber size, indicating that the lack of Pitx2 function in myogenic committed progenitors have not consequences in the developing muscle. However, we have detected dramatic defects on satellite cell function

Myf5Cre+/Pitx2loxp-/- conditional mutant mice due to high Pax7 expression. These findings together with the fact we observed that satellite cells of Pax3Cre+/Pitx2loxp+/- heterozygous mice also display defects on myogenic differentiation suggest that Pitx2 is important to satellite cell myogenic differentiation. Overall, our results shown that the lack of Pitx2 function at early stages of myogenesis on Pax3+ multipotent myogenic progenitors lead to deficient muscle formation during development (hypotrophy) and functional-defective satellite cells, whereas Pitx2 inactivation at a later point of myogenesis in Myf5+ progenitors only impact on satellite cell function with dramatic consequences in muscle regeneration.

MATERIAL AND METHODS

Generation of conditional tissue-specific null mutant mice.

Animals procedures were approved by the University of Jaen Ethics Committee, and it was conducted according the national and European community guidelines regulations for animal care and handling. All mice were maintained inside a barrier facility where food and water were administered *ad libitum*.

B6;129-Pax3tm1(cre)Joe/J (ref. 005549) transgenic mice were supplied by The Jackson Laboratory. Myf5Cre+ were kindly supplied by Victor Luis Ruiz Pérez, (Instituto de Investigaciones Biomédicas de Madrid). Both transgenic mice were crossed into homozygous Pitx2 floxed mice kindly supplied by Marina Campione (Pathophysiology of Striated Muscle Group, Universitá degli Studi di Padova). $Pax3Cre^{+/-}$ $Pitx2^{fl+/-}$ heterozygotes were backcrossed. In the same way, $Myf5Cre^{+/-}$ $Pitx2^{fl+/-}$ and $Myf5Cre^{+/-}$ $Pitx2^{fl+/+}$ were backcrossed too. The

littermates were PCR screened with Pitx2- and Cre-specific primers (Table 1). $Pitx2^{fl+/+}$ homozygotes mice were selected as wild-type controls. All mice were maintained inside a barrier facility, and experiments were performed in accordance with University of Jaen regulations for animal care and handling.

PCR genotyping.

The DNA was isolated from different tissues depending of the animal age. For adult animals, ear DNA was used for genotyping by PCR while for newborns the DNA was isolated from the tail and from the yolk sac for embryo stages. One microliter of neutralized DNA samples was used for PCR reaction using DreamTaq DNA Polymerase (ThermoFisher) with buffers supplied by the manufacturer with 0.4 mM dNTPs and 4 mM $MgCl_2$. The PCR products were resolved in agarose gel (2% for Pitx2 PCR product and 1,5% for $Pax3Cre^+$ and $Myf5Cre^+$ PCR product), stained with 0.5 µg ml^{-1} ethidium bromide (Gibco), and digitally imaged for record keeping.

Cardiotoxin (CTX) and muscle injury:

Cardiotoxin (Sigma) was prepared by dissolving a freshly opened tube in PBS at 10 µM. The solution was divided into Eppendorf tubes as 50 µl aliquot stocks, flash frozen, and stored at -80 °C. Each tube was thawed fresh before injection and not re-used. Animals were anaesthetized by intraperitoneal injection of ketamine/xylazine. The tibialis anterior muscles of 4 months old mice were injected with 50 µl of cardiotoxin using an insulin needle. Cardiotoxin animals

were kept on a warming blanket until recovery before being returned to a normal cage rack. For immunohistochemistry and histological analysis, the animals were killed and TA muscles were collected at 3, 7, 15 and 30 days after cardiotoxin injection.

Exercise tolerance test

An exhaustion treadmill was performed to evaluate the endurance of the mice by using the motorized treadmill LE8708 single mouse, Treadmill, PanLab, Harvard Apparatus supplied with shocker plate as described elsewhere [39]. The treadmill was run at an inclination of 0° at 5 m/min for 5 min, after which the speed was increased 1 m/min every minute. The test was then stopped when the mouse remained on the shocker plate for 20 seconds without any attempt to reengage the treadmill. Distance (meters) and the time to exhaustion (expressed in minutes) was determined. For immunohistochemistry and histological analysis, the animals were killed and TA muscles were collected, frozen in liquid nitrogen cooled isopentane for sectioning and preserved at -80ºC.

Tibialis anterior muscle collection

Mice were sacrificed by cervical dislocation. TA were collected and frozen in liquid nitrogen-cooled isopentane for sectioning or in liquid nitrogen for total RNA isolation and store at -80ºC.

For histological analysis tissue specimens were sliced using a cryostat microtome to 10 µm thick and mounted onto Thermo Scientific™ SuperFrost Ultra Plus™ Adhesion Slides.

Whole-mount in situ hybridization

Mouse embryos from E10.5 and E12.5 were fixed and store in 4% PFA at 4ºC. Complementary RNA digoxigenin-labelled probes of Pax3, Pax7, Myf5, MyoD and MyoG were generated using standard protocols. Embryos head were holed carefully to avoid the trapping. The embryos were washed in PBT (PBS x10, 0,1% Tween® 20) and MetOH to be dehydrated before be bleached (6% H_2O_2/MetOH) in darkness. After be rehydrated with PBT, the embryos were treated with Proteinase K and postfix (0,2% glutaraldehyde 4% PFA). Prehybridization washes (50% Formamide, 25% SSC x20 pH4.5, 2% SDS , 2% BBR, 0,025% yeast tRNA, 1% Heparin) and hybridization were carried out at 70ºC with following washes (50% Formamide, 20% SSC x20 pH4.5, 2% SDS) at the same temperature. The staining (0,15% NBT, 0,2% BCIP on NTMT) was realized at RT.

Inmunohistochemistry

Series of 10 µm transverse cryosections cut over the mouse tibialis anterior muscles (TA) length were examined by immunohistochemical staining. The tissue sections were fixed in 4% PFA for 10 min at RT. For PAX7,

immunostaining, epitopes were unmasked in citrate buffer (10 mM Sodium Citrate, 0.05% Tween-20, pH 6.0) in a pre-heat water bath 30 min at 95ºC. Afterwards, all samples were washed twice in PBS and incubated in TBSA-BSAT (10 mM Tris, 0.9% NaCl, 0.02% sodium azide, 2% BSA and 0.1% Triton X-100) at RT for 30 min. The antibodies were diluted to 5 µg/µl into TBSA-BSAT and incubated overnight at 4°C in a humidified chamber. The antibody solutions were removed and the samples were washed with TBSA-BSAT twice at RT. Alexa-conjugated secondary antibodies (Thermo Fisher Scientific, 1/200) were applied to the samples and incubated for 2 hours at RT. The antibody solutions were then removed and washed two times in PBS. Finally, sections were incubated with DAPI in PBS 1/2000 for 15 min at RT. The samples were mounted with Hydromount (National Diagnosis. HS-106) after two PBS and two H_2O milliQ washes. Images were acquired on a Leica TCS SPE-CTR6500 Confocal Microscope.

For tissue samples from paraffin, the slides were heated at 60ºC during 10 minutes and dewax in xylene washes and rehydrated in diminishing alcohol washes before be blocked with TBSA solution. Antibodies list is shown in Table 2.

Cross-section area

To analyse the size of skeletal muscle fibers, we measured the fibre cross-sectional area as described (Moresi et al., 2009) using ImageJ software on adult and neonatal TA sliced.

Total RNA extraction and reverse transcription

Muscle total RNA was extracted from treated tibialis anterior muscles by using Direct-zol™ RNA MiniPrep-Zymo Research kit (Zymo Research, R2050) following manufacturer's instructions. One microgram of total RNA was reverse transcribed using Maxima First Strand cDNA Synthesis Kit (Thermo Fisher, K1642) following manufacturer's instructions. As a reverse transcription negative control, each sample was subjected to the same process without reverse transcriptase.

qRT-PCR analyses:

Real-time PCR was performed by using an MxPro Mx3005p PCR thermal cycler (Stratagene, Spain) using SsoFast™ EvaGreen® Supermix (Bio-Rad, 1725201) and primers listed in supplementary information Table 3. The relative level of expression of each gene was calculated as the ratio of the extrapolated levels of expression of each gene and Gapdh and Gusb genes as mRNA normalizers. Each PCR reaction was performed in triplicate and repeated at least in three different biological samples to have a representative average. Relative measurements were calculated as described Pfaffl MW. qPCR program consisted in 95ºC for 30 seconds (initial denaturalization), followed by 40 cycles of 95ºC for 5 seconds (denaturalization); 60ºC for 10 seconds (annealing) and 75ºC for 7 seconds (extension). Finally melt curves were determined by an initial step of 95ºC for 5 seconds followed by 0,5ºC increments for 7 seconds

from 65 to 95ºC. The relative level of expression of each gene was calculated as the ratio of the extrapolated levels of expression of each gene and Gapdh and Gusb genes as normalizers. Primers used are shown in Table 3.

Quantification and statistical analysis

For comparison between two groups, two- tailed paired, unpaired Student's t tests were performed to calculate p-values and to determine statistically significant differences. The number of independent experimental replications (n value ≥ 3: mice, experiments, wells or counted cells/muscles). Mean ± SD and statistical test (p-value) are reported in each corresponding figure legend. All statistical analyses were performed with GraphPad Prism. Image were processed for quantification with ImageJ software.

Electroporation

Eggs are incubated with the blunt end up in a humidified incubator at 37ºC. To obtain HH10 embryos we incubated fertile eggs for approximately 38h.

Remove shell pieces until embryo is easily accessible and in a shallow angle inject ink-mix (1:500 PBS/ Pen Strep (PS) on with Indian ink beneath the embryo for contrast and apply 2 drops PBS/PS-solution on top to increase elasticity of extra-embryonic tissues (EET).

Use syringe needle to cut open the vitelline membrane. Perform injection in area of interest using a needle for microinjection (borosilicate glass capillaries 1.00 mm O.D. × 0.78 mm I.D.). Load needle with ~1.5 µl Morpholino (5'CCTTCATGCAACTCATCGGCGAGAG3') at 1 µM using Microloader™ (Eppendorf) and mount onto microinjector (20 Volts, 4 pulses, 950 milliseconds space, 50 milliseconds/pulse). Remove needle and visually confirm injection.

Slide the needle of the large syringe down along the inside of the egg shell and remove albumen until the embryo is sufficiently lowered and will not touch the sealing tape.

Apply a few drops PBS/PS-solution. Seal the egg using clear adhesive tape and Return the egg to an incubator immediately. Collect the embryos after 24h or 48h.

ACKNOWLEDGMENTS

This work was partially supported by grants, BFU2015-67131 (Ministerio de Economía y Competitividad, Gobierno de España), CTS-1614 (Junta de Andalucía), P08-CTS-03878, and by Duchenne Parent Project Spain-2016 and 2019 grants. VAG also acknowledges funding from the Health Institute 'Carlos III' (ISCIII, Spain) and the European Regional Development Fund, (ERDF/FEDER), (Grants CP12/03057 and CPII17/00004); Duchenne Parent Project Spain (grant 05/2016) and Ikerbasque (Basque Foundation for Science).

REFERENCES

1.- Margaret Buckingham. Gene regulatory networks and cell lineages that underlie the formation of skeletal muscle. 2017. PNAS. 114 (23): 5830-5837.

2.- Jérome Chaland Olivier Pourquie. Making muscle: skeletal myogenesis in vivo and in vitro. 2017. Development, 144:2104-2122.

3.- Francisco Hernandez-Torres, Lara Rodríguez-Outeiriño, Diego Franco1 and Amelia E. Aranega. Pitx2 in Embryonic and Adult Myogenesis. 2017. Frontiers in Cell and Developmental Biology. 5: article 46.

4.- Margaret Buckingham , Lola Bajard, Ted Chang, Philippe Daubas, Juliette Hadchouel, Sigolène Meilhac, Didier Montarras, Didier Rocancourt, Frédéric Relaix. The Formation of Skeletal Muscle: From Somite to Limb. 2003. J Anat , 202 (1), 59-68.

5.- Fabienne Lescroart , Wissam Hamou , Alexandre Francou , Magali Théveniau-Ruissy , Robert G Kelly , Margaret Buckingham . Clonal Analysis Reveals a Common Origin Between Nonsomite-Derived Neck Muscles and Heart Myocardium. 2015. PNAS. 112 (5), 1446-51.

6.- Swetha Gopalakrishnan, Glenda Comai, Ramkumar Sambasivan, Alexandre Francou, Robert G. Kelly, Shahragim Tajbakhsh. A Cranial Mesoderm Origin for Esophagus Striated Muscles. 2015. Developmental Cell, 34: 694-704.

7.- Eldad Tzahor. Head Muscle Development. 2015. Results Probl Cell. Differ, 56, 123-42.Gnes &

8.- Frédéric Relaix , Didier Rocancourt, Ahmed Mansouri, Margaret Buckingham. A Pax3/Pax7-dependent Population of Skeletal Muscle Progenitor Cells. 2005. Nature. 435 (7044), 948-53.

9.- Frédéric Relaix, Didier Montarras, Stéphane Zaffran, Barbara Gayraud-Morel, Didier Rocancourt, Shahragim Tajbakhsh, Ahmed Mansouri, Ana Cumano, and Margaret Buckingham. Pax3 and Pax7 have distinct and overlapping functions in adult muscle progenitor cells. 2006. J Cell Biol. 172(1): 91–102.

10.- Graziella Messina and Giulio Cossu. The origin of embryonic and fetal myoblasts: a role of Pax3 and Pax7. 2009Genes & Development. 23:902–905.

11.- Kitamura, K., Miura, H., Miyagawa-Tomita, S., Yanazawa, M., Katoh-Fukui, Y., Suzuki, R., Ohuchi, H., Suehiro, A., Motegi, Y., Nakahara, Y., Kondo, S., Yokoyama, M., 1999. Mouse Pitx2 deficiency leads to anomalies of the ventral body wall, heart, extra- and periocular mesoderm and right pulmonary isomerism. Development 126, 5749–5758.

12.- Shih, H.-P., Gross, M.K., Kioussi, C., 2007b. Cranial muscle defects of Pitx2 mutants result from specification defects in the first branchial arch. Proc. Natl. Acad. Sci. USA 104, 5907–5912. http://dx.doi.org/10.1073/pnas.0701122104.

13.- Aurore L'Honoré, Jean-François Ouimette, Marisol Lavertu-Jolin, Jacques Drouin. Pitx2 defines alternate pathways acting through MyoD during limb and somitic myogenesis. 2010. Development. 137: 3847-3856.

14.- Kioussi, C., Briata, P., Baek, S.H., Rose, D.W., Hamblet, N.S., Herman, T., Ohgi, K.A., Lin, C., Gleiberman, A., Wang, J., Brault, V., Ruiz-Lozano, P., Nguyen, H.D., Kemler, R., Glass, C.K., Wynshaw-Boris, A., Rosenfeld, M.G., 2002. Identification of a Wnt/ Dvl/beta-Catenin – > Pitx2 pathway mediating cell-type-specific proliferation during development. CELL 111, 673–685.

15.- Sergio Martínez-Fernandez , Francisco Hernández-Torres, Diego Franco, Gary E Lyons, Francisco Navarro, Amelia E Aránega. Pitx2c Overexpression Promotes Cell Proliferation and Arrests Differentiation in Myoblasts. 2006. Dev Dyn, 235 (11), 2930-9.

16.- Abu-Elmagd, M., Robson, L., Sweetman, D., Hadley, J., Francis-West, P., Münsterberg, A., 2010. Wnt/Lef1 signaling acts via Pitx2 to regulate somite myogenesis. Dev. Biol. 337, 211–219. http://dx.doi.org/10.1016/j.ydbio.2009.10.023.

17.- Lozano-Velasco, E., Contreras, A., Crist, C., Hernández-Torres, F., Franco, D., Aránega, A.E., 2011. Pitx2c modulates Pax3+/Pax7+ cell populations and regulates Pax3 expression by repressing miR27 expression during myogenesis. Dev. Biol. 357, 165–178. http://dx.doi.org/10.1016/j.ydbio.2011.06.039.

18.- Gage, P.J., Suh, H., Camper, S.A., 1999. Dosage requirement of Pitx2 for development of multiple organs. Development 126, 4643–4651.

19.- Lu, M.F., Pressman, C., Dyer, R., Johnson, R.L., Martin, J.F., 1999. Function of Rieger syndrome gene in left-right asymmetry and craniofacial development. Nature 401, 276–278.

20.- Lin, C.R., Kioussi, C., O'Connell, S., Briata, P., Szeto, D., Liu, F., Izpisua-Belmonte, J.C., Rosenfeld, M.G., 1999. Pitx2 regulates lung asymmetry, cardiac positioning and pituitary and tooth morphogenesis. Nature 401, 279–282. http://dx.doi.org/10.1038/45803.

21.- Chan WY, Cheung CS, Yung KM, Copp AJ. Cardiac neural crest of the mouse embryo: Axial level of origin, migratory pathway and cell autonomy of the Splotch (Sp2H) mutant effect. Development. 2004; 131:3367–3379. [PubMed: 15226254].

22.- Conway SJ, Henderson DJ, Copp AJ. Pax3 is required for cardiac neural crest migration in the mouse: Evidence from the Splotch (Sp2H) mutant. Development. 1997; 124:505–514. [PubMed: 9053326].

23.- Epstein JA, Li J, Lang D, Chen F, Brown CB, Jin F, Lu MM, Thomas M, Liu E, Wessels A, Lo CW. Migration of cardiac neural crest cells in Splotch embryos. Development. 2000; 127:1869–1878. [PubMed: 10751175].

24.- Brian L. Nelms, Elise R. Pfaltzgraff, and Patricia A. Labosky*Functional Interaction Between Foxd3 and Pax3 in Cardiac Neural Crest Development. 2010. Genesis. 2011 January ; 49(1): 10–23.

25.- Fanny Bajolle, Ste´phane Zaffran, Robert G. Kelly, Juliette Hadchouel, Damien Bonnet, Nigel A. Brown, Margaret E. Buckingham. Rotation of the Myocardial Wall of the Outflow Tract IsImplicated in the Normal Positioning of the Great Arteries. 2006. Circulation Research. 98:421-428

26.- Di Aia, Wei Liua, Lijiang Maa, Feiyan Donga, Mei-Fang Lua, Degang Wanga, Michael P. Verzid, Chenleng Caic, Philip J. Gageb, Sylvia Evansc, Brian L. Blackd, Nigel A. Browne, and James F. Martin. *Pitx2* regulates cardiac left-right asymmetry by pattering second lieage-derived myocardium. 2006. Dev Biol; 296 (2): 437-449.

27.- Hsiao-Yen Ma1, Jun Xu1, Diana Eng1, Michael K. Gross1, and Chrissa Kioussi. Pitx2-Mediated Cardiac Outflow Tract Remodeling. 2013. Dev Dyn. 242(5): 456–468.

28.- Neia Naldaiz-Gastesi, María Goicoechea, Sonia Alonso-Martín, Ana Aiastui, Macarena Lo´pez-Mayorga, Paula Garcı´a-Belda, Jaione Lacalle, Carlos San Jose´, Marcos J. Arau´zo-Bravo, Lidwine Trouilh, Ve´ronique Anton-Leberre, Diego Herrero, Ander Matheu, Antonio Bernad, Jose´ Manuel Garcı´a-Verdugo, Jaime J. Carvajal, Fre´de´ric Relaix, Adolfo Lopez de Munain, Patricia Garcı´a-Parra, and Ander Izeta. Identification

andCharacterization of the Dermal Panniculus Carnosus Muscle Stem Cells. 2016. Stem Cell Reports.7: 411-424.

29.- Stefano Biressia, Christopher R.R. Bjornsona, Poppy M.M. Carliga, Koichi Nishijob, Charles Kellerc, and Thomas A. Rando. Myf5 expression during fetal myogenesis defines the developmental progenitors of adult satellite cells. 2013. Dev Biol, 379(2): 195–207.

30.- Hugo C. Olguin, Zhihong Yang, Stephen J. Tapscott, and Bradley B. Olwin. Reciprocal inhibition between Pax7 and muscle regulatory factors modulates myogenic cell fate determination. 2007. J Cell Biol, 4; 177(5): 769–779.

31.- Olguin, H.C., and B.B. Olwin. 2004. Pax-7 up-regulation inhibits myogenesis and cell cycle progression in satellite cells: a potential mechanism for self-renewal. Dev. Biol. 275:375–388.

32.- Julia von Maltzahn, Andrew E. Jones, Robin J. Parks, and Michael A. Rudnicki. Pax7 is critical for the normal function of satellite cells in adult skeletal muscle. 2013. PNAS. 110 (41) 16474-16479.

33.-Sung Hee Baek , Chrissa Kioussi, Paola Briata, Degeng Wang, H D Nguyen, Kenneth A Ohgi, Christopher K Glass, Anthony Wynshaw-Boris, David W Rose, Michael G Rosenfeld. Regulated Subset of G1 Growth-Control Genes in Response to Derepression by the Wnt Pathway. 2003. PNAS. 100 (6), 3245-50.

34.- Mounia Lagha , Takahiko Sato, Béatrice Regnault, Ana Cumano, Aimée Zuniga, Jonathan Licht, Frédéric Relaix, Margaret Buckingham. Transcriptome Analyses Based on Genetic Screens for Pax3 Myogenic Targets in the Mouse Embryo. 2010. BMC Genomics. 11, 696.

35.-L'honoré, A., Coulon, V., Marcil, A., Lebel, M., Lafrance-Vanasse, J., Gage, P., Camper, S., Drouin, J., 2007. Sequential expression and redundancy of Pitx2 and Pitx3 genes during muscle development. Dev. Biol. 307, 421–433. http://dx.doi.org/10.1016/ j.ydbio.2007.04.034.

36.- Ai D, Liu W, Ma L, Dong F, Lu MF, Wang D, Verzi MP, Cai C, Gage PJ, Evans S, Black BL, Brown NA, Martin JF. Pitx2 regulates cardiac left-right asymmetry by patterning second cardiac lineagederived myocardium. Dev Biol. 2006; 296:437–449. [PubMed: 16836994].

37.- Chang, C.P., Stankunas, K., Shang, C., Kao, S.C., Twu, K.Y., Cleary, M.L., 2008. Pbx1 functions in distinct regulatory networks to pattern the great arteries and cardiac outflow tract. Development 135, 3577–3586.

38.- Michael Olaopa ,Hong-ming Zhou, Paige Snider , Jian Wang , Robert J. Schwartz , Anne M. Moon, Simon J. Conway. Pax3 is essential for normal cardiac neural crest morphogenesis but is not required during migration nor outflow tract septation. 2011. Dev Biol, 356: 308-322.

39.- Benchaouir R, Meregalli M, Farini A, D'Antona G, Belicchi M, Goyenvalle A, Battistelli M, Bresolin N, Bottinelli R, Garcia L & Torrente Y (2007) Restoration of Human Dystrophin Following Transplantation of Exon-Skipping-Engineered DMD Patient Stem Cells into Dystrophic Mice. *Cell Stem Cell* **1:** 646–657 Available at: http://www.ncbi.nlm.nih.gov/pubmed/18371406 [Accessed February 16, 2020]

Figure legends

Figure 1: The number of Pax3+ cells is reduced in the limb buds is reduced in homozygous conditional mutant embryos of Pax3Cre/Pitx2loxp-/-: A: Representative images of in situ hybridization for Pax3 in Pix2loxp/loxp, Pax3Cre/Pitx2loxp+/- and Pax3Cre/Pitx2loxp-/- embryo at E10.5 stage. **B:** Magnified view of representative images of in situ hybridization for Pax3 in Pix2loxp/loxp, Pax3Cre/Pitx2loxp+/- and Pax3Cre/Pitx2loxp-/- embryo at E10.5 stage. Pax3 positive cells are dotted.

Figure 2: Pitx2 is required for migration of CNC cells. A: Representative images of Pax3 and Pitx2 immunostaining in the mouse embryo at E10.5 stage. **B:** Representative images of in situ hybridization for Pax3 in Pix2loxp/loxp, Pax3Cre/Pitx2loxp+/- and Pax3Cre/Pitx2loxp-/- embryo at E10.5 stage. The arrows shown Pax3-expressing cells. **C:** Representative images showing the presence of DORV (arrow) in Pax3Cre/Pitx2loxp-/- embryo at E12.5. **D:** Pitx2 loss-of function experiments by Morpholinos in pre-migrating cardiac neural

crest of the chick embryo (HH10). The arrows indicate electroporated migrating CNC cells.

Figure 3: The onset of MyoD and miogenin expression is delayed in the myotome at E10.5 and reduced in the limb buds at E12.5 in Pax3Cre/Pitx2loxp-/- embryos. A: Representative images of in situ hybridization for MyoD in Pix2loxp/loxp, Pax3Cre/Pitx2loxp+/- and Pax3Cre/Pitx2loxp-/- embryo at E10.5 and E12.5 stages. **B:** Representative images of in situ hybridization for Myogenin in Pix2loxp/loxp, Pax3Cre/Pitx2loxp+/- and Pax3Cre/Pitx2loxp-/- embryo at E10.5 and E12.5 stages. **C:** Magnified view of representative images of in situ hybridization for MyoD and Myogenin in Pax3Cre/Pitx2loxp+/- and Pax3Cre/Pitx2loxp-/- embryo at E12.5 stage. The arrows indicate MyoD and Myogenin expression in the limb buds.

Figure 4: Pax3Cre/Pitx2loxp-/- mice display muscle hypotrophy and retarded secondary myogenesis at fetal stages. A: Representative images of MF20 immunostaining in Epaxial muscles, Hypaxial muscles and diaphragm in Pix2loxp/loxp, Pax3Cre/Pitx2loxp+/- and Pax3Cre/Pitx2loxp-/- embryo at E14.5 stage. **B:** Representative images of MF20 and Laminin immunostaining in Pix2loxp/loxp, Pax3Cre/Pitx2loxp+/- and Pax3Cre/Pitx2loxp-/- embryo at E14.5 stage. Percentage of secondary myotubes is shown.

Figure 5: A : Representative images of PAX7 and Laminin co-immunostaining in the TA muscles of Pix2loxp/loxp, Pax3Cre/Pitx2loxp+/- and Pax3Cre/Pitx2loxp-/- mice at neonatal stage. The percentage of PAX7 positive

cells, number of muscles fibers and distribution of cross-sectional area are shown. **B:** Representative images of PAX7 and Laminin in the TA muscles of Pix2loxp/loxp, Pax3Cre+/- and Pax3Cre/Pitx2loxp-/- mice at adult stage. The percentage of PAX7 positive cells, number of muscles fibers and skeletal fiber size distribution area are shown.

Figure 6: Muscle regeneration is impaired in *Pax3cre$^{+/-}$/Pitx2$^{+/-}$* heterozygote mice. **A** Representative image of Pax7+/MyoD+ cells at day 7 after cardiotoxin injection in tibialis anterioris muscle (TA) of *Pax3cre$^{+/-}$/Pitx2$^{+/-}$* heterozygote mice *vs.* controls *Pax3cre$^{+/-}$* mice. **B)** Percentage of Pax7+/MyoD+ cells at day 7 after cardiotoxin injection in *Pax3cre$^{+/-}$/Pitx2$^{+/-}$* heterozygote mice *vs.* controls *Pax3cre$^{+/-}$* mice. **C and D) C:** Cross-sectional area in tibialis anterioris (TA) muscles of *Pax3cre$^{+/-}$/Pitx2$^{+/-}$* heterozygote mice *vs.* controls *Pax3cre$^{+/-}$* mice at day 15 after cardiotoxin injection and representative images in **D**. **E)** Treadmill Test: Running time and distance of *Pax3cre$^{+/-}$/Pitx2$^{+/-}$* heterozygote mice *vs.* controls *Pax3cre$^{+/-}$* mice at day 30 after muscle injury. *p<0.1,**p<0.01, ***p<0.001,****p<0.0001.

Figure 7: Myf5Cre/Pitx2loxp-/- mice have normal survival rates but posses satellite cells with high Pax7 expression. A: Survival rates for Pitx2loxp/loxp, Myf5Cre/Pitx2loxp+/- and Myf5Cre/Pitx2loxp-/- mice. **B:** Representative images of PAX7 and Laminin co-immunostaining in the TA muscles of Pitx2loxp/loxp, Myf5Cre/Pitx2loxp+/- and Myf5Cre/Pitx2loxp-/- mice. The percentage of PAX7 positive cells is shown. **C:** RT-PCR analyses for Pax7 in the TA muscles of Pitx2loxp/loxp, Myf5Cre/Pitx2loxp+/- and Myf5Cre/Pitx2loxp-/- mice.

Figure 8: Muscle regeneration is dramatically affected in *Myf5cre$^{+/-}$/Pitx2$^{-/-}$* mice. **A:** Scheme of CTX injection in the TA of C57BL/6 mice Pitx2loxp/loxp, Myf5Cre/Pitx2loxp+/- and Myf5Cre/Pitx2loxp-/- mice and representative images of PAX7 and Laminin co-immunostaining in the TA muscles of Pitx2loxp/loxp, Myf5Cre/Pitx2loxp+/- and Myf5Cre/Pitx2loxp-/- mice at 15 days of cardiotoxin-muscle damage. The percentages of eMyHC positive myofibers and centralized nuclei are shown.

Supplementary Figure Legends

Figure S1: Mendelian ratios and survival rates for Pitx2loxp/loxp, Myf5Cre/Pitx2loxp+/- and Myf5Cre/Pitx2loxp-/- mice

Figure S2: Representative images of Desmin and Ki67 immunostaining in the myotome of Pix2loxp/loxp, Pax3Cre/Pitx2loxp+/- and Pax3Cre/Pitx2loxp-/- mice at E10.5 stage.

Figure S3: Satellite cell isolated from Pax3Cre+/-/Pitx2+/- heterozygote mice, in which Pitx2 expression is reduced by around 50% (A), exhibited a lower number of differentiated myotubes during in vitro differentiation (B-C), a decreased myogenin expression (D) as well as a diminished number ofmyogenin+ nuclei (E- F). *p<0.1, ***p<0.001, ****p<0.0001.

Figure 1

A

Pitx2loxp/loxp
E10.5

Pax3Cre+/-/Pitx2loxp+/-
E10.5

Pax3Cre+/-/Pitx2loxp-/-
E10.5

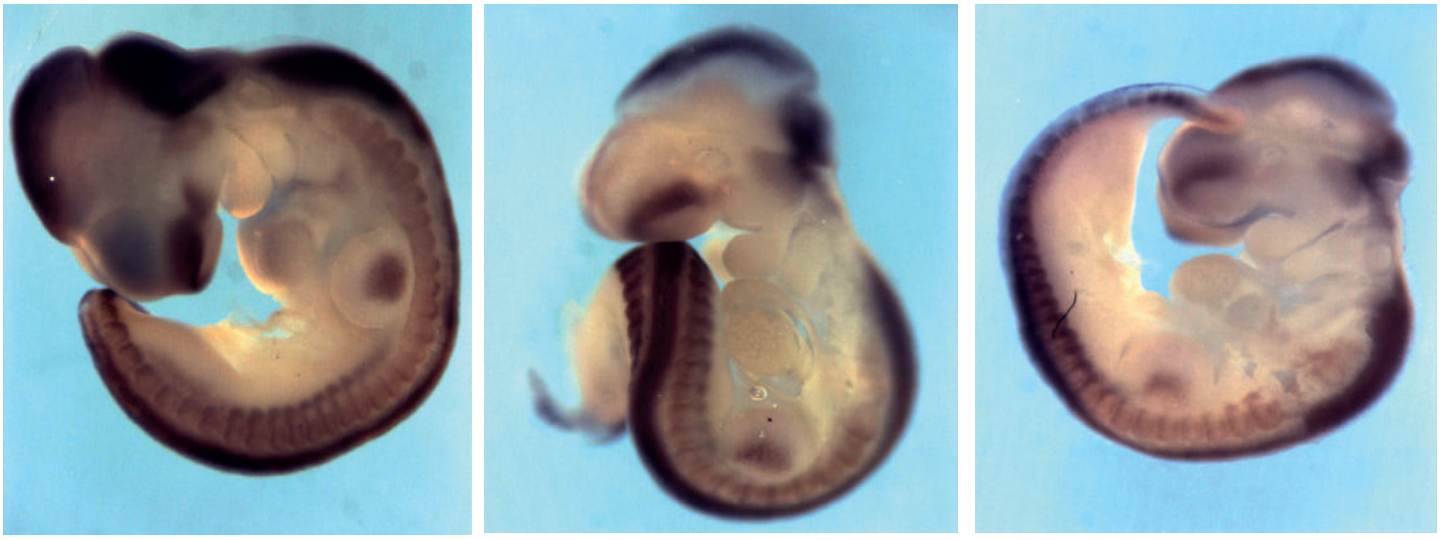

B

Pitx2loxp/loxp
E10.5

Pax3Cre+/-/Pitx2loxp+/-
E10.5

Pax3Cre+/-/Pitx2loxp-/-
E10.5

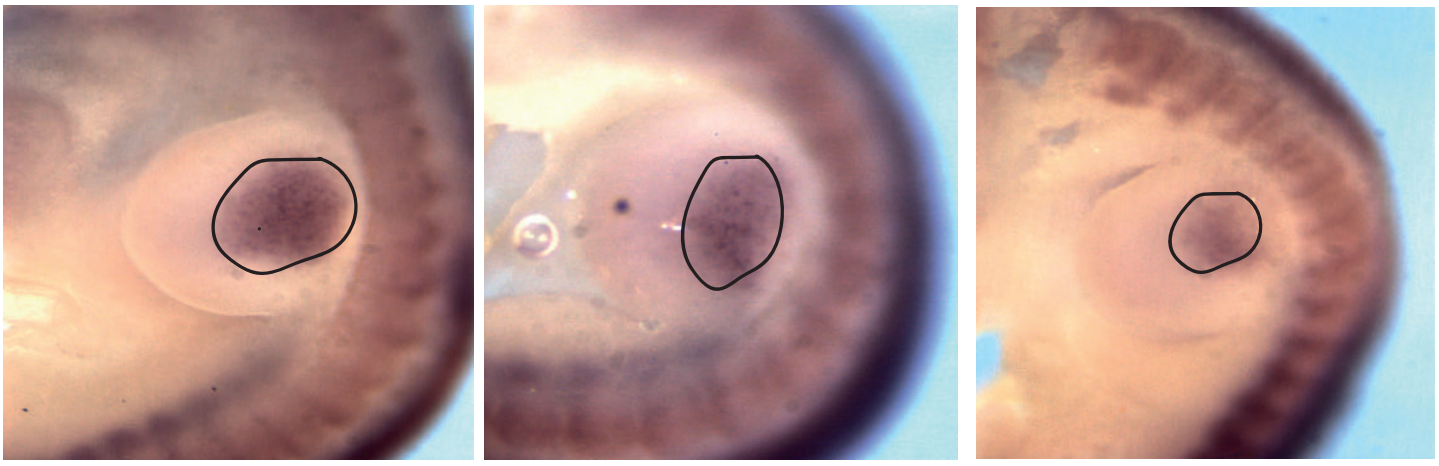

Figure 2

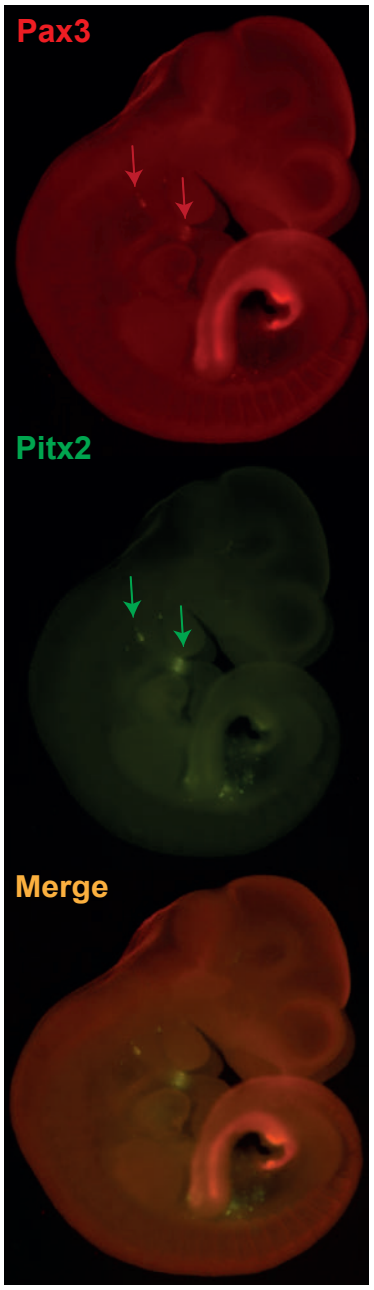
A
E10.5
Pax3
Pitx2
Merge

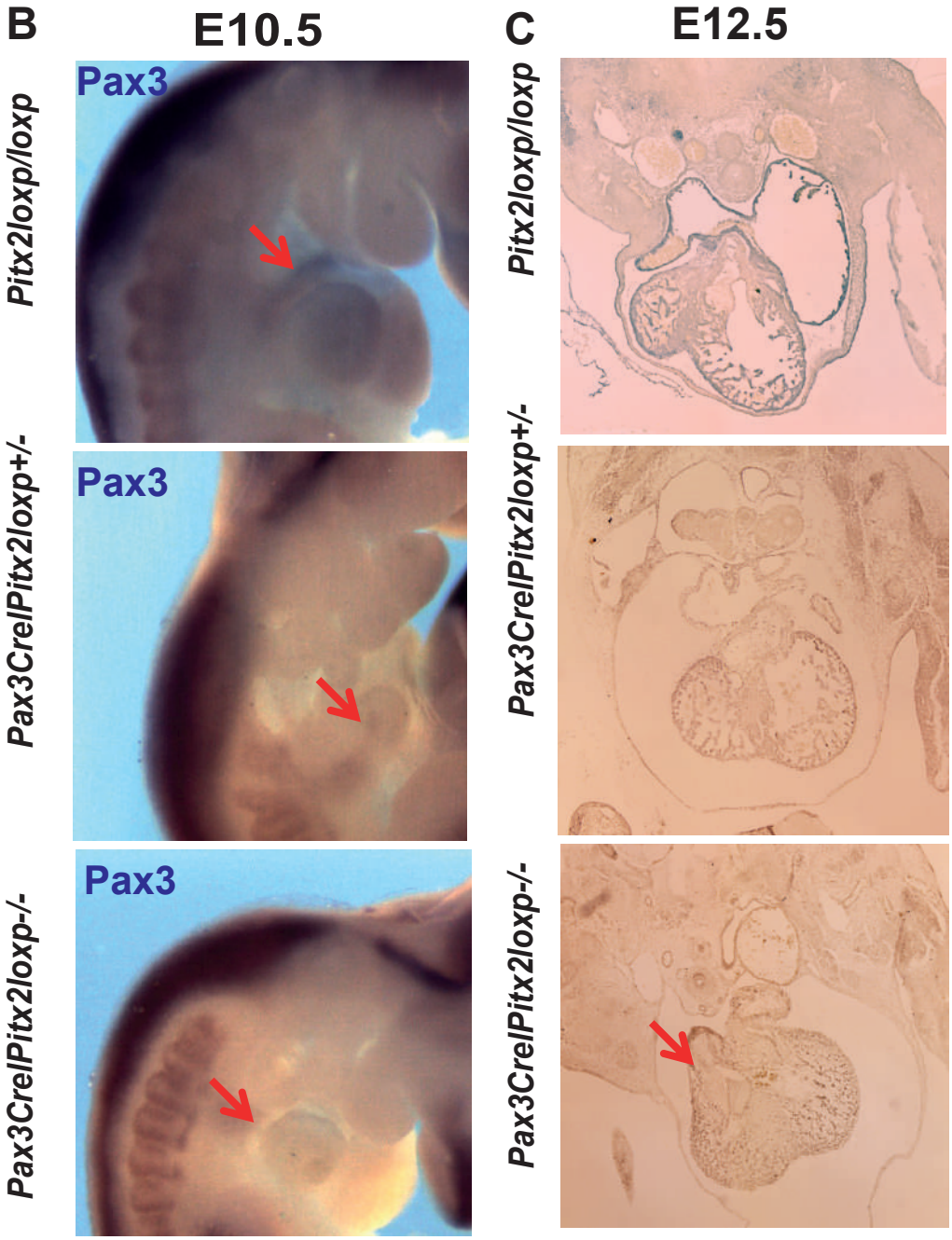
B
E10.5
C
E12.5
Pax3
Pax3
Pax3
Pitx2loxp/loxp
Pax3CrePitx2loxp+/-
Pax3CrePitx2loxp-/-
Pitx2loxp/loxp
Pax3CrePitx2loxp+/-
Pax3CrePitx2loxp-/-

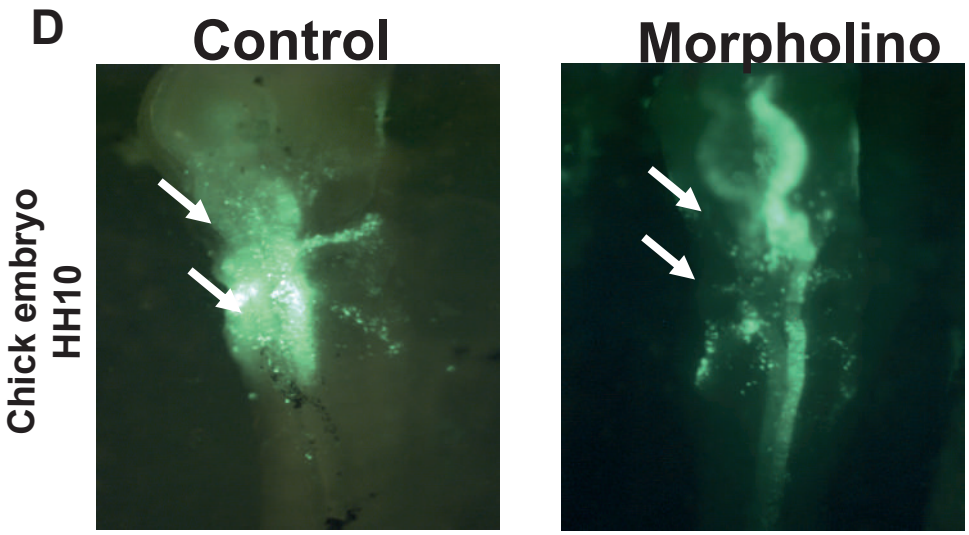
D
Control
Morpholino
Chick embryo
HH10

Figure 3

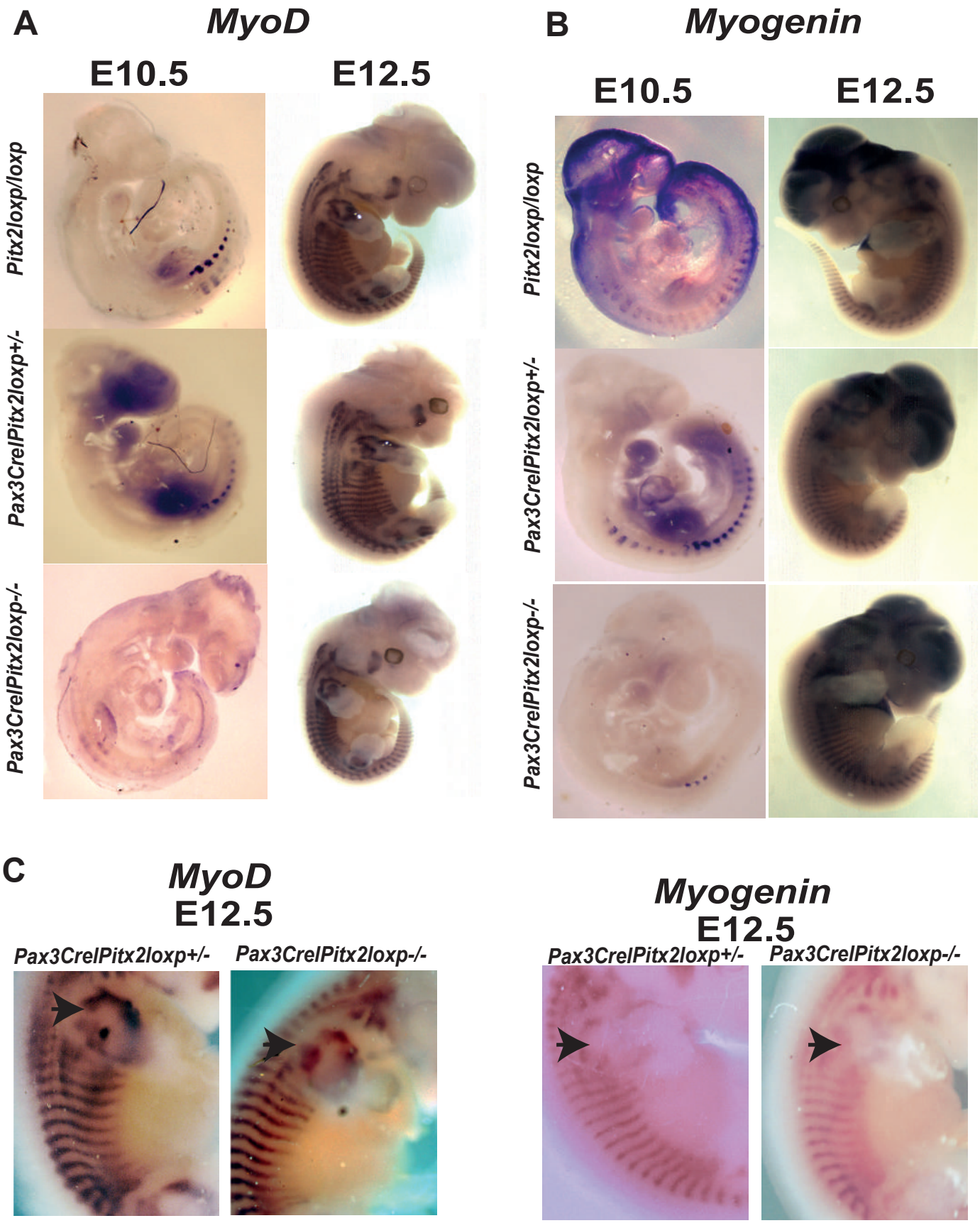
A
MyoD
E10.5
E12.5
Pitx2loxp/loxp
Pax3CrelPitx2loxp+/-
Pax3CrelPitx2loxp-/-
B
Myogenin
E10.5
E12.5
Pitx2loxp/loxp
Pax3CrelPitx2loxp+/-
Pax3CrelPitx2loxp-/-
C
MyoD
E12.5
Pax3CrelPitx2loxp+/-
Pax3CrelPitx2loxp-/-
Myogenin
E12.5
Pax3CrelPitx2loxp+/-
Pax3CrelPitx2loxp-/-

Figure 4

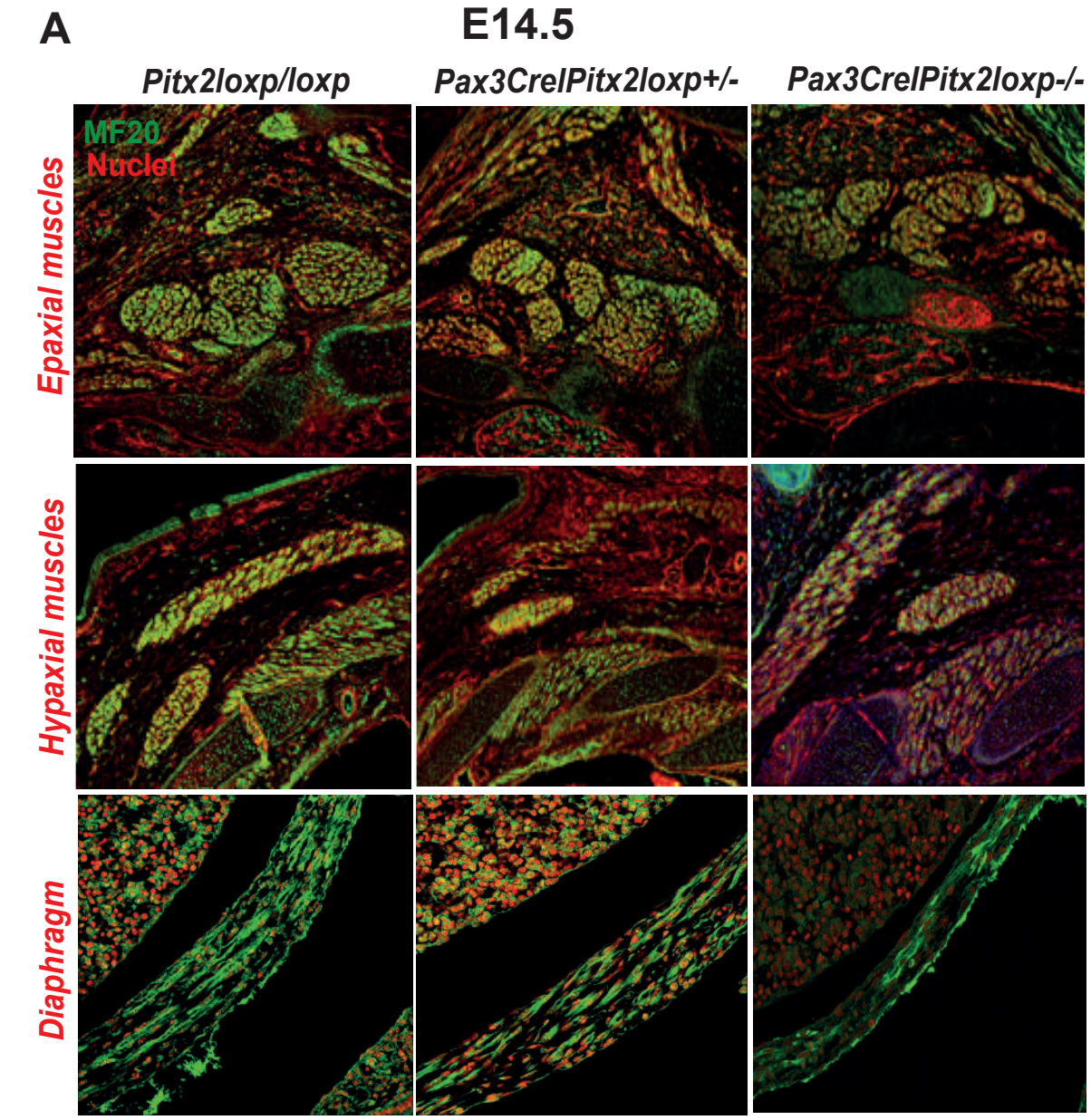
A
E14.5
Pitx2loxp/loxp
Pax3CrelPitx2loxp+/-
Pax3CrelPitx2loxp-/-
MF20
Nuclei
Epaxial muscles
Hypaxial muscles
Diaphragm

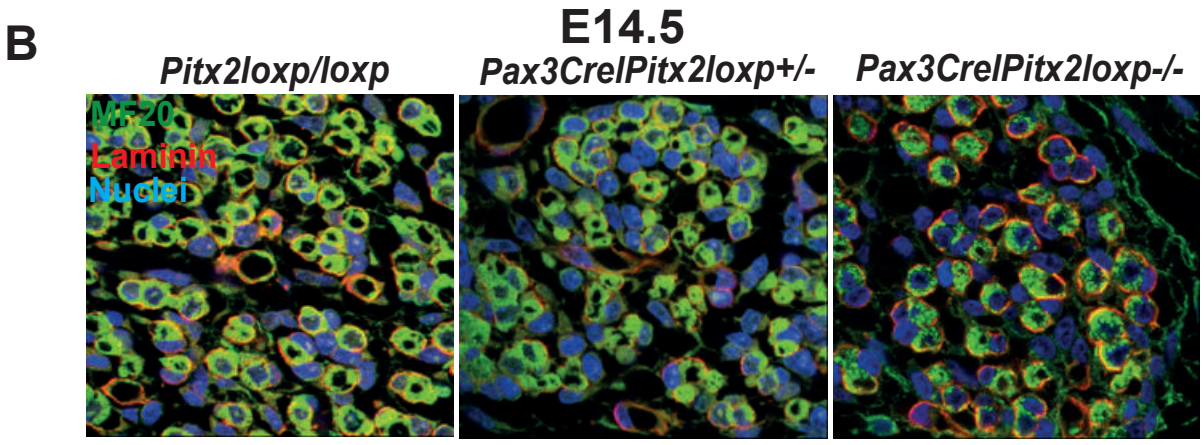
B
E14.5
Pitx2loxp/loxp
Pax3CrelPitx2loxp+/-
Pax3CrelPitx2loxp-/-
MF20
Laminin
Nuclei

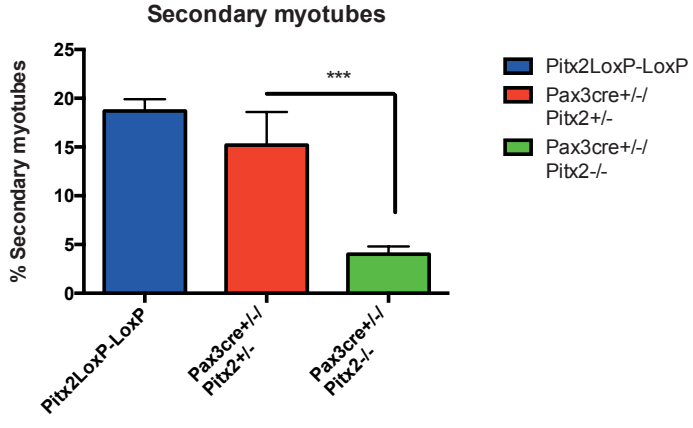
Secondary myotubes
% Secondary myotubes
25
20
15
10
5
0
***
Pitx2LoxP-LoxP
Pax3cre+/-/ Pitx2+/-
Pax3cre+/-/ Pitx2-/-
Pitx2LoxP-LoxP
Pax3cre+/-/ Pitx2+/-
Pax3cre+/-/ Pitx2-/-

Figure 5

A

Neonates

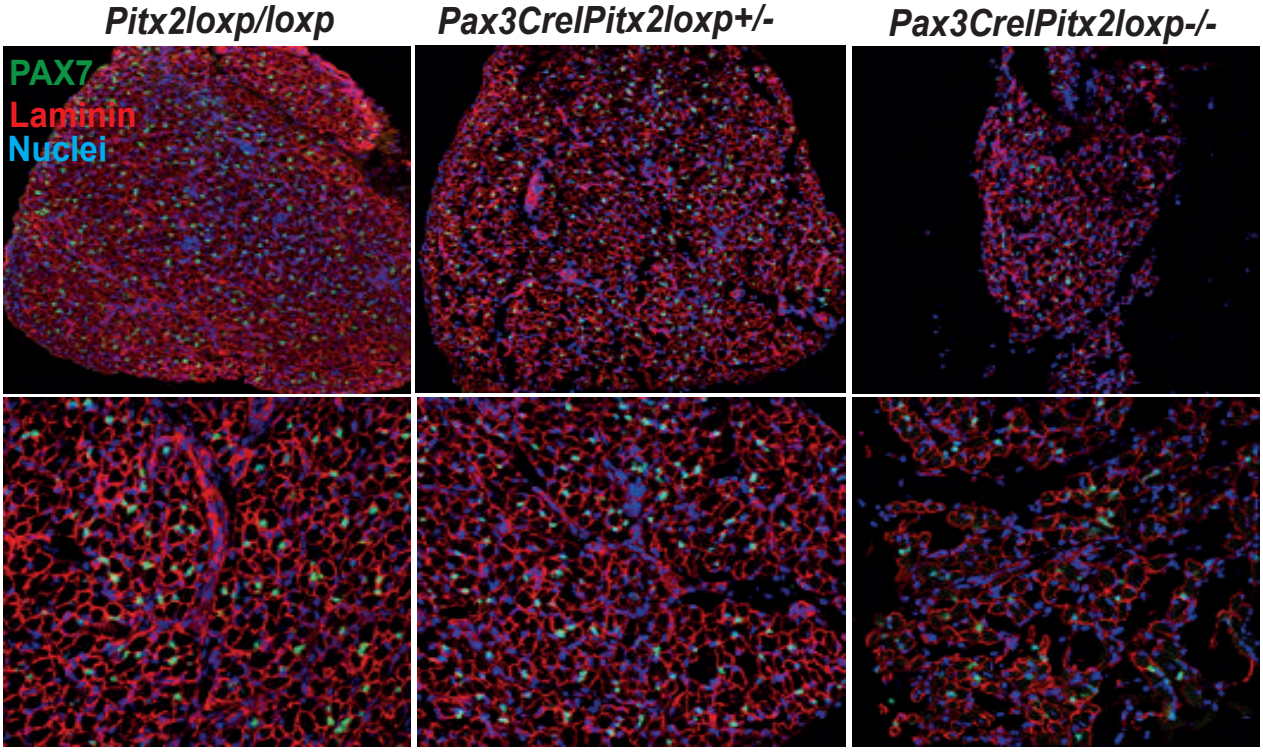

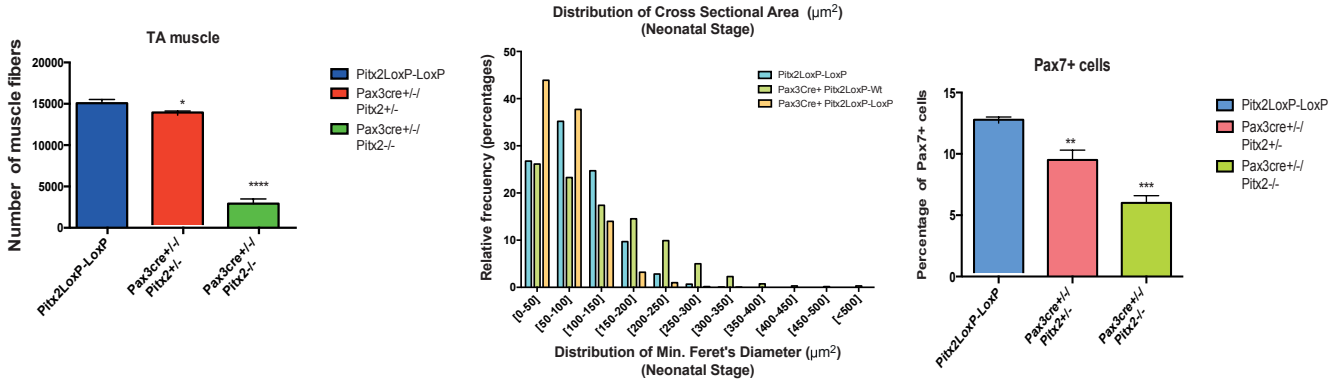

B

Adults

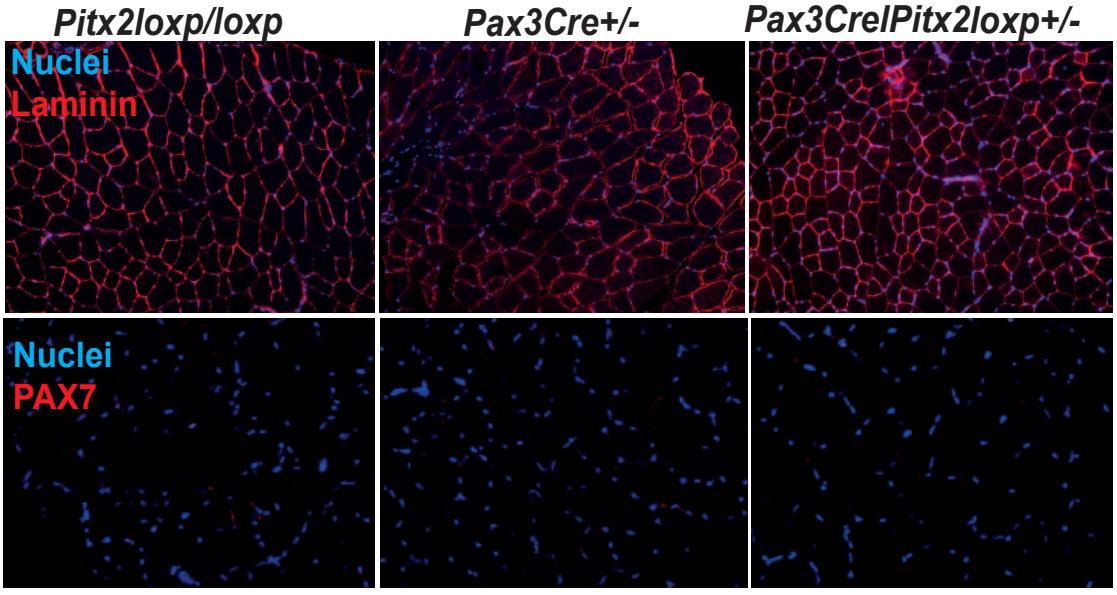

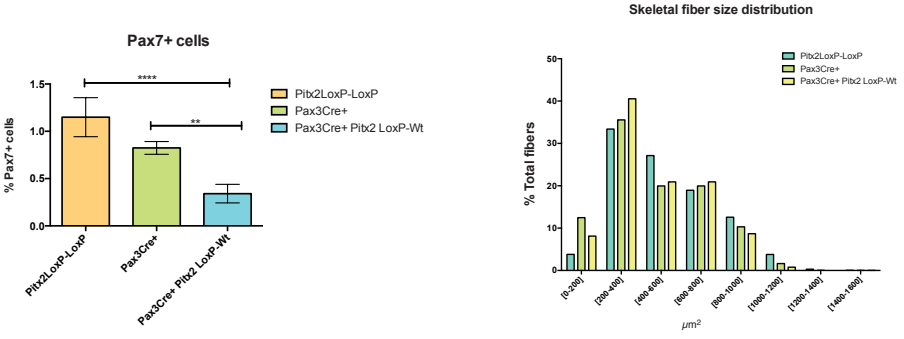

Figure 6

A

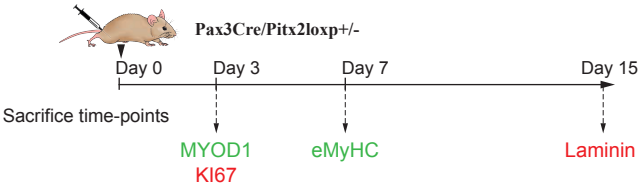

Day 7

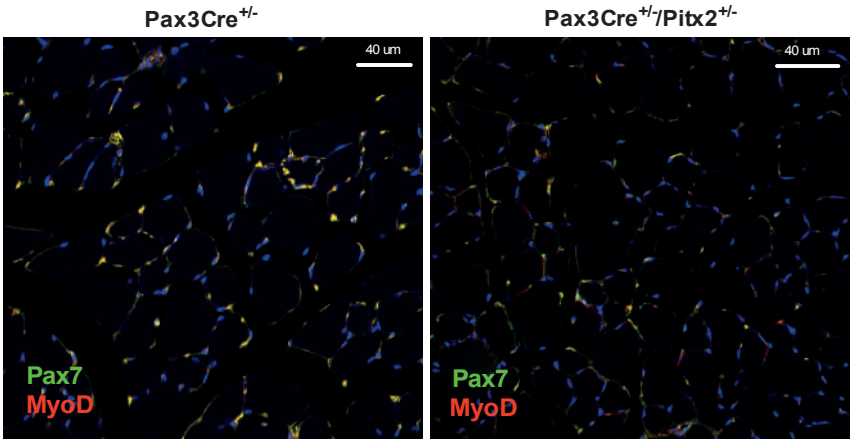

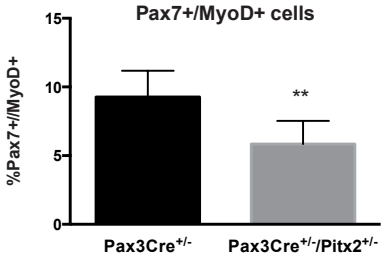

B

Day 15

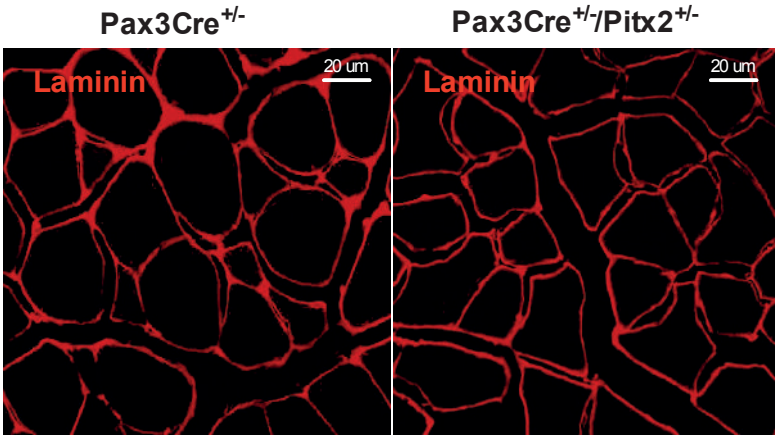

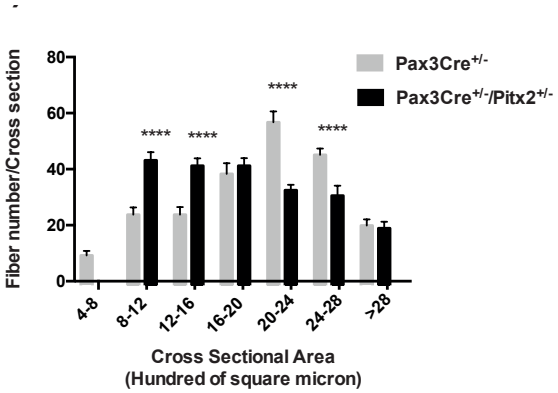

C

Day 30

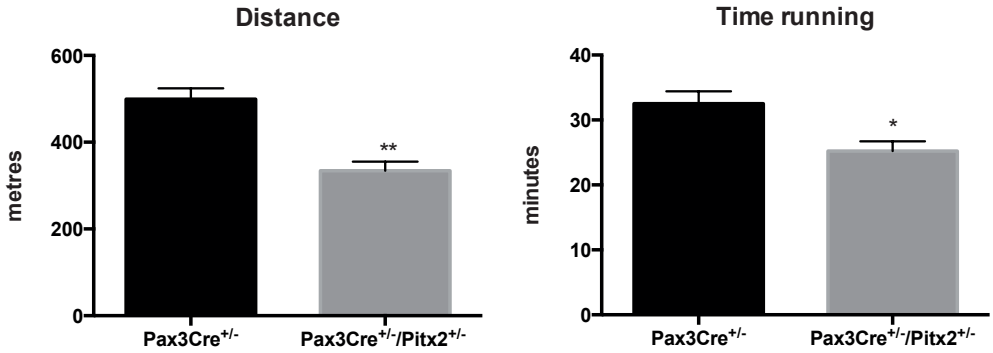

Figure 7

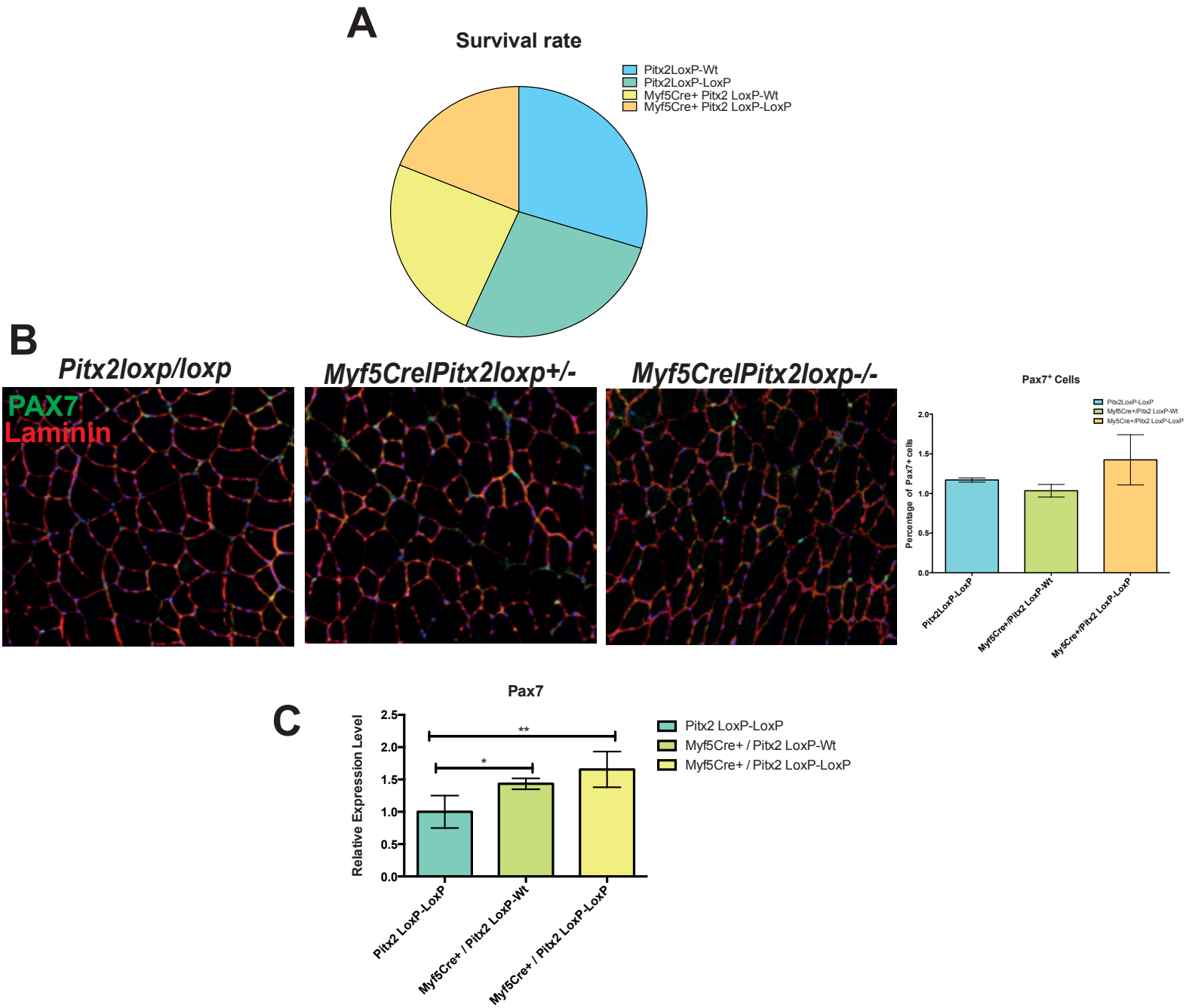
A
Survival rate
Pitx2LoxP-Wt
Pitx2LoxP-LoxP
Myf5Cre+ Pitx2 LoxP-Wt
Myf5Cre+ Pitx2 LoxP-LoxP
B
Pitx2loxp/loxp
Myf5CrelPitx2loxp+/-
Myf5CrelPitx2loxp-/-
PAX7
Laminin
Pax7+ Cells
Percentage of Pax7+ cells
2.0
1.5
1.0
0.5
0.0
Pitx2LoxP-LoxP
Myf5Cre+/Pitx2 LoxP-Wt
My5Cre+/Pitx2 LoxP-LoxP
Pitx2LoxP-LoxP
Myf5Cre+/Pitx2 LoxP-Wt
My5Cre+/Pitx2 LoxP-LoxP
C
Pax7
Relative Expression Level
2.5
2.0
1.5
1.0
0.5
0.0
**
*
Pitx2 LoxP-LoxP
Myf5Cre+ / Pitx2 LoxP-Wt
Myf5Cre+ / Pitx2 LoxP-LoxP
Pitx2 LoxP-LoxP
Myf5Cre+ / Pitx2 LoxP-Wt
Myf5Cre+ / Pitx2 LoxP-LoxP

Figure 8

A

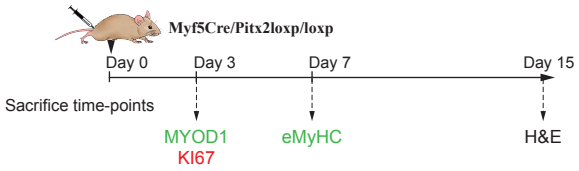

Day 3

Pitx2loxp/loxp | *Myf5CrelPitx2loxp+/-* | *Myf5CrelPitx2loxp-/-*

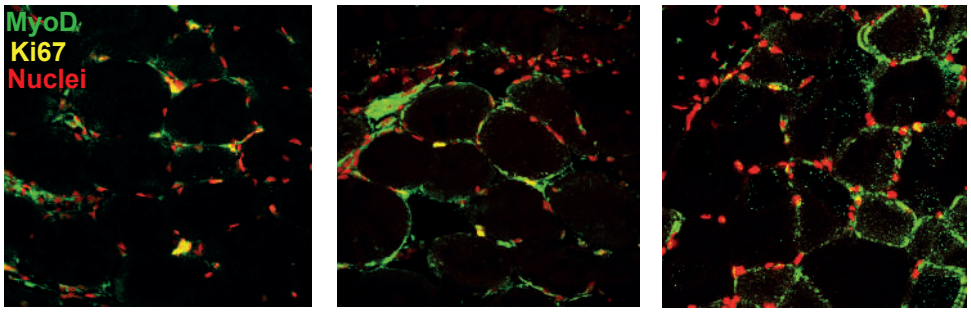

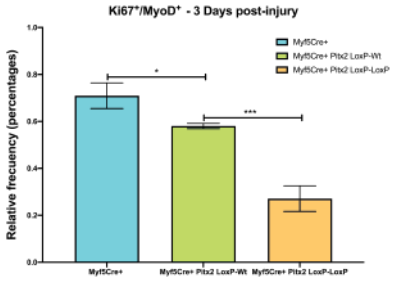

B

Day 7

Pitx2loxp/loxp | *Myf5CrelPitx2loxp+/-* | *Myf5CrelPitx2loxp-/-*

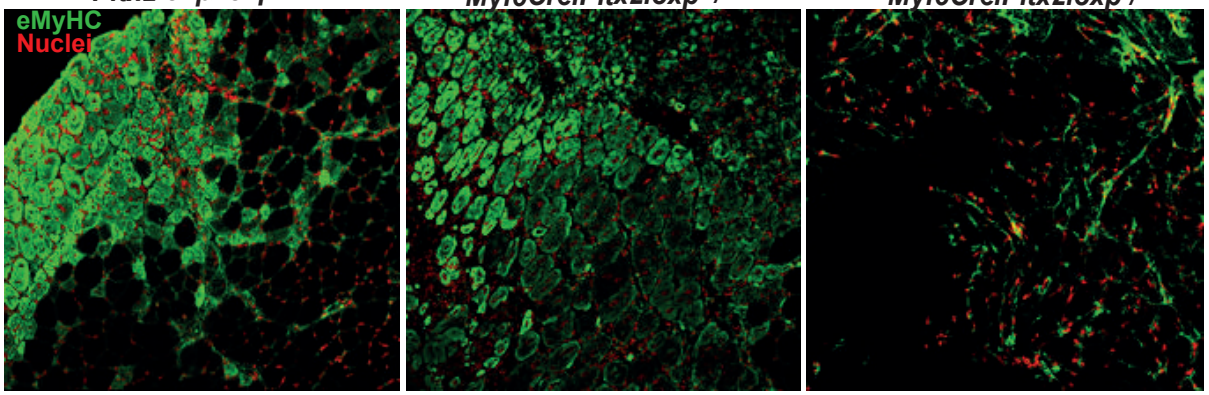

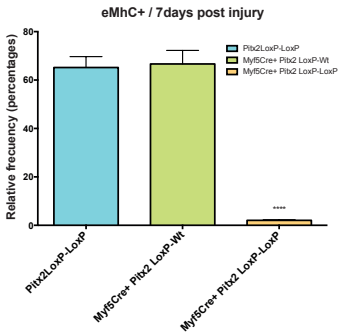

C

Day 15

Pitx2loxp/loxp | *Myf5CrelPitx2loxp+/-* | *Myf5CrelPitx2loxp-/-*

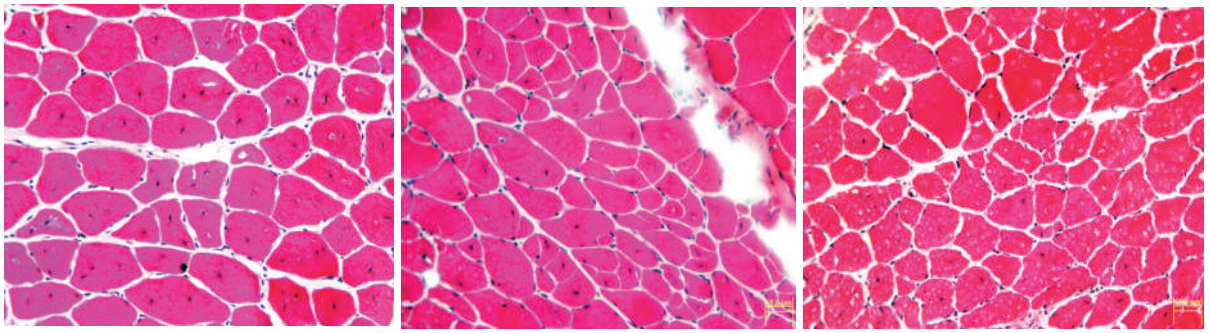

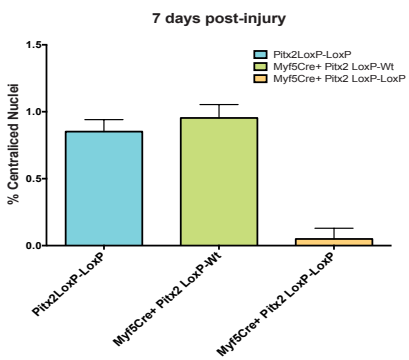

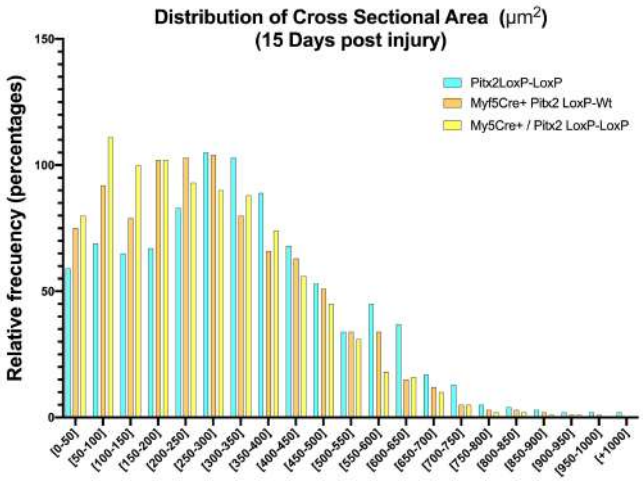

Figure S1

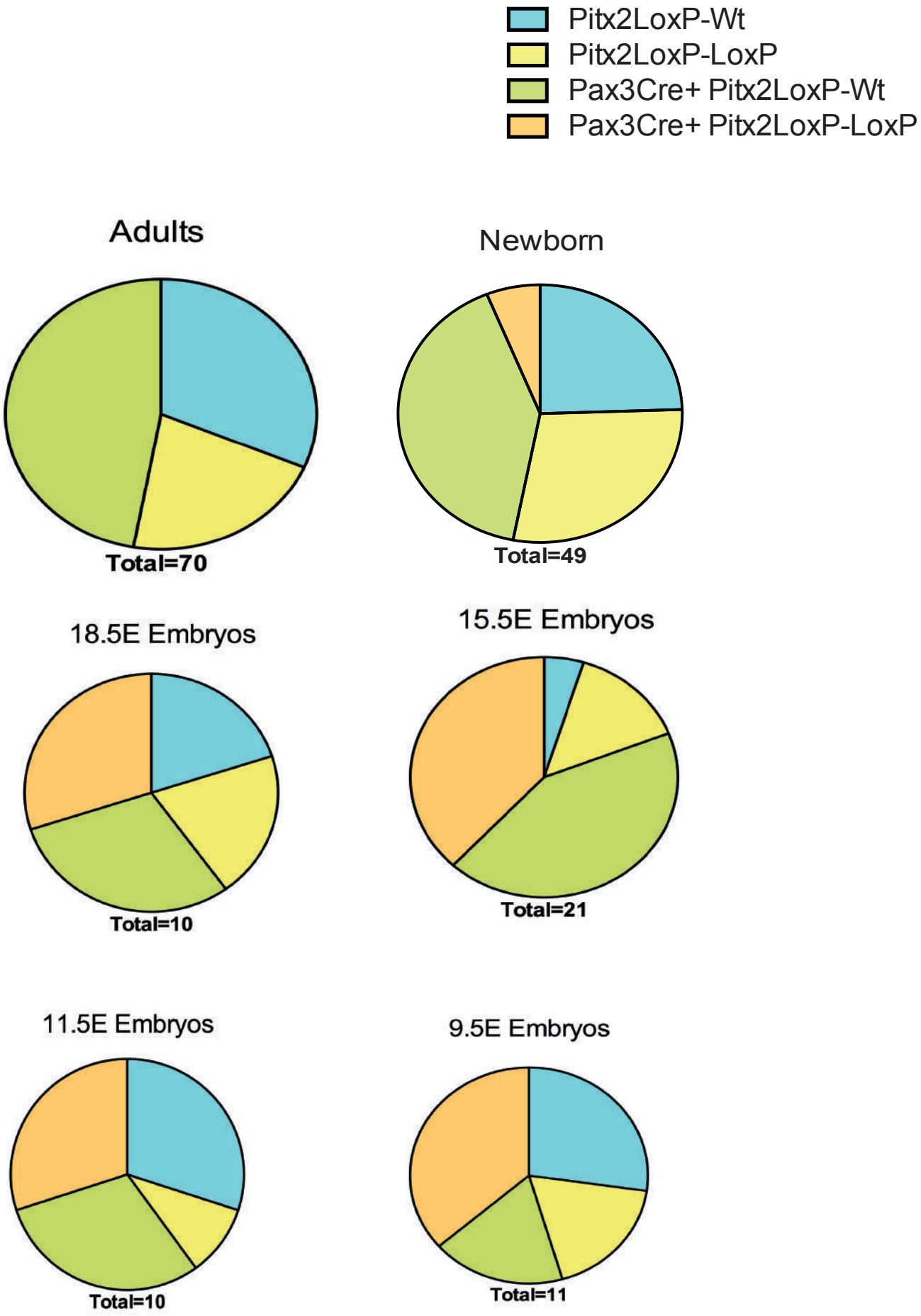
Pitx2LoxP-Wt
Pitx2LoxP-LoxP
Pax3Cre+ Pitx2LoxP-Wt
Pax3Cre+ Pitx2LoxP-LoxP
Adults
Total=70
Newborn
Total=49
18.5E Embryos
Total=10
15.5E Embryos
Total=21
11.5E Embryos
Total=10
9.5E Embryos
Total=11

Supplementary Figure 2

Lorem ipsum

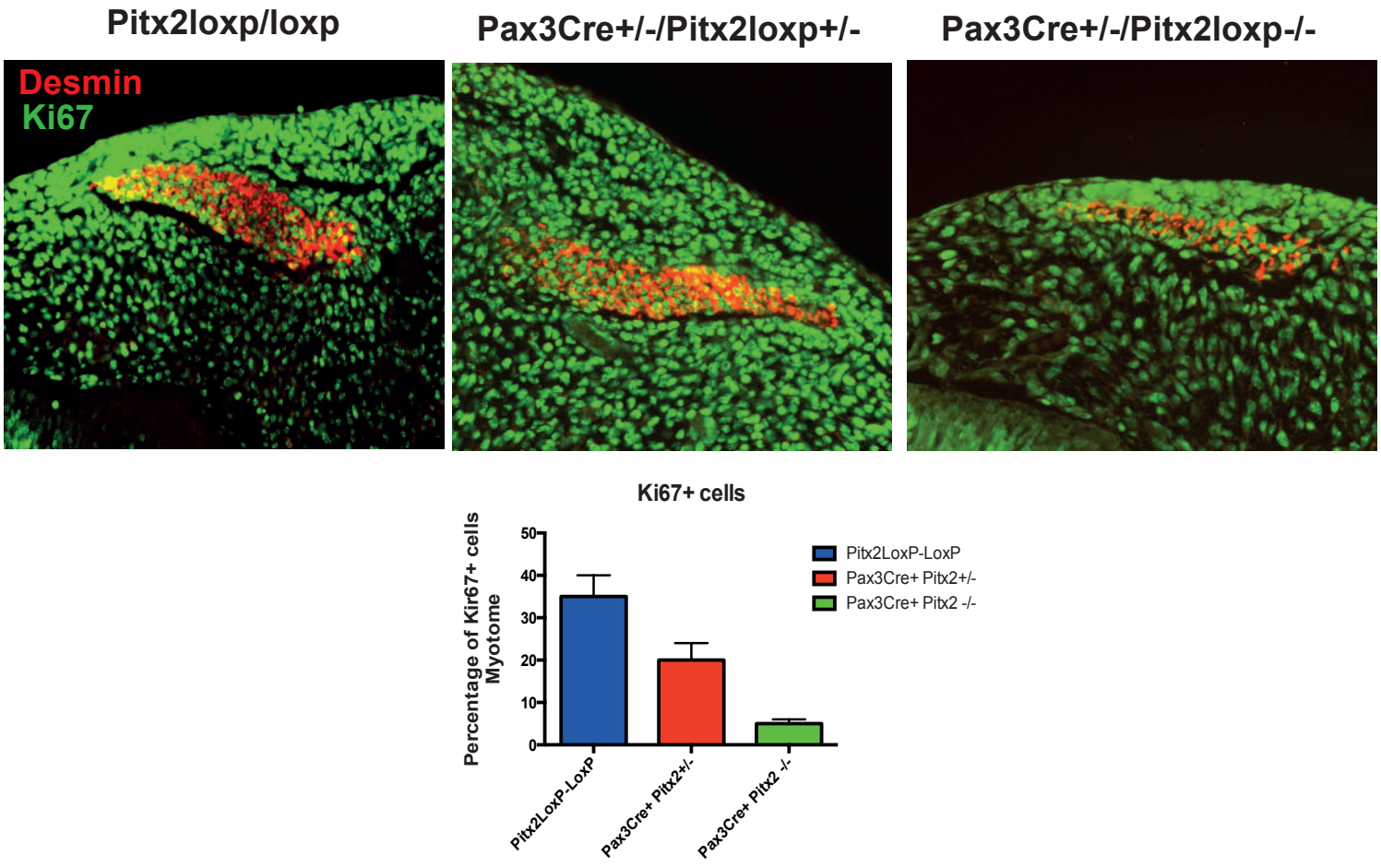

Supplementary Figure 3

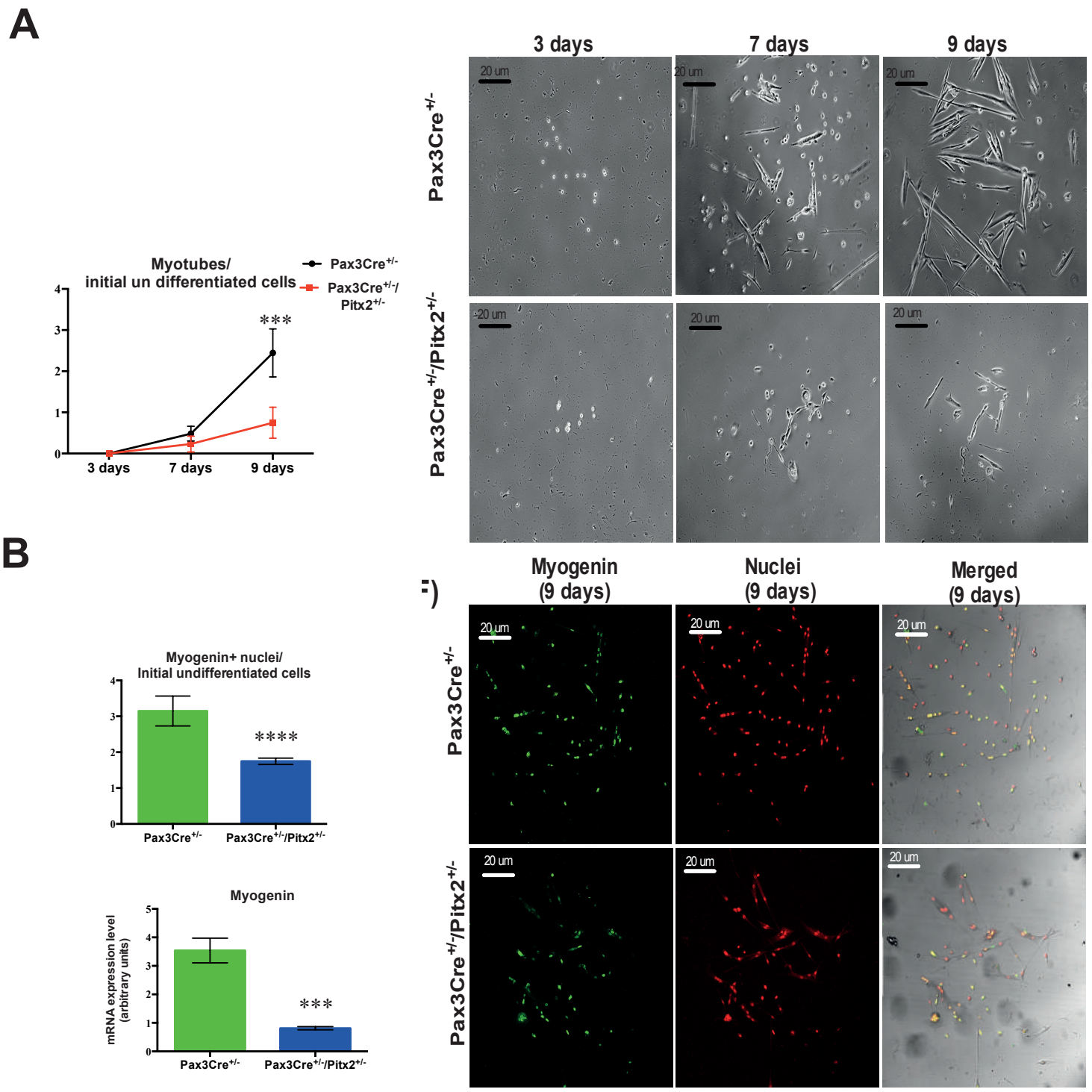

Table 1: Genotyping primers

Primer	Sequence	
Pitx2ln4_f01	GGTGGGGGTGTCTGTAAAAC	$Pitx2^{fl+/-}$
Pitx2ln5_r01	CAAGCCTTGCGTGTTTCTG	$Pitx2^{fl+/-}$
oIMR6977	CTGCACTCAAGGGACTCCTC	$Pax3Cre^{+/-}$
oIMR6978	GTGAAGGCGAGACGAAAAAG	$Pax3Cre^{+/-}$
oIMR9074	AGGCAAATTTTGGTGTACGG	$Pax3Cre^{+/-}$
AF-Cre1	CGGTCGATGCAACGAGTGATGAGG	$Myf5Cre^{+/-}$
AF-Cre2	CCAGAGACGGAAATCCATCGCTCG	$Myf5Cre^{+/-}$

Table 2: Antibodies list

Antibody	Source	Identifier
Rabbit Anti-Laminin	Sigma-Aldrich	L9393; RRID: AB_477163
Mouse Anti-MF20	Developmental Studies Hybridoma Bank (DSHB)	RRID: AB_2147781
Mouse Anti-Pax7	Developmental Studies Hybridoma Bank (DSHB)	RRID: AB_528428
Goat Anti-Pax3 (C-20)	Santa Cruz Biotechnology	Sc-34916
Mouse Anti-Desmin	Sigma-Aldrich	D1033
AlexaFluor® Goat Anti-rabbit 546	Thermo Fisher Scientific	A-11035; RRID: AB_2534093
AlexaFluor® Goat Anti-mouse 488	Thermo Fisher Scientific	A-11001; RRID: AB_2534069
DAPI	Thermo Fisher Scientific	D1306; RRID: AB_2629482

Table 3: Primers list for qRT-PCR

Gene	Primer sequence
Gapdh (NM_008084.2)	MmGapdhF: GGCATTGCTCTCAATGACAA MmGapdhR: TGTGAGGGAGATGCTCAGTG
Gusb (NM_010368.1)	MmGusbF: ACGCATCAGAAGCCGATTAT MmGusbR: ACTCTCAGCGGTGACTGGTT
Pitx2c (NM_001042502.1)	MmPitx2cF: CCTCACCCTTCTGTCACCAT MmPitx2cR: GCCCACATCCTCATTCTTTC
Pax7 (NM_011039.2)	MmPax7F: TCTTACTGCCCACCCACCTA MmPax7R: GTGGACAGGCTCACGTTTTT

Manuscript #	CDD-20-0282
Current Revision #	0
Submission Date	24th Feb 20
Current Stage	Under Consideration
Title	Stage-specific effects of Pitx2 inactivation during skeletal myogenesis
Running Title	Pitx2 and myogenesis
Manuscript Type	Article
Corresponding Author	Prof. Amelia Aranega (Cardiac and Skeletal Myogenesis Group, Department of Experimental Biology, University of Jaen.)
Contributing Authors	Mrs. Felicitas Ramirez de Acuña , Mrs. Lara Rodriguez-Outeiriño , Prof. Francisco Hernández-Torres , Dr. Jorge Dominguez-Macias , Dr. Diego Franco
Abstract	During embryonic development, the skeletal muscles of the trunk derive from transitory structures called somites. Multipotent muscle progenitor cells (MPCs) that express Pax3 arise from the dermomyotome and acquire their definitive identity via the myogenic regulatory factors (MRFs) Myf5, Mrf4, and MyoD. Moreover, the muscle stem cells (satellite cells) of the body and limbs also arise from somites, in common with the muscle that they are associated with. Several previous evidences have revealed that the transcription factor Pitx2 might be a player within the molecular pathways controlling somite-derived muscle progenitors' fate. However, the hierarchical position occupied by Pitx2 within the genetic cascade that control somite-derived myogenesis remain unsolved. To get insight into this issue, we have differentially generated two conditional Pitx2 mutant mice to specifically inactivate Pitx2 in multipotent Pax3+ muscle progenitors (Pax3Cre+/Pitxloxp/loxp mice) and in myogenic committed progenitors (Myf5Cre+/Pitx2loxp/loxp mice). Our analyses revealed that Pitx2 inactivation in Pax3+ precursors lead defective migration of Pax3+ cells and muscle hypotrophy while the loss of Pitx2 in Myf5+ myogenic cells have an impact in satellite stem properties with severe consequences in muscle regeneration. Overall our results suggest a Pitx2 requirement for MPCs migration as well as for the acquisition of a proper satellite cell function.